UNIVERSITÉ FRANÇOIS RABELAIS DE TOURS

Écoles Doctorales SSBCV et MIPTIS

Unité de Recherche Avicole (INRA-UR 0083)

Laboratoire de Mathématiques et Physique Théorique (CNRS-UMR 7350)

THÈSE présenté par :

Masoomeh TAGHIPOOR

soutenue le : 24 septembre 2012

pour obtenir le grade de : Docteur de l'université François Rabelais - Tours

Discipline/ Spécialité : Mathématiques/ Biomathématique

MODÉLISATION DU TRANSPORT, DE LA DÉGRADATION ET DE L'ABSORPTION DES ALIMENTS DANS L'INTESTIN GRÊLE

THÈSE DIRIGÉE PAR :

LESCOAT Philippe	Ingénieur de Recherche HDR, INRA - Nouzilly
BARLES Guy	Professeur, Université François Rabelais - Tours

RAPPORTEURS :

LAROCHE Béatrice	Directeur de Recherche, INRA - Jouy en Josas
FIORAMONTI Jean	Directeur de Recherche, INRA - Toulouse

JURY :

BARLES Guy	Professeur, Université François Rabelais - Tours
BROSSARD Ludovic	Ingénieur d'études, INRA - Rennes
DUITTOZ Anne	Professeur, Université François Rabelais - Tours
FIORAMONTI Jean	Directeur de Recherche, INRA - Toulouse
FOUILLET Hélène	Chargé de Recherche, INRA - Paris
LAROCHE Béatrice	Directeur de Recherche, INRA - Jouy en Josas
LESCOAT Philippe	Ingénieur de Recherche HDR, INRA - Nouzilly
SUPPO Christelle	Professeur, Université François Rabelais - Tours

Remerciements

.

Abstract

The purpose of this study is to represent a generic model of digestion in the small intestine.

In the first part of this work, a model based on ordinary differential equations is used to represent the digestion : the equations describe the evolution of the position and composition of the bolus of feedstuffs coming from the stomach. Each bolus is identified as a cylinder. This model considers simultaneously the different aspects of digestion i.e. transport of the bolus all along the small intestine, feedstuffs degradation according to the enzymes and local physical conditions, and nutrients absorption.

In the second part of this study, we use the homogenization method to sustain the simplified digestion model developed in the first part. We show that this model can be considered as a macroscopic version of more realistic models which contain the biological phenomena at lower scales of the small intestine : (i) the high frequency peristaltic pulses (microcopic time scale) and their effects on the velocity of bolus, (ii) the presence of the intestinal villi (microscopic scale of space) and their influence on the digestion.

Finally, in the third part of this study, we investigate the digestion of a non-homogeneous feedstuffs matrix by integrating the dietary fibre in the bolus. The two main physiochemical characteristics of dietary fibre which interact with the function of the small intestine, i.e. viscosity and water holding capacity are modelled. This leads us to consider some features of the digestion which have not been taken into account previously, particularly the interrelationship between the evolution of dry matter and water in the bolus. Although this model is generic and contains a large number of parameters, to our knowledge, it is among the first qualitative dynamical modelling of fibre influence on intestinal digestion.

Keywords : Modelling, ODE, Digestion, Small intestine, Peristaltic, Homogenization, Viscosity solutions, Dietary fibres.

Résumé

L'objectif de ce travail est de présenter un modèle générique de la digestion dans l'intestin grêle.

Dans la première partie de ce travail, un modèle mécaniste basé sur les équations différentielles ordinaires est utilisé pour présenter la digestion : les équations décrivent l'évolution de la position et de la composition du bolus provenant de l'estomac. Chaque bolus est représenté par un cylindre. Ce modèle prend en compte simultanément les différents aspects de la digestion à savoir le transport du bolus dans la lumière intestinale, la dégradation des aliments par des enzymes, et l'absorption des nutriments.

Dans la deuxième partie de cette étude, nous utilisons les méthodes d'homogénéisation mathématique pour justifier le modèle de la digestion développé dans la première partie. Nous montrons que ce modèle peut être considéré comme une version macroscopique des modèles plus réalistes, qui contiennent des phénomènes biologiques à des échelles inférieures de l'intestin grêle : (i) les ondes péristaltiques à haute fréquence (échelle du temps microscopique) et leurs effets sur la vitesse du bolus, (ii) la présence des villosités intestinales (échelle microscopique de l'espace) et leur influence sur la digestion.

Enfin, dans la troisième partie de ce travail, nous étudions l'influence du changement de la structure de bolus sur la digestion en intégrant les fibres alimentaires dans sa composition. Les deux principales caractéristiques des fibres alimentaires qui interagissent avec la fonction de l'intestin grêle, à savoir, la viscosité et la capacité de rétention d'eau ont été modélisées. Ce modèle nous a permis de considérer, en particulier, la relation entre l'évolution de la matière sèche et de l'eau au sein du bolus. Bien que ce modèle est générique et contient un grand nombre de paramètres, à notre connaissance, il est parmi les premiers modèles dynamiques qualitatives de l'influence des fibres sur la digestion intestinale.

Table des matières

Liste des tableaux

Table des figures

Nomenclature

Symboles	Unités	Définitions
A_{nd}	g	Matière non-dégradable
A_{ns}	g	Matière non-solubilisée
A_s	g	Matière solubilisée
A_s^{dm}	g	Proportion de la matière sèche présente dans A_s
B_{int}	g	Matière intermédiaire (non-absorbable)
B_{int}^{dm}	g	Proportion de la matière sèche présente dans B_{int}
B_{abs}	g	Matière absorbable par la paroi intestinale
B_{abs}^{dm}	g	Proportion de la matière sèche présente dans B_{abs}
F_{sol}	g	Fibres solubles
F_{sol}^{dm}	g	Proportion de la matière sèche présente dans F_{sol}
F_{insol}	g	Fibres non-solubles
F_{insol}^{dm}	g	Proportion de la matière sèche présente dans F_{insol}
W	g	Quantité d'eau présente dans le bol alimentaire
M	g	Masse totale du bol alimentaire
V	m^3	Volume du bol alimentaire
e	—	Enzymes pancréatiques et stomacaux
e_{exo}	—	Enzymes exogènes
R	m	Rayon
ℓ	m	Longueur du bol alimentaire
x	m	Distance
W_{as}	g	Quantité d'eau associée à A_s^{dm}
W_{int}	g	Quantité d'eau associée à B_{int}^{dm}
W_{abs}	g	Quantité d'eau associée à B_{abs}^{dm}

Introduction générale

En recherche, les disciplines biologiques s'appuient souvent sur l'expérimentation animale. En effet, les phénomènes naturels sont complexes et rarement strictement identiques d'une espèce à l'autre. La démarche expérimentale permet le recueil des données concernant chaque espèce et dans des conditions variées, ces données peuvent être ensuite analysées, traitées et comparées permettant la compréhension de mécanismes d'intérêt. Pourtant les interrogations de la société concernant l'utilisation des animaux à des fins de recherche ont nécessité la mis en œuvre d'alternatives à l'expérimentation animales. Ainsi, Russel et Burch [2], ont proposé la règle des "3R" de l'utilisation des animaux dans les recherches biologique : remplacer, raffiner et réduire.

Les modèles mathématiques sont souvent cités comme une alternative à l'expérimentation animale et sont utilisés notamment quand la complexité du phénomène observé ne permet pas à l'intuition ou à des approches analytiques de comprendre son fonctionnement et son évolution (J. VanMilgen et P. Lescoat [3]). La modélisation mathématique consiste à tenter de comprendre les lois régissant les phénomènes naturels du vivant à travers leur représentation par des équations mathématiques. Mais, une condition sine qua non est que la complexité des phénomènes biologiques implique l'adoption d'une approche réductionniste par le modélisateur. En d'autres termes en fonction de l'objectif, le modélisateur choisit de négliger dans le modèle les variables d'état qui n'interviennent que très peu dans l'évolution du système biologique tout du moins au regard de la question traitée (J. Clairambault. [4]).

a. *Pourquoi un modèle mathématique ?*

La contribution de la modélisation aux "3R" de l'expérimentation animale révèle son intérêt dans les recherches biologiques. Ainsi, les modèles mathématiques, par leur rôle dans l'orientation des recherches biologiques (*raffinement*) ont pu contribuer à la *réduction* de l'expérimentation animale. De plus, les différents logiciels informatiques permettent des simulations numériques du modèle construisant des expérimentations virtuelles (*in-silico*), ce qui pourrait *remplacer* (ou au moins limiter) des redondances expérimentales.

D'autre part, la complexité des phénomènes naturels peut rendre l'interprétation des expérimentations "*in-vivo*" difficile et même impossible. Or, après la construction du modèle, son analyse mathématique, permet de vérifier l'existence et l'unicité des solutions, l'analyse de leur stabilité ainsi qu'une analyse qualitative sur le comportement du système [4]. Mais cela ne doit pas faire oublier que les résultats ainsi obtenus par modélisation ne sont valides que dans le cadre des hypothèses posées initialement. En outre, la mise en œuvre de théorèmes mathématiques rend valide les résultats, ceci soulignant l'importance en modélisation appliquée à la biologie de l'utilisation des connaissances mathématiques.

Par exemple, les systèmes du vivant ont souvent plusieurs échelles emboîtées, de la molécule à la cellule, de la cellule à l'organe ou tissu, de l'organe à l'individu, etc. Les propriétés macroscopiques de l'individu sont souvent liées au fonctionnement à l'échelle inférieure (ex. influence de la quantité des cellules matures des villosités intestinales sur l'absorption) et inversement, l'évolution à l'échelle microscopique du système dépend de son état à l'échelle supérieure (ex. influence de la composition du bol alimentaire dans la lumière intestinale sur l'utilisation des transporteurs pour l'absorption active). Un modèle mathématique peut décrire l'évolution du système dans l'un de ces niveaux, mais il peut aussi intégrer plusieurs échelles simultanément (ex. modèle d'évolution de la digestion en fonction de la composition du bol alimentaire ainsi que la maturité des cellules sur les villosités). Cette approche par modélisation permet aussi d'étudier l'influence respective de modification des propriétés à chaque échelle sur l'évolution du système.

Suite à la phase de modélisation mathématique, la simulation numérique du modèle à l'aide de logiciels appropriés est indispensable pour permettre à l'utilisateur d'effectuer ses propres expériences "*in-silico*". Cela permet d'étudier différentes hypothèses simultanément et de s'affranchir de certaines limites existant dans les approches expérimentales, notamment en termes de nombre de combinaisons et de domaines explorés par le modèle.

b. *Limites d'utilisation d'un modèle mathématique*

Un modèle mathématique contient très souvent de nombreux paramètres dont les valeurs sont fixées grâce aux données expérimentales ou à dire d'expert par absence de mesures existantes ou disponibles. Ce grand nombre et la difficulté de les obtenir sont des questions clés quant à la possibilité d'utiliser les modèles et quant à leur portée. D'autre part, une étape importante qui suit la modélisation est la confrontation des sorties du modèle à des données issues de l'expérimentation afin de valider le modèle, ou pour tout le moins son comportement.

En conclusion, de la même façon que l'expérimentation est nécessaire pour valider la modélisation, un modèle devrait permettre de mieux définir des plans d'expérimentation.

Il est toutefois illusoire de croire que les phénomènes du vivant, d'une complexité hors de notre portée, peuvent se réduire à des équations mathématiques, aussi complexes soient-elles. C'est un débat depuis les origines de la connaissance scientifique [3].

c. *Modélisation pour comprendre la digestion*

L'intestin grêle est la partie la plus longue du tube digestif. Elle a des conditions favorables pour la dégradation des macromolécules (motricité, activité enzymatique, conditions physico-chimiques, etc). La connaissance de la dynamique de la digestion dans l'intestin grêle des différentes espèces permettrait de mieux valoriser les aliments fournis et donc d'optimiser les intrants et de limiter les rejets dans l'environnement. Or, les méthodes expérimentales et les mesures *in-vivo* provoquent des perturbations dans le fonctionnement de l'intestin grêle et ne permettent pas d'étudier la digestion en prenant simultanément en compte les différentes échelles présentes dans l'intestin grêle. La modélisation permet de surmonter certaines des difficultés qui existent dans des approches expérimentales sous réserve d'une prise en compte argumentée des phénomènes biologiques connus et pertinents pour l'objet étudié. .

L'objectif de ce travail est de construire un modèle générique de la digestion dans l'intestin grêle c'est-à-dire le transport des aliments le long de l'intestin grêle, la dégradation des macromolécules au sein du bol alimentaire et l'absorption des nutriments à travers de la paroi intestinale chez les monogastriques.

Nous rappellerons d'abord les principaux éléments de la digestion dans l'intestin grêle chez les monogastriques, puis abordera des différentes méthodes de la modélisation que nous avons testées. Cette thèse est organisée en trois chapitres dont les résumés sont présentés à la fin de l'introduction.

1 Intestin grêle et digestion des aliments

L'intestin grêle est un organe multifonctionnel, il est d'une part responsable du transit des aliments dans la lumière intestinale et de leur mélange avec des enzymes et, d'autre part, il est un lieu idéal pour la dégradation par l'hydrolyse enzymatique et l'absorption des nutriments.

L'intestin grêle comporte trois segments : le duodénum qui suit le pylore, le jéjunum qui est le lieu principal de l'absorption à cause de la présence d'une quantité importante des villosités intestinales et l'iléon. La Figure 1 présente un schéma de l'intestin grêle.

La longueur de l'intestin grêle varie selon les espèces ; par exemple pour le porc [1] en croissance la longueur de l'intestin grêle est de 17 à 20 m et le diamètre est de 4 à 5 cm.

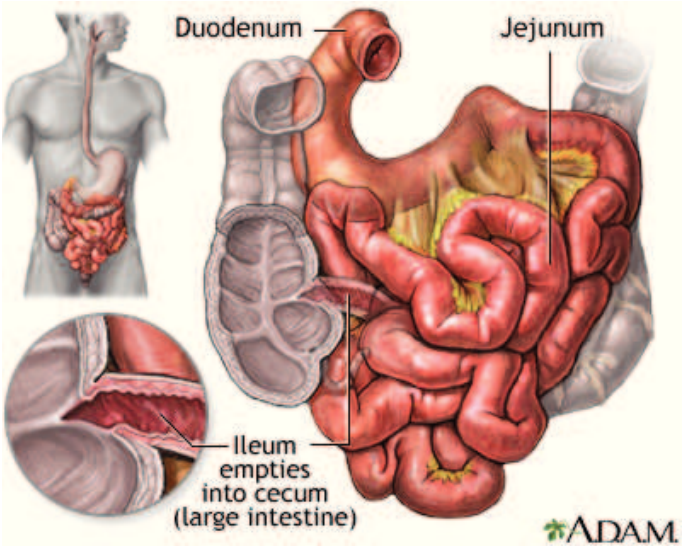

FIGURE 1: Schéma général de l'intestin grêle (U.S. National Library of Medicine).

La digestion est le processus par lequel les molécules organiques sont réduites pour être rendues absorbables à travers la paroi du tube digestif. L'intestin grêle est l'organe majeur de la dégradation des aliments et de l'absorption des nutriments. Dans le cadre de ce travail, la digestion est représentée par trois phénomènes principaux : le transport des aliments le long de l'intestin grêle par les ondes péristaltiques, la dégradation des macromolécules par l'hydrolyse enzymatique et l'absorption des nutriments par absorption active et passive [5].

L'étude de la digestion nécessite la connaissance des divers caractéristiques anatomiques de l'intestin grêle qui se représentent selon quatre échelles (Figure 2) :

- Échelle macroscopique ($17\,m$) qui correspond à la longueur de l'intestin grêle.
- Échelle mésoscopique ($1\,cm$) qui correspond à la longueur des villosités intestinales (leur rôle étant d'augmenter la surface d'absorption) et la muqueuse intestinale.
- Échelle sous mésoscopique ($1\,mm$) qui correspond aux micro-villosités et aux cryptes.
- Échelle microscopique ($10\,\mu m$) qui correspond aux cellules épithéliales.

Par la suite, nous expliquons brièvement chacun de ces phénomènes.

1. Toutes le mesures utilisées dans cette thèse correspondent à celles du porc en croissance.

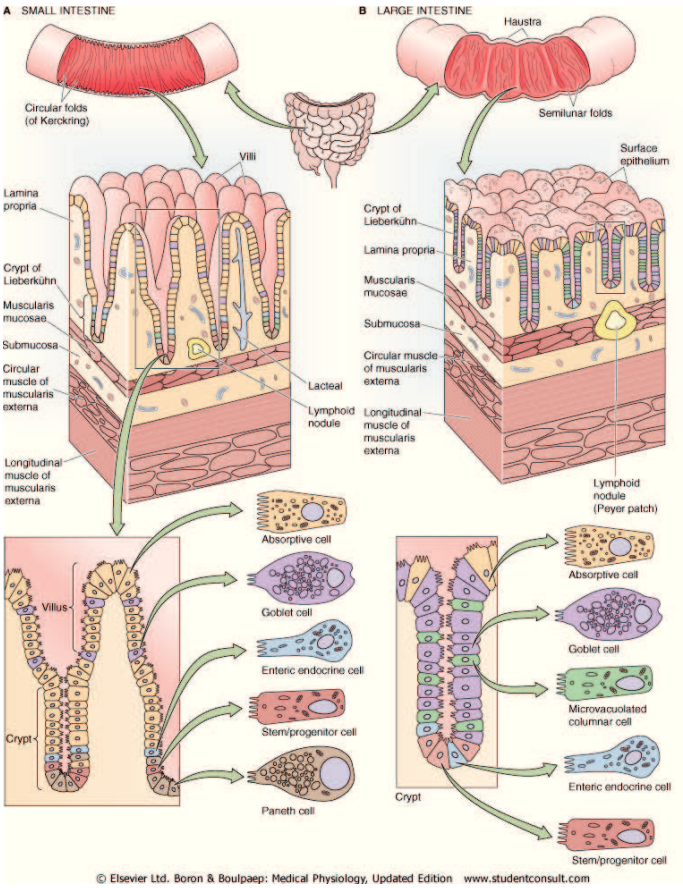

FIGURE 2: Différentes échelles spatiales de l'intestin grêle et du côlon.

Dégradation

La dégradation dans l'intestin grêle est principalement due à l'hydrolyse enzymatique. L'hydrolyse est une réaction spontanée très lente qui est accélérée par des enzymes. L'intestin grêle reçoit les sécrétions digestives du foie et du pancréas qui contiennent des enzymes nécessaires pour les diverses réactions d'hydrolyse : des enzymes protéolytiques (peptidases, trypsine et chymotrypsine), des amylases et des lipases. Ces sécrétions ont notamment pour rôle de neutraliser le contenu acide provenant de l'estomac et d'émulsifier des lipides par les sels biliaires. En outre les enzymes intestinaux, les enzymes de la bordure en brosse interviennent dans le processus final de la digestion, en complétant l'hydrolyse commencée par les enzymes gastriques et pancréatiques. Parmi ces enzymes citons la lactase, la maltase, les aminopeptidases A et N, la phsosphatase alcaline, etc (cours de L. Montagne [6]).

Absorption

L'absorption est le passage des nutriments à travers la paroi intestinale et les cellules absorbantes. (P. Meunier [5]). L'absorption dans l'intestin grêle se fait selon deux mécanismes : (i) la diffusion passive et le transport facilité (par un transporteur membranaire) selon un gradient de concentration, (ii) le transport actif permet l'absorption contre un gradient chimique ou électrique, ce processus nécessite la consommation d'énergie. Dans le cadre de ce travail nous nous intéressons à la diffusion passive et au transport actif. Cette étude nécessitera l'intégration des propriétés du système à l'échelle microscopique dans le modèle.

Transport

Le mouvement de l'intestin grêle a pour objectif de mélanger son contenu ainsi que de le propulser. En période inter-digestive, ce mouvement se propage le long de l'intestin grêle selon un cycle régulier. Ce phénomène est appelé le *complexe moteur migrant* (CMM) et son rôle est de vider l'intestin grêle des résidus alimentaires et d'éviter sa colonisation par des bactéries coliques. Chez toutes les espèces la durée de la propagation de CMM est de 90 à 120 minutes, ce qui veut dire une propagation plus rapide chez les espèces avec un intestin plus long. En période digestive le CMM s'interrompt et c'est une activité contractile continue et irrégulière, un mélange de contractions segmentaires et péristaltiques, qui prend sa place et permet le brassage des aliments et leur propulsion aborale.

Dans le cadre de ce travail, nous modéliserons la propagation des ondes péristaltiques et leur influence sur l'avancement du bol alimentaire. Ces ondes sont générées à l'entrée de l'intestin grêle avec une période de l'ordre de la seconde. Leur intégration dans le modèle de digestion implique une étude à deux échelles du temps :

- Échelle de la génération des ondes péristaltiques ($12\,sec$)
- Échelle de la durée de la digestion intestinale (4 à $5\,h$).

2 Méthodes mathématiques

Nous présentons ici des méthodes utilisées pour modéliser la digestion. Ces méthodes sont basées sur deux approches souvent utilisées pour étudier des modèles en physique ou en chimie :

- l'approche eulérienne : en adoptant cette approche, l'observateur est dans une posi-

tion fixe et observe l'évolution du bol alimentaire. Dans la Section 2.1, un modèle de la digestion basé sur les équations aux dérivées partielles (EDP) est présenté. Ce modèle est un exemple d'approche eulérienne en modélisation. Nous étudions ensuite des avantages et des inconvénients de cette méthode pour modéliser la digestion.

- l'approche lagrangienne : en adoptant cette approche, l'observateur se déplace avec le même mouvement que les bols alimentaires. C'est l'approche que nous avons adapté dans cette thèse pour modéliser la digestion.

2.1 Équations de transport-dégradation-absorption

Un premier modèle basé sur des équations aux dérivées partielles a été construit par l'équipe MODINGRE [2]. Les équations de type transport-dégradation- absorption ont été utilisées.

Dans ce modèle, l'intestin grêle est représenté par l'intervalle $]0, L[$ et un flux de nutriments est injecté en $x = 0$ qui représente le pylore. Les notions suivantes sont utilisées afin de représenter le contenu de l'intestin grêle :

(a) $x \in]0, L[$ représente la position dans l'intestin grêle.

(b) $A(x, t)$ est la concentration des aliments à l'instant t et à la position x.

(c) Ces nutriments sont digérés grâce à une enzyme de concentration $e(x, t)$.

(d) $B(x, t)$ est la concentration en aliments digérés, donc assimilables par l'organisme.

La réaction de dégradation de A en B le long de l'intestin grêle est catalysée par l'enzyme e, ce phénomène est représenté par une réaction du type ($A + e \mapsto B + e$). L'efficacité de ces enzymes dépend du *pH* de l'intestin grêle à la position x.

Le mélange des aliments ($A + B$) et les enzymes (e) sont transportés à la vitesse c qui peut dépendre de x et t :

$$\frac{\partial e}{\partial t} = -c\frac{\partial e}{\partial x} - \bar{k}e \ , \tag{1}$$

le premier terme du membre de droite, décrit le transport par la vitesse c et le deuxième explique la décroissance exponentielle des enzymes par un taux de dégradation $\bar{k}$.

Les aliments sont transportés par une vitesse c et sont dégradés par les enzymes

$$\frac{\partial A}{\partial t} = -c\frac{\partial A}{\partial x} - k(pH(x))Ae \ , \tag{2}$$

2. Équipe qui regroupe des chercheurs de l'INRA et du Laboratoire de Mathématiques et Physique Théorique (LMPT).

le premier terme explique l'avancement de la matière A avec une vitesse c, le deuxième terme décrit la dégradation de A qui est proportionnelle à A (*loi d'action de masse*) et à la quantité d'enzymes e avec une efficacité qui dépend du pH de l'intestin grêle en position x.

L'évolution de la matière absorbable (par la paroi intestinale) est décrite par

$$\frac{\partial B}{\partial t} = -c\frac{\partial B}{\partial x} + k(pH(x))Ae - \tilde{k}B \,, \tag{3}$$

comme précédemment le premier terme représente le transport, le deuxième terme représente la production de B par A et le dernier terme l'absorption de B par la paroi intestinale au taux $\tilde{k}$.

Les condition initiales sont $A(x,0) = B(x,0) = e(x,0) = 0$. Les conditions aux limites en $x = 0$ sont

- $A(0,t) = \phi(t)$ est une fonction périodique (ex. une indicatrice ou une fonction constante par morceau valant 0 et 1) modélisant la vidange gastrique.
- $B(0,t) = 0$ est la quantité de matière dégradée à la sortie de l'estomac. En effet, la dégradation au niveau de l'estomac est considérée comme négligeable.
- $e(0,t) = \bar{e}\phi(t)$, par cette hypothèse, nous supposons que les enzymes sont injectés avec A dans l'intestin grêle, et de plus leur quantité est proportionnelle à celle de A.

Comme le système qui représente la digestion est basé sur les équations du transport avec un terme de réaction-absorption, il est classique d'utiliser la **méthode des caractéristiques** pour calculer sa solution théorique. Nous présentons ici l'utilisation de cette méthode pour calculer la solution théorique à travers un exemple. Nous comparons ensuite cette solution avec la solution numérique obtenue par des méthodes numériques.

Courbes caractéristiques

Pour $\bar{k} = 0$ et c constante dans l'équation (2), nous avons

$$\frac{\partial A}{\partial t} + c\frac{\partial A}{\partial x} = -ke_0 A \,. \tag{4}$$

Nous introduisons

$$a(t) = A(x(t), t) \,,$$

ce qui implique

$$\frac{da(t)}{dt} = \frac{\partial A(x(t),t)}{\partial t} + \dot{x}(t)\frac{\partial A(x(t),t)}{\partial x} = -ke_0 A(x(t),t) = -ke_0 a(t) \,, \tag{5}$$

donc par identification, nous avons

$$\dot{x}(t) = c\,. \tag{6}$$

Les solutions de cette équation différentielle sont les courbes caractéristiques associées à l'équation (4). Pour ces courbes la solution A de l'équation (4) est déterminée par l'équation différentielle ordinaire (EDO) (5).

De la même manière, la solution B de l'équation (3) et la solution e de l'équation (1) peuvent être déterminées par une EDO. En conclusion, nous obtenons un système d'EDO (à résoudre, suivant les cas, explicitement ou numériquement) qui permet de calculer la solution du système d'EDP.

Nous avons aussi utilisé la méthode des différences finies afin de calculer la solution numérique de l'équation (4). La Figure 3 montre la différence entre la solution théorique de l'Équation (4) et sa solution calculée par des méthodes numériques [3]. Dans la première courbe (Figure 3.a), avec le pas de l'espace $\Delta x = 5cm$ et le pas du temps $\Delta t = 4s$, la différence entre les deux solutions théorique et numérique est plus que décevante. Les pas du temps et de l'espace ont été affinés ($\Delta x = .25cm$ et $\Delta t = 1s$) afin d'améliorer le résultat, mais la différence entre les deux solutions théorique et numérique, affichée dans le Figure 3.b, n'est toujours pas acceptable.

Cet exemple met en évidence des difficultés de l'approche eulérienne pour modéliser la digestion. Nous avons constaté que la différence entre la solution obtenue par la méthode des différences finies et la solution théorique n'est pas acceptable. Ce problème est lié au fait que d'une part, l'équation du transport est connue pour être intrinsèquement délicate à résoudre et d'autre part, les échelles multiples à prendre en compte aggravent la situation.

Le développement d'un modèle edp ne semble donc pas être une approche adéquate pour modéliser la digestion. Nous avons donc décidé de changer l'approche et d'adopter une approche lagrangienne qui est inspirée par la méthode des caractéristiques. Dans la nouvelle approche, un modèle basé sur des équations différentielles couplées (l'analogue des équations de la méthode des caractéristiques couplées avec celles de la dégradation et de l'absorption) a été mis au point. Ce modèle a permis dans un premier temps, de prendre en compte un aspect plus sophistiqué de la digestion comme l'effet des ondes péristaltiques ainsi que la dégradation par des différents types d'enzymes.

3. Illustrations par Isaline Aubert, Stagiaire du magistère de l'ENS de Cachan

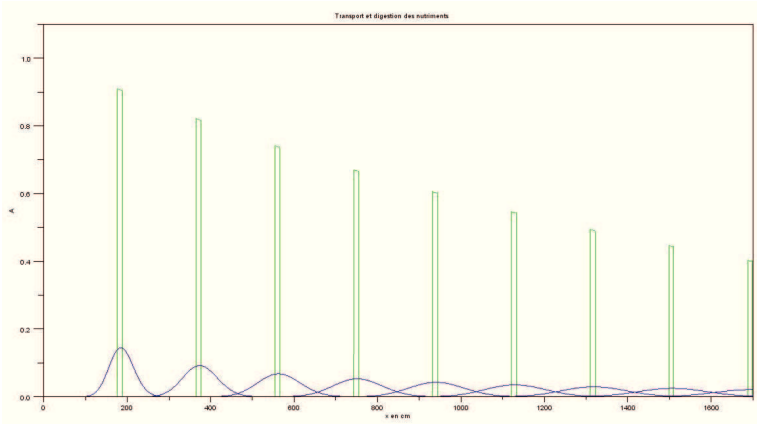

(a) $\Delta x = 5cm$, $\Delta t = 4s$

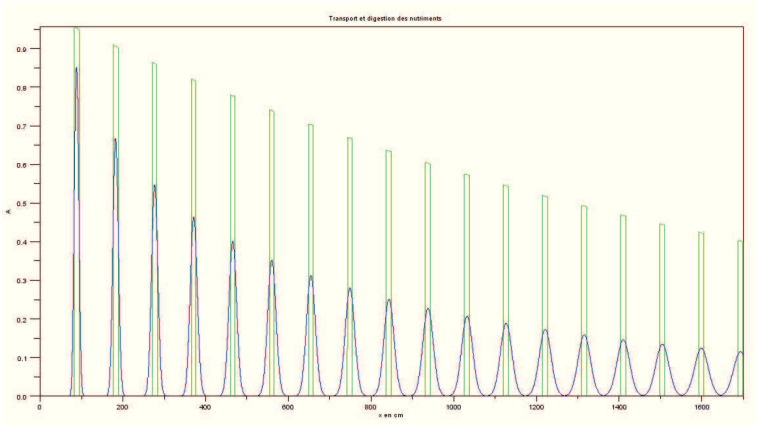

(b) $\Delta x = 0.25cm$, $\Delta t = 1s$

FIGURE 3: La différence entre la solution théorique en verte et la solution numérique en bleu. L'axe des abscisses représente la longueur de l'intestin grêle et l'axe des ordonnées la concentration de la matière. Les quantités Δt et Δx représentent le pas du temps et de l'espace dans le schéma numérique.

2.2 Système d'équations différentielles ordinaires couplées

Dans cette approche, les aliments dans la lumière intestinale forment des paquets que nous appelons *bolus* (ici des cylindres de rayon $R(t)$, de longueur ℓ et de centre $x(t)$) qui ont des évolutions indépendantes les uns par rapport aux autres. Les inconnues sont la position $x(t)$, le rayon $R(t)$ et la quantité d'enzymes $e(t)$. Ici, nous étudions l'évolution d'un seul bolus dans la lumière intestinale.

Dans ce premier modèle, la digestion se fait *via* la surface de contact, en plus nous supposons que la vitesse de disparition de A est proportionnelle à la surface du cylindre

et à l'activité enzymatique :

$$\frac{dA}{dt}(t) = -k(pH(x(t)), e(t)).2\pi R(t)\ell A(t)\,,$$

où e est la concentration en enzyme au point $x(t)$ qui suit toujours la loi $\frac{de}{dt}(t) = -\bar{k}e(t)$. Bien évidemment, il y a la création de nutriments assimilables $B(t)$ qui sont absorbés par la paroi avec un taux $\tilde{k}$:

$$\frac{dB}{dt}(t) = k(pH(x(t)), e(t)).2\pi R(t)\ell A(t) - \tilde{k}B(t)\ .$$

Le transport du bol alimentaire est assuré par des ondes péristaltiques qui sont générées périodiquement. La Figure 4 montre un exemple d'ondes générées toutes les minutes,

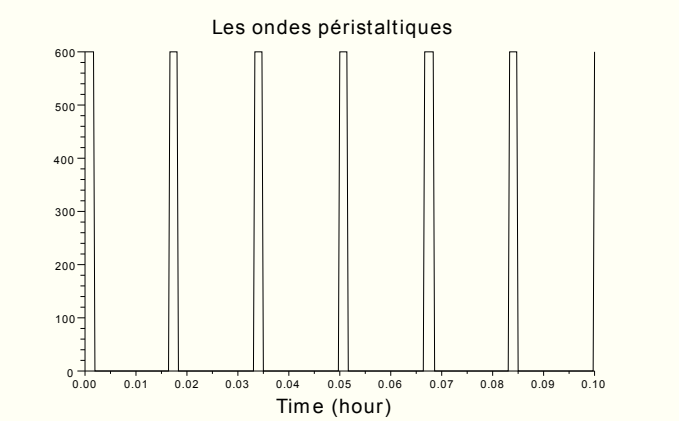

FIGURE 4: Représentation des ondes péristaltiques générées à $x = 0$ par une fonction périodique $W(t)$.

L'efficacité de ces ondes est proportionnelle à la taille du bolus

$$\frac{dx}{dt}(t) \ \propto\ (A+B)(t)$$

pour $(A+B)(t) = \pi R^2(t)\ell\rho$, où ρ représente la masse volumique du bolus. D'autre part, l'efficacité du transport décroît avec la distance

$$\frac{dx}{dt} \ \propto\ \frac{1}{x}.$$

Enfin, la vitesse est atténuée par un terme constante K de viscosité. L'équation suivante modélise alors l'avancement du bol alimentaire le long de l'intestin grêle :

$$\frac{dv}{dt}(t) = \frac{c_0 + c_1(A+B)(t)/\rho}{a + bx(t)}(1 - v(t)/c)W(1 - x(t)/c) - Kv(t)\ .$$

la fonction $v(t) = \dfrac{dx}{dt}(t)$ représente la vitesse d'avancement du bol alimentaire. La vitesse moyenne des ondes péristaltiques est représentée par c.

Ce modèle, basé sur une approche lagrangienne, nous permet de calculer la solution numérique avec moins d'erreurs et d'autre part de prendre en compte conjointement la complexité du bolus et celle du milieu intestinal.

Nous avons donc retenu et développé ce modèle pour obtenir un modèle plus réaliste qui permet de tenir compte des phénomènes qui jouent un rôle important dans la digestion intestinale (viscosité du bol alimentaire, interactions entre les différentes composantes du bol, effet de l'eau sur la digestion, etc). Le modèle initial ne prend pas en compte la présence des villosités intestinales ainsi que les absorptions active et passive. Cependant, au Chapitre II, nous démontrons que les propriétés à l'échelle microscopique peuvent être moyennées et insérées dans un modèle de digestion à l'échelle macroscopique.

Ce travail est organisé de la manière suivante :

Chapitre I Les trois étapes clés qui guident la première partie de ce travail sont : le transport du bol alimentaire par les ondes péristaltiques, la dégradation des aliments par de nombreuses réactions biochimiques et l'absorption des nutriments via des processus actifs ou passifs au sein de la paroi intestinale

Dans le premier chapitre, une succession de modèles génériques de la digestion dans l'intestin grêle a été construit. Le bol alimentaire est assimilé à un cylindre homogène avec une longueur fixe ℓ et rayon variable $R(t)$. Il se déplace dans la lumière intestinale à l'aide des ondes péristaltiques. La dégradation des aliments est le résultat de l'hydrolyse enzymatique par des transformations volumiques et surfaciques. Ces phénomènes sont présentés par un système d'équations différentielles ordinaires couplées qui se résout par les méthodes classiques d'intégration numérique de Runge-Kutta.

Nous détaillons les différentes étapes de la modélisation de la digestion sous forme de quatre modèles, chaque modèle étant une version "améliorée" du précédent. Ainsi, chaque nouveau modèle contient plus de phénomènes biologiques que le précèdent. Le Tableau 1 représente les hypothèses de trois premiers modèles. Le modèle 4 est une simplification du modèle 3 par des méthodes mathématiques d'homogénéisation. Nous démontrons mathématiquement que l'accélération due aux ondes péristaltiques peut être moyennée de façon à obtenir une variation plus lente de la vitesse.

Chapitre II L'une des difficultés de l'étude de la digestion dans l'intestin grêle vient du fait que l'environnement du système est complexe. Ainsi la paroi intestinale joue un rôle clé dans le transfert des nutriments dans le sang et dans la dégradation du bolus tout autant que dans le transit du bol alimentaire par les ondes péristaltiques. Afin de prendre en compte cette complexité tout en la réduisant partiellement, la seconde partie de ce travail

Modèles	Composition (forme de matière)	Enzymes	Réactions enzymatiques
Modèle 1	Solubilisé A_s Absorbable B_{abs}	Gastriques	$A_s \to B_{abs}$
Modèle 2	Solubilisé A_s Intermédiaire B_{int} Absorbable B_{abs}	Gastriques Pancréatiques Brush-border	$A_s \to B_{int}$ $A_s \to B_{abs}$ $B_{int} \to B_{abs}$
Modèle 3	Non dégradable A_{nd} Non solubilisé A_{ns} Solubilisé A_s Intermédiaire B_{int} Absorbable B_{abs} Eau W	Gastriques Pancréatiques Brush-border	$A_s \leftrightarrow A_{ns}$ $A_s \to B_{int}$ $A_s \to B_{abs}$ $B_{int} \to B_{abs}$

TABLE 1: La composition du bol alimentaire, les enzymes inclus et les réactions enzymatiques au sein du bol alimentaire dans les différents modèles présentés dans le Chapitre I.

consiste à utiliser une méthode d'homogénéisation pour simplifier le modèle du transport initial et à analyser et justifier le choix du taux d'absorption par la paroi intestinale.

D'abord, le transport des bolus à l'intérieur de l'intestin grêle est induit par des impulsions à haute fréquence. Ces impulsions entraînent une variation rapide de la vitesse du bolus dans l'intestin grêle. Nous démontrons mathématiquement que les impulsions peuvent être moyennées d'une manière appropriée. Par conséquent, la vitesse à variation rapide dans le modèle peut être remplacée par cette nouvelle vitesse moyennée.

Ensuite, afin de prendre en compte l'influence des villosités intestinale sur la digestion à l'échelle macroscopique (intestin grêle), nous définissons un taux effectif moyen d'absorption à l'aide des méthodes mathématiques d'homogénéisation.

L'homogénéisation est une méthode rigoureuse pour démontrer des propriétés de moyennisation. En d'autres termes, en prenant en compte le comportement du système à l'échelle microscopique, l'homogénéisation permet de décrire son comportement à l'échelle macroscopique. Dans l'étude de la digestion, au lieu d'étudier un seul problème à l'échelle microscopique de taille $\epsilon \ll 1$, nous étudions une suite de problèmes pour ϵ qui tend vers zéro. La question est donc de trouver la limite de cette suite des problèmes (G. Allaire [7]).

Dans ce but, nous supposons que les villosités intestinales sont distribuées périodiquement avec la période $\epsilon \ll 1$ le long de l'intestin grêle, une équation aux dérivées partielles tri-dimensionnelle de diffusion-transport-réaction pour modélise la digestion dans ses différentes échelles. Les conditions aux limites de type Neumann représentent le taux d'absorption à travers la paroi de l'intestin grêle.

Notre méthode consiste à un passage à la limite de ce modèle tri-dimensionnel pour obtenir une équation de transport uni-dimensionnelle avec un taux d'absorption moyen. Ce taux d'absorption tiendra compte de l'influence des villosités intestinales sur l'absorption. En effet, nous démontrons qu'un modèle complexe tri-dimensionnel peut être simplifié à un modèle uni-dimensionnel sans perdre des propriétés importantes du système.

Chapitre III Le passage d'un bolus homogène à un mélange de nutriments en interaction au sein du bol alimentaire est une étape importante à intégrer dans notre modèle. Afin d'étudier l'influence des propriétés physicochimiques de l'aliment sur la digestion, la présence des fibres alimentaires dans la composition du bolus a été prise en compte.

Les objectifs sont de modéliser l'impact de l'enrichissement de l'aliment en fibres sur, d'une part, la digestibilité des nutriments et d'autre part, la vitesse de transit du bolus. Le modèle tient compte de deux catégories principales des fibres, solubles et non solubles. Les résultats des expériences numériques en présence des différents pourcentages des fibres apparaissent cohérents avec les études bibliographiques. Ces dernières ne précisent pas la raison des effets observés mais proposent des hypothèses que nous avons mises en œuvre dans le modèle.

Enfin, une dernière partie de la thèse abordera quelques éléments de la discussion et les principales perspectives de ce travail.

Chapitre I

Mathematical Modeling of Transport and Degradation of Feedstuffs in the Small Intestine

We describe a mathematical model of digestion in the small intestine. The main interest of our work is to consider simultaneously the different aspects of digestion i.e. transport of the bolus all along the intestine, feedstuffs degradation according to the enzymes and local physical conditions, and nutrients absorption. A system of coupled ordinary differential equations is used to model these phenomena. The major unknowns of this system are the position of the bolus and its composition. This system of equations is solved numerically. We present several numerical computations for the degradation, absorption and transport of the bolus with acceptable accuracy regarding the overall behavior of the model and also when challenged versus experimental data. The main feature and interest of this model are its genericity. Even if we are at an early stage of development, our approach can be adapted to deal with contrasted feedstuffs in non-ruminant animal to predict the composition and velocity of bolus in the small intestine [1].

1. Ce chapitre a fait l'objet d'une publication au journal of Theoretical Biology [8] :
Mathematical modeling of transport and degradation of feedstuffs in the small intestine
Masoomeh Taghipoor, Philippe Lescoat, Jean-René Licois, Christine Georgelin, Guy Barles
Received 15 April 2011. Revised 3 October 2011. Accepted 18 October 2011. Available online 10 November 2011.

1 Introduction

The main step of digestion and absorption along the gastrointestinal tract takes place in the small intestine for non ruminant animals. To reach an optimized composition of available nutrients due to their behavior in the digestive system, it is necessary to understand and predict the digestion and absorption of the ingested feedstuffs in the small intestine [9, 10, 11]. It is also now well-known that the use of implanted experimental devices may modify the dynamic of digestion in the small intestine [12, 13].

Several models have been developed representing the digestion and transport of bolus in the small intestine. In the model of [14] digestion and absorption are integrated and represented considering only the polymers and individual absorbable end products. The transit through the small intestine is modeled mainly as a result of gastric emptying. No peristaltic wave is taken into account, and the bolus contained only the dry matter. [15] describe the digestion and absorption using the plug flow reactors to encapsulate complex digestion phenomena in a simple set of equations. Different rate of absorption and degradation are involved : first order kinetics, Michaelis-Menten and the sigmoid ones. A detailed model of the intestinal propulsion is provided by [16, 17]. However, these models portray the transport of bolus simplistically, or they represent only a limited number of different processes involved in digestion.

This article tries to go further in the modeling of digestion in the small intestine by considering the different steps of digestion i.e. the transport of the bolus all along the intestine, feedstuffs degradation according to the enzymes and local physical conditions, and nutrient absorption. Therefore a system of coupled ordinary differential equations is used. The major unknowns of this system are the position of the bolus and its composition.

In fact, several models are presented reflecting the modeling process at its different stages with our attempts to make it more realistic by inclusion of more sophisticated and relevant biological phenomena and chemical transformations. We decided to describe the different steps with the assumptions leading us to our choices instead of presenting only the last model since the whole process by itself may help to underline relevant questions to be further discussed. Of course, this modeling process is an iterative one and is still going ahead in directions which are described in Section 6.

Our models intend to be a mechanistic approach of feedstuffs digestion even though simplifications were included according to participatory approaches between biologists and mathematicians. However they involve a lot of different unknowns and parameters, and require a numerical software to obtain suitable approximation of the solutions since it is hopeless to obtain explicit ones. Scilab software was used to perform these numerical computations [2] .

2. The reader can perform its own numerical experiments, with the possibility of changing the parame-

In all our models, we try to estimate the parameters using data from scientific literature. When these data are not available, we assume the reasonable values for the parameters.

The article is organized as follows : Section 2 is devoted to present the main assumptions of our models and most of our notations. In Section 3, we describe the transport equations. In our four different models, we point out that there are only two different ways of modeling the transport of the bolus in the intestinal tract. The main differences concern the degradation itself, with several possibilities for the composition of the bolus, for the enzymatic reactions and the water influence. The outcoming stages (4 different models) are presented in Section 4, with the key assumptions and characteristics of each model. Section 5 is a comparison of these four models and of the numerical results of the most sophisticated model (Model 3) versus some experimental data from the literature. Finally, in Section 6, we criticize our models and describe the perspective.

2 General Hypothesis and Synthetic Presentation of the Different Models

Common assumptions to all models are the following ones.

(i) The first simplification concerns the small intestine representation itself. Instead of taking into account its complex geometry, it is represented as a one-dimensional interval $[0, L]$. The position of the bolus in the small intestine at time t is given by $x(t) \in [0, L]$ (cf. Figure I.1). The equation of the transport of bolus along the small intestine is described on $x(t)$.

(ii) The bolus is treated as a homogeneous cylinder with a fixed length ℓ and variable radius $R(t)$ which is a function of time t. To locate this cylinder, we use the position $x(t)$ of its center. This assumption is justified by the general shape of the small intestine's segments as well as the observation of the real bolus in animals' small intestines. As the length of bolus is assumed fixed, the degradation only changes the radius. Degradation of substrates is obtained by enzymatic reactions with possible subsequent absorption by the intestinal wall [5].

(iii) The enzymes which participate in enzymatic hydrolysis included in our models consist systematically in pancreatic and brush-border ones with the possibility of including exogenous and gastric ones. The enzymes' activity depends on the *pH* of the small intestine at each point along its length. The brush-border enzymes on the intestinal wall are assumed to be always in excess [5].

The bolus moves through the intestinal tract because of the pulses resulting from peristaltic waves and gastric emptying which gives an initial velocity to the bolus [5]. Peristalsis are series of wavelike contractions occurring in the smooth muscle layer of the

ters, using our Scilab software online at the URL : http://www.lmpt.univ-tours.fr/modingre

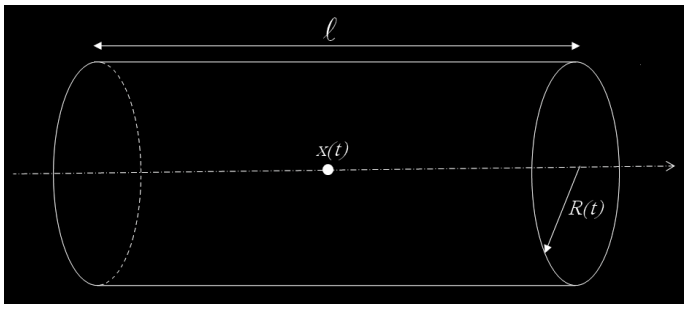

FIGURE I.1: The cylindric bolus with its different characteristics

gastrointestinal tract. It is a physiological process that results in intestinal motility and propulsion of ingested food along the intestine. It starts as a ring-like constriction initially which later moves mostly forward along the intestine. Moreover it might be assumed that it helps the bolus to be digested by spreading the food particles along the intestinal wall for effective digestion and absorption. Therefore to model the transport, bolus movement is connected to pulses all along the intestine with the initial velocity coming from the gastric emptying effect. Efficiency of pulses is proportional to the volume of the bolus and it is inversely correlated to the distance between the bolus and the pylorus [18, 19]. The bolus speed is assumed to be slowed down by the local conditions in the small intestine lumen (friction on the borders, viscosity effects, etc). The effects of these different local factors depends on the composition of the bolus, and in particular its dilution.

For the bolus content, the following assumptions and notations are used throughout this paper

- The bolus includes a single species whose total mass is denoted by A. In the most sophisticated model presented in this work, A is composed of A_s, A_{ns} and A_{nd}, in other words $A = A_s + A_{ns} + A_{nd}$. A_s is the mass of solubilized fraction of A which can be hydrolyzed in the presence of the enzymes. The index s stands for "solubilized". A_{ns} is the mass of "non-solubilized" fraction of A, for example dry starch or the non-emulsified lipids. Transformation of A_{ns} into A_s requires a sufficient quantity of water. Regarding lipids emulsion, we assume that the bile salts are in excess. The mechanism $A_{ns} \leftrightarrow A_s$ is described through an equilibrium property depending on the water quantity in the bolus. Finally A_{nd} is the mass of non-degradable A, which enters and leaves the small intestine without any change. For example the vegetal fiber in feed are poorly digestible. Moreover the fiber matrix of feedstuffs or the anti-nutritional factor content can be responsible for a reduction in the

digestibility of some amino acids in some feedstuffs [20].

- The quantity B is the mass of product obtained from A_s by enzymatic reactions, it is composed of B_{int} and B_{abs}

$$A_s\big(\overset{enzymes}{\longrightarrow} B_{int}\big)\overset{enzymes}{\longrightarrow} B_{abs}.$$

  The quantity B_{int} is the product of hydrolysis due to gastric and pancreatic enzymes, the index int stands for "intermediate" substrate which is not yet absorbable since it is not fully degraded. This transformation has to be completed by a second one at the border of the small intestine via the brush-border enzymes (e.g. : proteins being degraded to polypeptides and afterwards to dipeptide or amino acids, which are absorbable). This second transformation is also able to give B_{abs} directly from A. The quantity B_{abs} is the absorbable fraction with index abs indicating "absorbable".
- The quantity e represents the gastric and pancreatic enzymes.
- The quantity W is the mass of water in the bolus and $[W]$ indicates the proportion of water in the bolus : $W/(A+B+W)$.
- The quantity $V(t)$ denotes the volume of bolus which is equal to $(A+B+W)/\rho$, where ρ denotes the density. For the sake of simplicity, we assume that all the substrates of bolus have the same density ρ. The total mass of the bolus is $(A+B+W)(t)$ at each moment.

Digestion consists in the transformation of digesta to absorbable nutrients through enzymatic hydrolysis. Volumic transformation is the degradation of A_s into B_{int} inside the bolus and transformation on the bolus surface is the degradation of both A_s and B_{int} into B_{abs} on a thin layer around the bolus. The following hypothesis are added progressively with upgraded versions of the model.

Model 1. In the first model, the whole bolus is considered to be solubilized ($A = A_s$). A is hydrolyzed thanks to gastric enzymes and becomes directly absorbable nutrients ($B = B_{abs}$). In this model, brush-border or pancreatic ones are not taken into account. Such mechanisms are associated for example with the consumption of disaccharides (resp. monosaccharides) such as milk sugar(resp. glucose).

Model 2. This model is an attempt to have a more realistic modeling of degradation. The bolus is still assumed to be completely solubilized. The absorbable nutrients can be obtained by two ways : either by a direct surfacic transformation $A \to B_{abs}$ or through a first volumic degradation $A \to B_{in}$ followed by a second one $B_{int} \to B_{abs}$ at the bolus surface by brush-border enzymes.

Model 3. This model includes the solubilization of the bolus in presence of water. A is splitted into A_s, A_{ns} , A_{nd} . Equations are added to express the equilibrium $A_s \leftrightarrow A_{ns}$ which depends on the quantity of water. The non-degradable part of bolus enters and leaves the small intestine without any mechanical or chemical change in its initial form. A key feature of this model concerns the transport of bolus along the small intestine since it is connected to the quantity of water through lubrification effects.

Model 4. This model is a simplification of the previous one by mathematical arguments. Through homogenization methods it is shown that the acceleration can be averaged and an equation with this averaged acceleration is substituted for the pulses in transport equation. Detailed models are described in Section 4.

3 Transport

We present a mathematical formulation of the transport of bolus in the small intestine. It is based on the physiology of the pig's small intestine to get consistent parameters. The duodenum is characterized by oscillatory electrical events (slow waves) occurring at a rate of 18/min. After food intake, some of these waves are associated with spikes bursts which are responsible for contractions and therefore propelling the bolus through the small intestine. We assume only 6 of the 18 slow waves by minute are followed by the spikes. It leads to one efficient contraction every 10 seconds [18]. The mean transit time of each peristaltic wave is assumed to be 150 minutes to move along small intestine from duodenum to the end of ileum according to [21] and [22]. We assume also that the pig's small intestine is about 18 meters [23], hence the average velocity c of these waves is $7,2$ m/h. Each peristaltic wave takes $x(t)/c$ seconds to reach the bolus in position $x(t)$, therefore the pulse which pushes the bolus in time t is generated in duodenum at time $t - x(t)/c$.

If $v(t)$ denotes the velocity of the bolus ($v(t) = \dfrac{dx}{dt}(t)$), the effect of pulses is modeled through the following equation

$$\frac{d^2}{dt^2}x(t) = \frac{d}{dt}v(t) = \frac{d}{dt}y\left(t - x(t)/c\right),$$

the term $\dfrac{d}{dt}y$ represents the pulses which are defined as a periodic function of period 10 seconds such that

$$\int_0^{10} \frac{d}{dt}y(t)dt = 1$$

and for $t < 0$, we assume $y^{'}(t) = 0$.

Over a period, each pulse is an approximation of a Dirac mass of the origin. Therefore we define it as a function with the value $1/\epsilon$ during a very short interval of time ϵ and 0 at all other time.

According to [19] and [24] the efficiency of the peristaltic waves increases with the size of the bolus and decreases with the distance from pylorus. We assume that all these

dependences are affine, namely

$$\frac{d^2x}{dt^2}(t) = \frac{d}{dt}\left[y\left(t - x(t)/c\right)\right]\frac{c_0 + c_1 V(t)}{a + bx(t)},$$

where, c_0 and c_1 are determined under the assumption that the acceleration depends linearly on $V(t)$. THe constants a and b are obtained from experimental data.

The intestinal lumen is a confined environment which prevents the bolus to move perfectly according to the previous equation : the bolus has to work its way through the small intestine and is also submitted to the friction with the intestinal wall. All these friction effects are related to the "viscosity" of the bolus and we have two different ways to model the friction term : either as a constant effect which is independent of the bolus composition (models 1 & 2) or with a lubrification effect coming from the proportion of water in the bolus (models 3 & 4). More specifically, in Equation (I.1) below, the coefficient $K(t)$ is either constant in models 1 & 2 or $\tilde{K}/[W]$ in models 3 & 4, where $\tilde{K}$ is a constant.

The final equation of transport is therefore the following one

$$\begin{aligned} \frac{d^2x}{dt^2}(t) &= \frac{d}{dt}[y(t - x(t)/c)]\frac{c_0 + c_1 V(t)}{a + bx(t)} - K(t)\frac{dx}{dt}(t) \\ \frac{dx}{dt}(0) &= v_0, \;\; x(0) = 0 \end{aligned} \tag{I.1}$$

4 Digestion

Digestion is a mechanical and chemical process by which the feedstuffs molecules are broken down to the smaller ones by enzymes in order to to make them available for absorption. The uptake of the obtained nutrients is mainly by absorption. In this section the different steps of modeling are detailed.

4.1 Model 1

In this model the bolus is assumed to be completely solubilized (A=A_s). We also assume that the necessary enzymes for hydrolysis are mixed with the bolus in the stomach. The product of following reaction is directly absorbable ($B = B_{abs}$)

$$A + e \to B.$$

e denotes the gastric enzymes. The first aim of this model is to define the variation of the bolus which means the amount of the different substrates A, B and e at every time in the

cylinder, and the second is to locate the bolus along the small intestine. We assume that, the evolution of A or its volumic transformation depends on its mass at each moment and the enzyme activity. This equation follows the law of mass action

$$\frac{dA}{dt} = -Ck(x,e)A$$

where C denotes the degradation rate and, $k(x,e)$ is the enzyme activity which depends on the pH of the small intestine and the presence of the enzymes at each point along it.

The product B of the volumic transformation of A is absorbed by intestinal wall with a constant rate k_{abs}

$$\frac{dB}{dt} = Ck(x,e)A - k_{abs}B.$$

There are also the degradation and inactivation of the enzymes along the small intestine

$$\frac{de}{dt} = -k_e e$$

where k_e is the rate of degradation of the enzymes which depends on their types. The activity of each enzyme as a function of pH of small intestine is roughly known. We know also the pH of each point along the small intestine. The composition of these two functions gives the enzyme activity at each point x along it.

4.2 Model 2

In this second model, the presence of pancreatic enzymes in the small intestine as well as the brush-border ones on its wall are considered. The pancreatic secretions help neutralizing the stomach acid as they enter the small intestine. They also contain pancreatic enzymes. The level of the secretions is a function of volume and composition of the bolus entered the small intestine. The brush border enzymes are the enzymes for the terminal stage of digestion which is the surfacic hydrolysis. Contrary to the pancreatic enzymes they are not free in the intestinal lumen, but rather, in the plasma membrane of the enterocyte.

We assume that the bolus is completely solubilized. The product of the hydrolysis B consists in B_{int} and B_{abs} ($B = B_{int} + B_{abs}$).

The following scheme represents the chemical reactions of the bolus in this model

$$A_s \to B_{int}, \qquad A_s \to B_{abs}, \qquad B_{int} \to B_{abs}.$$

The first reaction takes place inside the bolus by pancreatic and gastric enzymes, the second and the third ones take place on the surface of the bolus.

The degradation of A in this model is the result of the volumic hydrolysis of A as in Model 1, and its surfacic hydrolysis by brush-border enzymes

$$\begin{aligned}\frac{dA}{dt} &= -Ck(x,e)A - C_{abs}(2\pi R\ell)\frac{A}{A+B_{int}+B_{abs}} \\ &= -Ck(x,e)A - 2C_{abs}\sqrt{\pi l/\rho}\frac{A}{(A+B_{int}+B_{abs})^{1/2}},\end{aligned}$$

the second term represents surfacic transformation of A to B_{abs}. We recall that the mass of the bolus in this model is

$$A(t)+B_{int}(t)+B_{abs}(t)=\rho V(t)=\rho\pi R^2(t)l,$$

and therefore the lateral surface of the cylinder is given by

$$2\pi R\ell = 2\sqrt{\pi l/\rho}(A+B_{int}+B_{abs})^{1/2}\ .$$

This transformation depends on the fraction of A on the surface of the bolus which is written by $(2\pi R\ell)\dfrac{A}{A+B_{int}+B_{abs}}$. The unit of the degradation coefficient per unit of surface and time, C_{abs} , is $g.m^{-2}.s^{-1}$.

After a distance traveled by bolus of about 5% of the total length of the small intestine which is approximatively $85\,cm$ in an growing pigs, the input of secretions starts and it stops after a distance of α meters traveled by bolus. We assume their mass is about $\beta\%$ of the bolus mass. In the following equation, the effect of these secretions on the variation of A is taken into account

$$\frac{dA}{dt} = ... + \ln(1.\beta)\frac{1}{\alpha}\frac{dx}{dt}\chi\left(\left(x(s)-0.85\right)/\alpha\right)A,$$

where χ is a localization function in the above equation which reflects the fact that secretions arrive in the small segment of the intestine, say between 0.85 cm and $0.85+\alpha$ cm.

The product of volumic hydrolysis, B_{int} , participates in the creation of B_{abs} on the surface of the bolus. Therefore its variation is modeled by

$$\begin{aligned}\frac{dB_{int}}{dt} &= Ck(x,e)A + \ln(1.25)\frac{1}{\alpha}\frac{dx}{dt}\chi((x(s)-0.85)/\alpha)B_{int} \\ &\quad -2C_{iabs}\sqrt{\pi l/\rho}\frac{B_{int}}{(A+B_{int}+B_{abs})^{1/2}}.\end{aligned}$$

The absorbable nutrients on the bolus are not absorbed instantaneously [15]. In this model we assume that the absorption rate follows Michaelis-Menten mechanism. The constant k_{abs} is the maximal rate of absorption at saturation, k is the Michaelis constant which is half saturation

$$\frac{dB_{abs}}{dt} = 2\sqrt{\pi l/\rho}\frac{C_{abs}A + C_{iabs}B_{int}}{(A + B_{int} + B_{abs})^{1/2}} - k_{abs}\frac{B_{abs}}{k + B_{abs}}.$$

4.3 Model 3

In this model the ingested food consists in A_{ns}, A_{nd}, A_s and water ($A = A_{ns} + A_{nd} + A_s + W$). We incorporate two effects of water on digestion : the first one is the dilution of the bolus and its impacts on degradation and absorption and the second one is the lubrification and its consequences on the transport.

We assume that the evolution of A_s and A_{ns} aims at reaching an equilibrium in which the ratio between A_s and A_{ns} is fixed and depends only on the proportion of water, namely $A_s = \mu([W])\,A_{ns}$ stressing that solubilization of A_{ns} depends on bolus dilution. From the mathematical standpoint, we write this evolution as

$$\frac{dA_{ns}}{dt} = -k_s\Big(\mu([W])\,A_{ns} - A_s\Big), \tag{I.2}$$

where μ is a linear function of water and the constant k_s represents the return rate to equilibrium.

The amount of water in the intestinal lumen is regulated by several complex biological phenomena. In fact the proportion of water in the bolus aims at reaching $[W_0]$ in a rather fast way which we translate it on a mathematical standpoint

$$\frac{d[W]}{dt} = -k_w([W] - [W_0]) + \ln(1.\beta)\frac{1}{\alpha}\frac{dx}{dt}\chi((x(s) - 0.85)/\alpha)[W] \tag{I.3}$$

where k_w is large enough to reach the equilibrium in an adequate time. The second term of above equation is the fraction of water in pancreatic secretions.

The variation of A_s depends on its degradation by volumic and surfacic hydrolysis, and contribution of pancreatic secretions as in previous models. It also depends on the equilibrium with A_{ns} resulting from equation (I.2) which is the first term of equation below

$$\begin{aligned}\frac{dA_s}{dt} &= k_s\Big(\mu([W])\,A_{ns} - A_s\Big) - Ck(x,e)A_s(t)\\ &\quad - 2C_{abs}\sqrt{\pi l/\rho}\frac{A_s}{(A_s + A_{ns} + A_{nd} + B_{int} + W + B_{abs})^{1/2}}[W]\\ &\quad + \ln(1.25)\frac{1}{\alpha}\frac{dx}{dt}\chi\left((x(s) - 0.85)/\alpha\right)A_s.\end{aligned} \tag{I.4}$$

The variation of absorbable nutrients depends on the creation of B_{abs} by enzymatic hydrolysis of A_s and B_{int} and its absorption by intestinal wall

$$\begin{aligned}\frac{dB_{abs}}{dt} =& 2\sqrt{\pi l/\rho}\frac{C_{abs}A + C_{iabs}B_{int}}{(A_s + A_{ns} + A_{nd} + B_{int} + W + B_{abs})^{1/2}}[W] \\ & - k_{abs}\frac{B_{abs}}{k + B_{abs}}. \end{aligned} \tag{I.5}$$

The non-degradable fraction of A, namely A_{nd}, enters in the small intestine and leaves it without any change in its structure.

As we already indicated in Section 5.1, lubrification of the bolus depends on the presence of water. For this model, the friction coefficient in equation (I.6) is written as

$$K(t) = \frac{\tilde{K}}{[W](t)}.$$

4.4 Model 4

This model is a mathematical simplification of the transport equation by means of homogenization theory. Homogenization theory is concerned with equations with rapidly oscillating coefficients and its aim is to provide an "homogenized" or "averaged" equation which is a limiting equation when the frequency of the oscillations tends to infinity. Advantages of homogenization theory are clear : on most occasions, it is simpler to use homogenized equations (for example to compute the solution) and, when the frequency of oscillations is over a given value, this approximation of the real equation by the homogenized one may be rather accurate as seen in the next section.

Homogenization problems for ODEs were studied by [25] but it is worth pointing out that our particular case does not fall into the theory described in [25]. Fortunately the specific structure of the transport equation allows us to do a complete analysis of the problem and even to compute explicitly the averaged equation.

More specifically, in the transport equation, pulses reach the bolus every 10 seconds approximately. Compared to the time scale of digestion phenomena (the bolus stays in the small intestine for several hours [13, 1]), this represents a very high frequency and causes very rapid variations in the velocity of the bolus (see the velocity profile in Figure I.3).

We can prove mathematically that the pulses can be averaged out in an appropriate way and we can replace the rapidly varying velocity by a slowly one.

In the simplest case, by normalizing the pulses, we assume that their mean effect over a period is $e(\epsilon)$. Thus, over a time $t = N\epsilon$, their mean effect is $Ne(\epsilon) = te(\epsilon)/\epsilon$. On the other hand we assume

$$\lim_{\epsilon \to 0} e(\epsilon)/\epsilon = \tau$$

the mean effect over a time t is therefore

$$\lim_{\epsilon \to 0} Ne(\epsilon) = te(\epsilon)/\epsilon = t\tau.$$

Inserting this equality in transport equation (I.1), the homogenized transport equation reads

$$\begin{aligned} \frac{d^2x}{dt^2}(t) &= \bar{a}(t)\frac{c_0 + c_1 V(t)}{a + bx(t)} - \frac{\tilde{K}}{[W](t)}\frac{dx}{dt}(t) \\ \frac{dx}{dt}(0) &= v_0, \;\; x(0) = 0 \end{aligned}$$

where $\bar{a}$ is the averaged effect of the pulses. Its value is

$$\bar{a}(t) := \tau(1 - \frac{1}{c}\frac{dx}{dt}(t)).$$

5 Results

In the first part of this section, the graph of degradation of model 4, and the graph of transport of model 3 and 4 are developed. The second part concerns the evaluation of the last model by comparing its outputs with experimental data. Only a limited number of outputs can be compared because of the lack of experimental data. However, the model is evaluated in relation to our objective which is developing a mathematical model that takes into account the physiology of the small intestine and process of digestion in it.

5.1 Digestion

The graph of digestion of model 4 is shown in figure I.2. We should at first initiate the bolus composition. These initial conditions vary following the different types of feedstuffs. We fixed the initial value of A_{ns} as three times that of A_s. We dilute A_{ns} by two times its volume water. Solubilized substrate A_s and non-solubilized one A_{ns} reach a dynamic equilibrium all along the small intestine, as explained in Section 4. This balance is reached rapidly at the beginning of the small intestine due to the large difference in quantity between these two substrates. The result of this equilibrium is the increases of the

value of A_s and the decreases of the values of A_{ns}, as seen in the graph of digestion. The inverse process might take place by lack of water. The absorption curve corresponds to the collected absorbable nutrients from $x = 0$ to $x = x(t)$, where x indicates the location of bolus in the small intestine. Obviously, the graph of the fourth model contains more details about different steps of digestion than the first two graphs thanks to the model structures. The digestion graph of model 4 is similar that of model 3. The only change in model 4 deals with the transport equation.

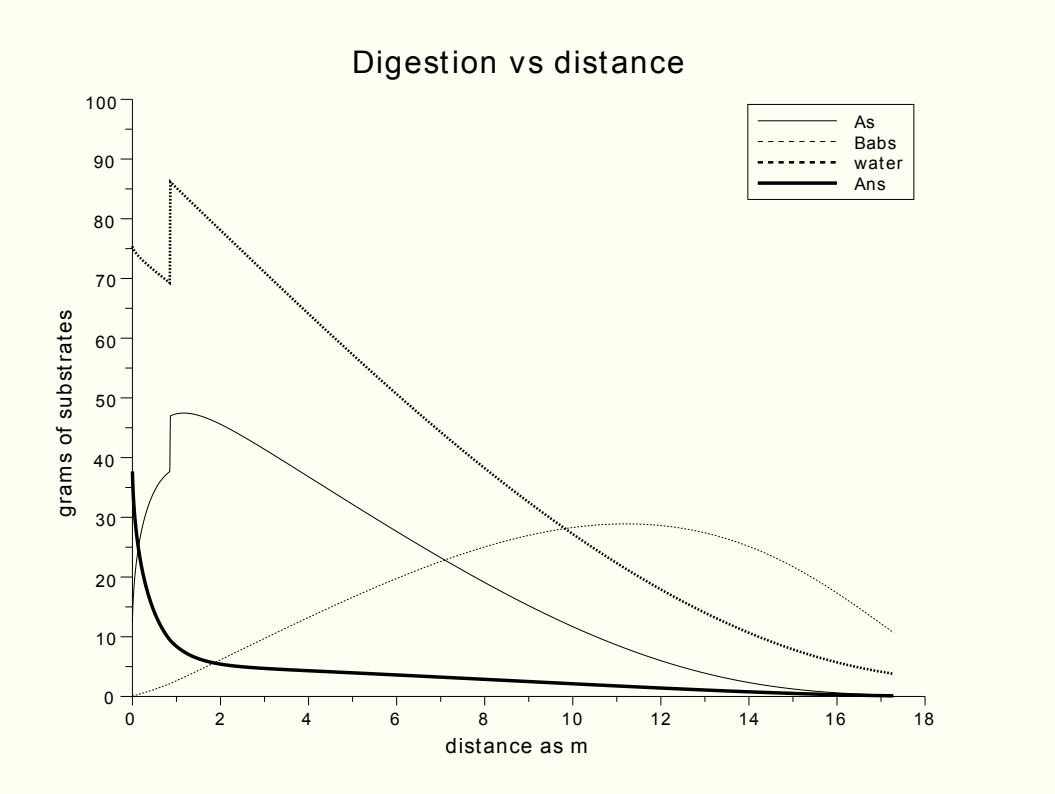

FIGURE I.2: Digestion through Model 4

5.2 Velocity

Figure I.3 provides a numerical evidence of the homogenization phenomena. The graph of transport resulting from models 3 and 4 is shown in figure I.3. The effect of pulses on the curve of velocity is obvious. However, using the homogenization theory in Model 4, we obtain a smooth graph of velocity which replaced that of Model 3.

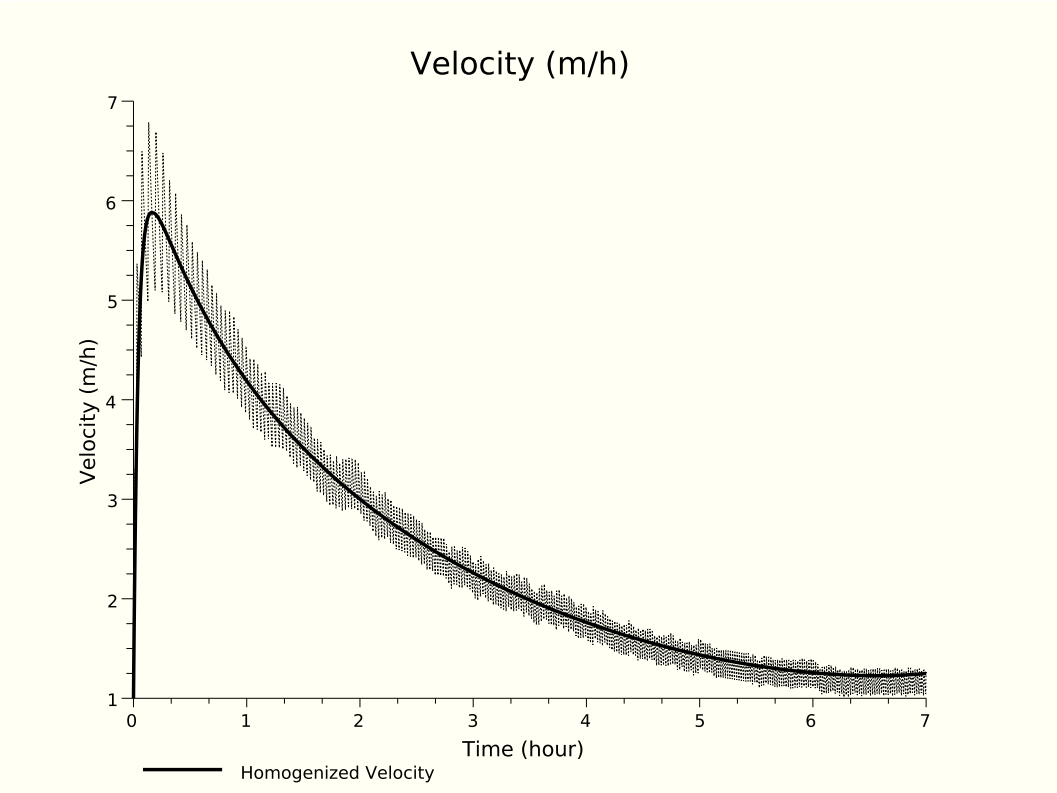

FIGURE I.3: Velocity of the bolus versus Time

5.3 Model evaluation

For a specific family of nutrients, here starch, digestion is calculated using Model 4 and is compared to data reported by [1]. To parameterize adequately the model, we adapt the enzyme activity of the last model to the activity of amylase in the small intestine. Amylase is the enzyme required for degradation of starch. The optimal activity of pancreatic amylase is in neutral pH [5].

Pancreatic secretions have no impact on the variation of A_s since there is no starch from this source.

The inputs of model are only A_{ns} and W which are Starch and Water. The outputs are the values of these substrates at the end of ileum. The data in the article of [1] are for purified protein free wheat starch, agreeing with our hypothesis for the composition of the bolus 1. The outputs concerns the collected data after at the end of ileum.

TABLE I.1: Digestion of starch in pigs by modeling : Comparison between simulated and experimental data by [1]

	Experimentation		Modeling	
	Input(g)	Output(%)	Input(g)	Output(%)
wet digesta	2571	8	113.10	5.33
dry matter	688	0.50(g)	37.70	0.04

Regarding the data presented table I.1, percentages of dry matter and wet digesta collected at the end of the ileum are approximatively the same as the output of model 4. The difference between inputs is due to the simulation calibration which takes into account only one bolus i.e. a fraction of the daily meal. However, differences between outputs are low in percentage enabling to conclude that the model can roughly simulate very simple situations.

5.4 Sensitivity analysis

Sensitivity analysis is performed to identify the key parameters affecting the digestion process. The chosen parameters are set at 5% and 50% of their original values.

Output	Parameters
A_s	C, C_{abs}
B_{abs}	C_{abs}, C_{iabs}, k_{abs}
v	a,b, c_0, c_1, K

Studied digestion parameters are C and C_{abs} for degradation of A_s, and C_{abs}, C_{iabs} and k_{abs} for the absorption of B_{abs}.

If y is the output and θ the parameter, the relative variation of y can be expressed as follows

$$\frac{|y_\theta - y_{\theta+\Delta\theta}|}{y_\theta}.$$

a. Influence on A_s

Both parameters C and C_{abs} are overestimated by 5 and 50%. The figure I.4 shows the relative variation of A_s at each moment. The relative variation of A_s resulting from 5 and 50% values of C is not meaningful. The parameter C_{abs} has the largest effect on A_s degradation. Observing the graph of relative variation of A_s, figure I.4, we conclude that increasing the value of C_{abs} increases the relative variation value with time. .

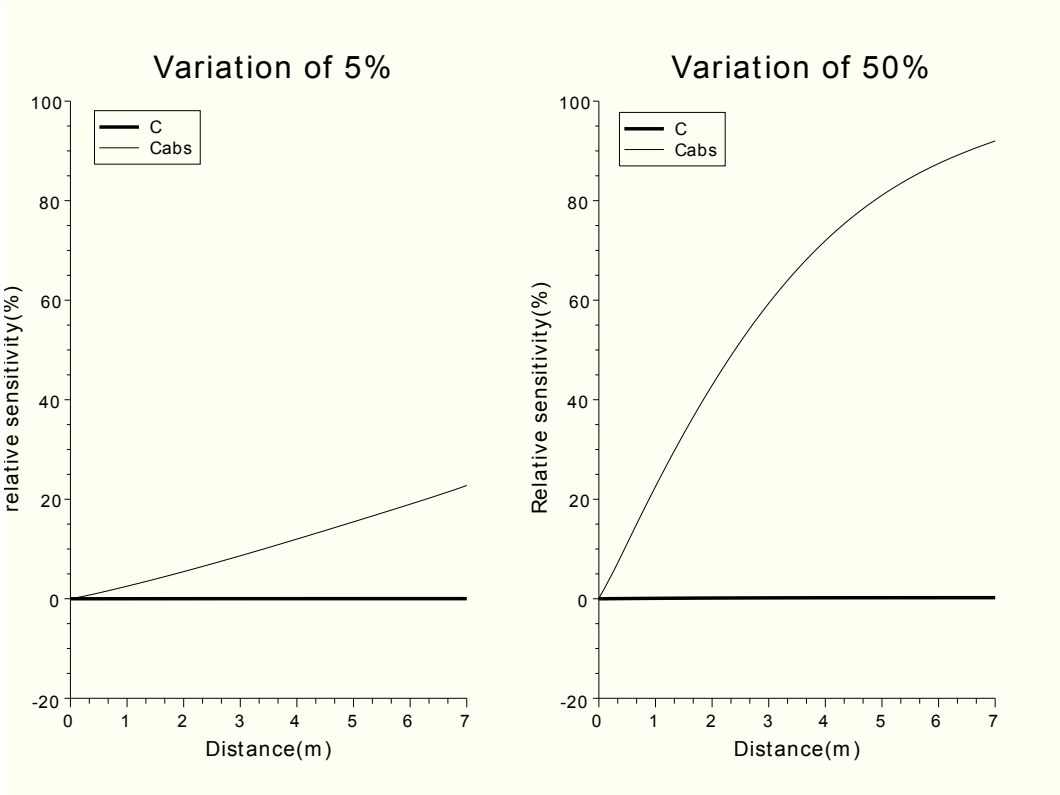

FIGURE I.4: Relative variation of A_s regarding to C, C_{abs}.

b. Influence on B_{abs}

The parameters k_t, C_{abs} and C_{iabs} are overestimated by 5 and 50%. The figure I.5 shows the relative variation of B_{abs} by time. The quantity of B_{int} being very small in the model, the effect of changing the parameter C_{iabs} is neglectible on the relative variation of B_{abs} by time. The quantity B_{abs} is very sensitive to the variation of parameter C_{abs} firstly because of the high quantity of A_s, then its influence decreases because of decreasing quantity of A_s over time. The quantity B_{abs} is dependent on kt because of the large impact of kt on the nutrient absorption rate.

6 Conclusion and Perspectives

This model is obtained from simplified biological assumptions and it can be used to illustrate generically the rate of degradation and absorption all along the small intestine. This is a global model of digestion of a bolus composed of one substrate and water. This section is devoted to a discussion on the current state of our modeling, our assumptions,

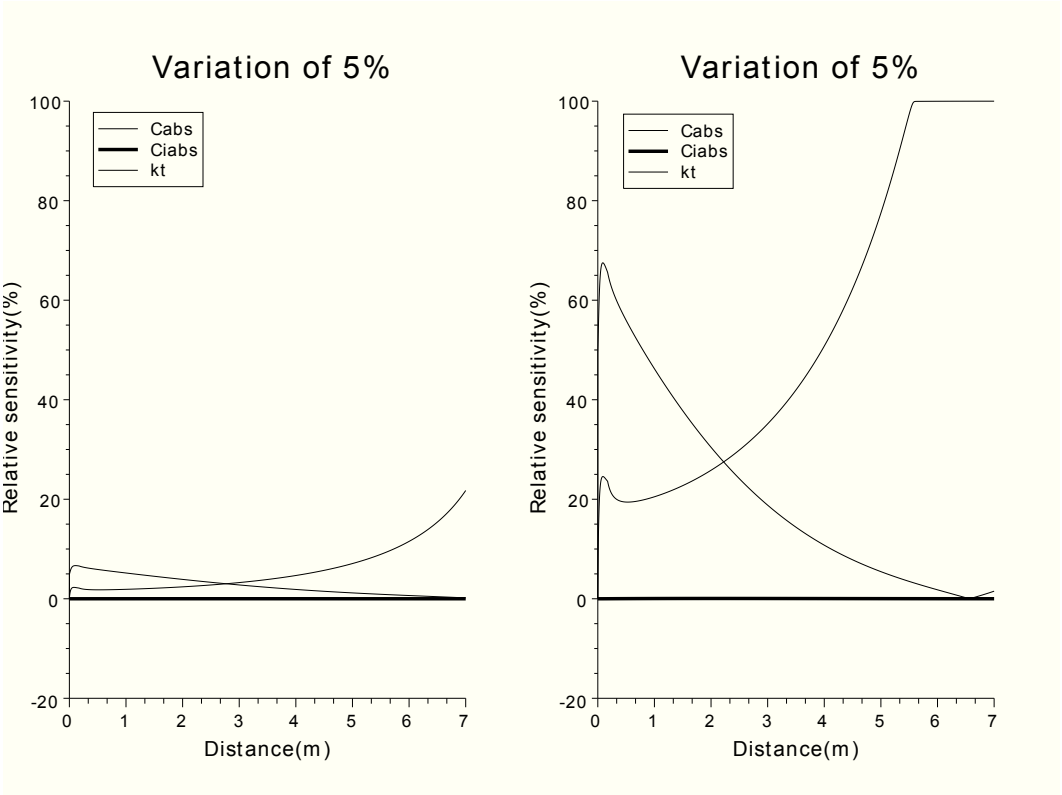

FIGURE I.5: Relative variation of B_{abs} regarding to C_{abs}, C_{iabs} and kt

difficulties and on the future development of the model.

The first assumption to be discussed is the "cylinder" one. As mentioned earlier, it was introduced for technical reasons. Our aim was to solve a partial differential equation with very different scales of times (pulses arising every 10 seconds while whole digestion process in the small intestine lasts for several hours [13, 1]) and with an highly variable domain with contrasted scales (few centimeters for the bolus compared to the 18 meters of the small intestine). Solving this PDE seems unreasonable since it was leading to the usual diffusive phenomena and large errors. We also notice that these 18 meters of the small intestine were rather empty and therefore we were spending a lot of time to compute functions which were very often 0.

From the transport standpoint, the "cylinder" assumption can be seen as a Lagrangian method, the ordinary differential equations on $x(\cdot)$ being (essentially) the *characteristic curves* of the transport equation. This is the first justification of this hypothesis, the second being the direct observation of animals bolus which convinces us that it can be represented as a cylinder, even if its geometrical characteristics could be more complicated. However we have to work more on the evolution of the length of the cylinder.

A more Eulerian "compartmental approach" is studied simultaneously but we are still facing difficulties for modeling the transport and, specifically to reproduce some features of the "cylinder" model.

The transport equation seems to take into account rather closely the phenomena which are described by the experts . It will be difficult to validate the term $\frac{c_0 + c_1 A}{a + bx}$ and to have a precise idea of the value of the different constants but such a modeling seems more appropriate than trying to use a complicated fluid mechanics approach whose laws may not be valid in this very confined domain. The same remarks hold for the effects of the water : it seems correct even if a relevant validation will be difficult.

For food digestion and absorption, we are only at a first stage of modeling. The absorption phenomena were not studied explicitly leading to required further development with a focus on the assumed interactions between the animal physiological status and absorption. The spatial aspects (location of the absorption) were clearly neglected so far.

For digestion, the next step will be to mix different nutrients and adapt the enzyme breakdown to each of them. We have also to examine more closely the respective effects of the different categories of enzymes together with the role of the water. Moreover interactions between nutrients on the digestion processes should be questioned.

As a conclusion of this first stage of modeling, consistent behaviors of the model were reached. Moreover, the simplicity of the current model allows easy developments in any directions. Our next target will therefore be to iterate the model development according to the above proposed research areas.

7 Acknowledgement

The multidisciplinary collaboration on this research project between the INRA Center of Nouzilly and the Laboratoire de Mathématiques et Physique Théorique was initiated within and supported by the CaSciModOT program (CAlcul SCIentifique et MODélisation des universités d'Orléans et de Tours) which is now a Cluster of the french Region Centre. This collaboration also takes place in a CNRS-INRA PEPS program "Compréhension et Modélisation du devenir de l'aliment dans le tube digestif". This work is part of the PhD thesis of Masoomeh Taghipoor, financed by CNRS and INRA.

Chapitre II

Mathematical Homogenization in the Modelling of Digestion in the Small Intestine

Digestion in the small intestine is the result of complex mechanical and biological phenomena which can be modelled at different scales. In a previous article, we introduced a system of ordinary differential equations for describing the transport and degradation-absorption processes during the digestion. The present article sustains this simplified model by showing that it can be seen as a macroscopic version of more realistic models including biological phenomena at lower scales. In other words, our simplified model can be considered as a limit of more realistic ones by averaging-homogenization methods on biological processes representation. [1]

1. Ce chapitre a fait l'objet d'une publication au journal de MathSinAction [26] :
Mathematical Homogenization in the Modelling of Digestion in the Small Intestine,
Masoomeh Taghipoor, Guy Barles, Jean-René Licois, Christine Georgelin, Philippe Lescoat.

1 Introduction

When building a model for digestion in the small intestine, difficulties occur. The first one is the extreme complexity of the mechanical/biological phenomena. Transport of the bolus through the peristaltic waves, feedstuffs degradation by numerous enzymatic reactions and the active/passive absorption of the nutrients by the intestinal wall are known to be the key steps but they are not biologically nor fully understood and neither quantitavely parameterized. Modelling approaches are a way to integrate complex mechanisms representation of these phenomena helping to improve our understanding of them. Since it is almost impossible to build direct experiments for studying the digestion in the small intestine, modelling is a way to test in silico hypotheses that could be challenged through limited in vivo experiments.

A second difficulty relies on the complex environment within the digestive tract. For example, the intestinal wall plays a key role in the transfer of the digested food in the blood and interferes in the degradation of the bolus via the brush-border enzymes and causes the transit of the bolus by transmitting the pulses coming from the peristaltic waves.

Thirdly, digestion in the small intestine has contrasted but relevant macroscopic and microscopic scales, both in space and time. To give few figures, the length of the small intestine in a growing pig reaches 18 meters, which is a large figure compared to its radius (2-3 centimeters) and even more compared to the size of the villi (around 1 millimeter). In the same way, the bolus stays in the small intestine for several hours, while the efficient peristaltic waves which ensure the transport of the bolus, start approximatively every 12 seconds from the pylorus.

Because of these different scales, a model based on partial differential equations and capturing all the interesting phenomena, would be too complicated and impossible to solve numerically. Therefore we have adopted in [8] a model based on ordinary differential equations (ode in short) : each bolus of feedstuffs coming from the stomach is identified as a cylinder and the odes describe the evolution of the position and composition of the cylinder. Since digestion could be described by a transport equation (or a system of such equations) with reacting terms, our strategy was essentially to use the Characteristics of this equation. At least numerically this type of Lagrangian method appears to be more efficient. We refer to [8] for details on our different models since several stages of the modelling process were developped in this paper.

The aim of the present article is to provide mathematical justifications of some assumptions of the modelling presented in [8]. We focus on the bolus transport and on the effects related to absorption and enzymatic breakdown by the brush border enzymes, phenomena which are related to averaging/homogenization type processes.

More precisely, in Section 2, we examine the effects of the pulses generated by the

peristaltic waves. Considering that the time scale for these pulses is small compared to the duration of the digestion i.e. that their frequency is high, we rigorously establish that their effect is the same as the one of a constant driving force. This result is biologically very interesting since it allows to get rid of this very small time scale and to do the numerical computations in a much more efficient way opening ways to alternative experimental approaches on digestive tract studies. Related and more general results on the homogenization of odes can be found in L. C. Piccinini[25] but we point out that our case does not fall into the scope of [25].

In Section 3, we consider the complex phenomena related to the villi and micro-villi : the active/passive absorption by the intestinal wall and the brush border enzymatic reactions. In order to study these phenomena, we introduce a 3-d model where we focus on the boundary effects. As a consequence, the other phenomena are highly simplified. The lumen of the small intestine is modelled as a cylindrical type, periodic domain whose axis is $\mathbb{R}e_1$, where $e_1 := (1, 0, 0)$. In order to model the villi, this domain has an highly oscillatory boundary of order ε^{-1} while its radius is of order ε. In this domain, we have a system of parabolic, transport-diffusion equations with oscillatory coefficients for the absorbable and non-absorbable nutrients. The key feature is the Neumann boundary condition which describes the phenomena on the intestinal wall : the effects of the brush-border enzymes together with the active-passive absorption.

Using homogenization method, we prove that, when ε tends to 0, this problem converges to a 1-d system of transport-reaction equation. The key issue is to show how the effects of the diffusion and the degradation- absorption on the highly oscillatory boundary are combined in order to produce the final reaction terms. For the readers convenience, we provide both a formal and a rigorous proof of this result. The formal proof gives rather explicit formulas which can easily be interpreted from the biological point of view. Moreover we point out that, even if we are using a very simplified framework, we show that it captures the key features of the absorption process.

The homogenization methods used in Section 3 are based on viscosity solutions' theory and in particular the "perturbed test function method" of L. C. Evans [27, 28] : we refer to [29] and references therein for the applications of such methods for problems with Neumann boundary conditions and oscillatory boundary. To our knowledge, it is the first time that such methods are used to obtain a convergence of a 3-d problem to a 1-d problem.

Acknowledgement. The multidisciplinary collaboration on this research project between the INRA Center of Nouzilly and the Laboratoire de Mathématiques et Physique Théorique was initiated within and supported by the CaSciModOT program (CAlcul SCIentifique et MODélisation des universités d'Orléans et de Tours) which is now a Cluster of the french Region Centre. This collaboration also takes place in a CNRS-INRA PEPS program "Compréhension et Modélisation du devenir de l'aliment dans le tube digestif". This

work is part of the PhD thesis of Masoomeh Taghipoor, financed by CNRS and INRA.

2 Transport Equation

Peristalsis is the phenomenon in which a progressive wave of contraction or expansion (or both) propagates along a tube [30, 16, 31, 8]. The peristaltic waves are responsible for the fluid dynamics of the contents of the small intestine and can be divided into segmentation and propulsive contractions. The segmentation motion are responsible for mixing the bolus. Propulsive contractions are responsible for transporting the bolus through the small intestine. The effective peristaltic waves generated in the pylorus reach the bolus approximatively every 12 seconds. This is very small compared to the time scale of digestion phenomena which lasts several hours. This causes the observation of very rapid variations in the velocity of the bolus.

In [8], the authors present a first simplified model of bolus transport along the small intestine. We use Homogenization Theory to simplify this equation to replace the periodically oscillating velocity by an averaged one (II.1). This section provides a rigorous mathematical justification of this transport equation.

2.1 Position of the problem

In this section, we formulate a simplified version of the transport problem. The small intestine is represented by the interval $[0, +\infty)$ and the position of the bolus at time t is given by $x(t) \in [0, +\infty)$. Roughly speaking, $x(t)$ is the distance between the center of bolus and the pylorus.

The bolus is composed of different types of nutrients, say nutrients $1, 2, \cdots, K$ and the quantity of nutrient i at time t is denoted by $y_i(t)$ for $i = 1, 2, \cdots, K$ and we set $y(t) := (y_1(t), y_2(t), \cdots, y_K(t))$. The variation of the different y_i depends on its production and degradation rate which is summarized through the equation

$$\dot{y}(t) = d(x(t), y(t)) \ , \tag{II.1}$$

where $d := (d_1, d_2, ...d_n)$ with $d_i : [0, +\infty) \times \mathbb{R}^K \to [0, +\infty)$ a Lipschitz continuous function. Since we are mainly interested in the transport equation in this section, this simple equation is written to fix ideas but also because the transport equation will depend on the composition of the bolus y.

The peristaltic waves are created at the pylorus and they travel along the intestinal wall at a quasi-constant velocity : the average wave velocity of each peristaltic wave is about

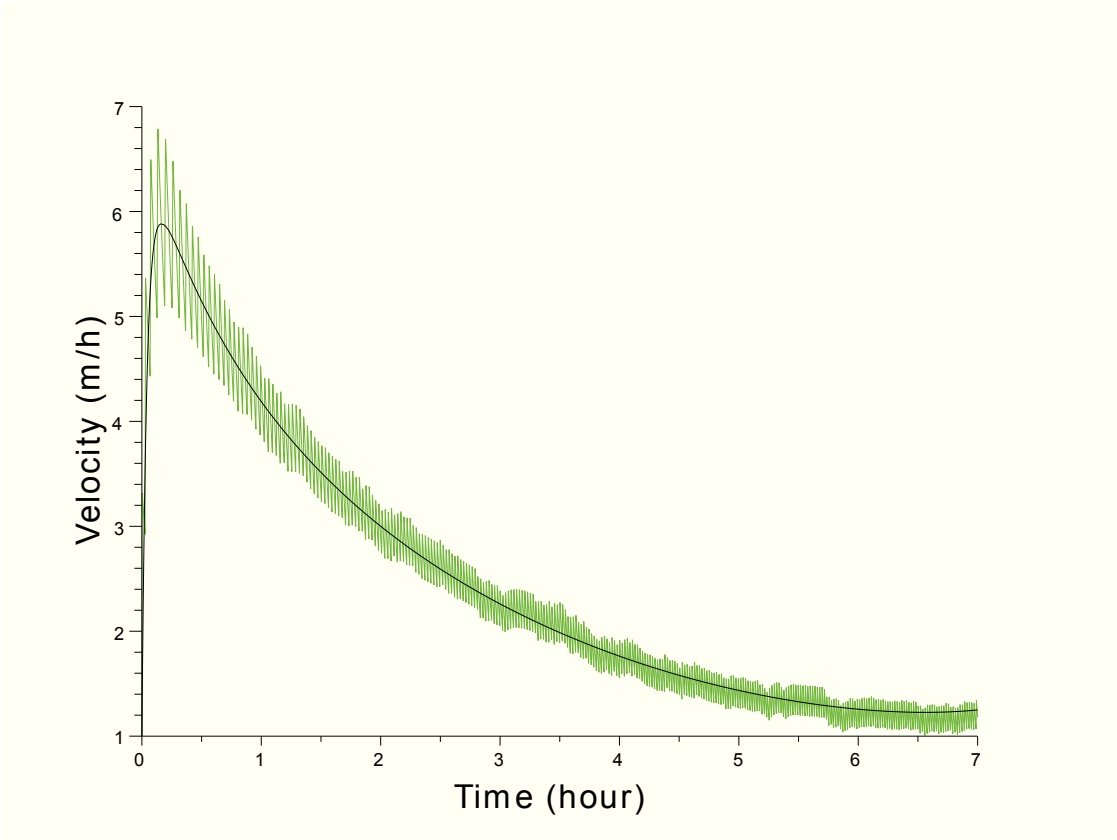

FIGURE II.1: Periodically oscillating velocity and averaged one.

$c \simeq 7.2m/h$. These waves are periodic of period denoted by $\epsilon \ll 1$ and to model them, we can say that at time t, an electric signal of size $\psi(t/\epsilon)$ starts from the pylorus and reaches a point x of the small intestine at time $t + x/c$. Here we assume that $\psi(s) \equiv 0$ if $s \leq 0$ and on $[0, +\infty)$, ψ is the restriction of a smooth, 1-periodic function on $\mathbb{R}$.

At time t, the bolus is at the position $x(t)$ and is reached by the wave generated at time $s = t - x(t)/c$ whose intensity is $\psi(s/\epsilon)$. we assume moreover that the impact of this pulse on acceleration of the bolus is given by a smooth, positive function $g_\epsilon(s, v, x, y)$ where, as above, s is the time when the pulse was generated, v is the relative velocity of a pulse with respect to the bolus velocity ($v = (c - \dot{x}(s))/c$), x is the position of the bolus and y its composition.

Indeed, according to [32] and [24] the efficiency of the peristaltic waves increases with the size of the bolus which is roughly speaking the sum of the y_i for $1 \leq i \leq K$, and decreases with the distance from pylorus $x(t)$.

The function g_ϵ is also ϵ-periodic in s, we emphasize this fact by writing

$$g_\epsilon(s, v, x, y) = g(s/\epsilon, v, x, y) \ ,$$

where $g(s, v, x, y)$ is a smooth function which is 1-periodic in s for $s > 0$.

Taking into the friction inside the small intestine as in [8] through a $-k(t)\dot{x}(t)$-term where $k(t) > 0$ for any t, the equation for the transport of the bolus reads

$$\ddot{x}(t) = g\left(\epsilon^{-1}(t - x(t)/c), 1 - \dot{x}(t)/c, x(t), y(t)\right) - k(t)\dot{x}(t) \tag{II.2}$$

with $x(0) = 0$ and $\dot{x}(0) = v_0$ where $v_0 < c$.

Having in mind the example of a water wave in a channel, if the bolus velocity is the same or is close to the wave one, then obviously the peristaltic wave will have either no effect or at least a small effect on the bolus velocity. Translated in term of g, this means that $g(t, 0, x, y) = 0$ and even $g(t, v, x, y) = 0$ if $v \leq 0$. Thus there exist a smooth function $\tilde{g} : \mathbb{R} \times \mathbb{R} \times [0, +\infty) \times \mathbb{R}^K \to [0, +\infty)$ such that $g(s, v, x, y) = \tilde{g}(s, v, x, y)v$. We notice that, since we assume g to be positive, then $\tilde{g}(s, v, x, y) \geq 0$ if $v \geq 0$ while we have $\tilde{g}(s, v, x, y) \equiv 0$ if $v \leq 0$.

Because of the dependence of Equation (II.2) on ϵ, we denote their solutions by x^ϵ, y^ϵ and our aim is to study the behavior of these solutions as ϵ tends to 0, and in particular the behavior of x^ϵ.

2.2 The asymptotic behavior

We first rewrite the equation satisfied by x^ϵ, y^ϵ. For Equation (II.2), we have

$$\ddot{x}^\epsilon = (1 - \dot{x}^\epsilon/c)\tilde{g}(\epsilon^{-1}(t - x^\epsilon/c), 1 - \dot{x}^\epsilon/c, x^\epsilon, y^\epsilon) - k(t)\dot{x}^\epsilon \tag{II.3}$$

while Equation (II.1) reads

$$\dot{y}^\epsilon = d(x^\epsilon, y^\epsilon). \tag{II.4}$$

The initial conditions are

$$x^\epsilon(0) = 0, \quad \dot{x}^\epsilon(0) = v_0, \quad y^\epsilon(0) = y_0, \tag{II.5}$$

where $v_0 < c$ because of physiological reasons.

In order to formulate our result, we introduce the function $F(t, V, X, Y)$ given by

$$F(t, V, X, Y) = \int_0^t \tilde{g}(s, V, X, Y)ds \tag{II.6}$$

and, recalling that $\tilde{g}(s, V, X, Y)$ is 1-periodic for $s \geq 0$, we denote the averaged of F over a period by $\bar{F}(V, X, Y)$. Of course we have

$$\bar{F}(V, X, Y) = F(1, V, X, Y) = \int_0^1 \tilde{g}(s, V, X, Y)ds,$$

and $F, \bar{F}$ are smooth functions since $\tilde{g}$ is a smooth function.

Example 2.1. *In [8], the authors introduce the the function g as*

$$g(s,v,x,y) := \dot{\psi}(t - x/c) \cdot v \frac{c_0 + c_1 y}{a + bx},$$

for the real non-negative values c_0, c_1, a and b. Where $y = \Sigma_{i=1}^{n} y_i$.

Our main result is the

Theorem 2.1. *Let (x^ϵ, y^ϵ) the unique solution of equations (II.3)-(II.4)-(II.5), then the sequence $(x^\epsilon, y^\epsilon)_{\epsilon>0}$ converges strongly in $C^1([0,T],[0,+\infty))$ to (x,y) the unique solution of the averaged system of equations*

$$\begin{aligned} \ddot{x}(t) =& \frac{c - \dot{x}(t)}{c} \bar{F}(1 - \dot{x}(t)/c, x(t), y(t)) - k(t)\dot{x}(t) \\ \dot{y}(t) =& d(x(t), y(t)) \end{aligned} \tag{II.7}$$

with the initial conditions

$$x(0) = 0, \quad \dot{x}(0) = v_0, \quad y(0) = y_0. \tag{II.8}$$

The key interpretation of this result is the following : the effect of frequent pulses on the transport of the bolus is the same as the one obtained through an averaged constant signal.

Proof of Theorem 2.1. We prove it in two steps : first we obtain various estimates showing that the sequences $(x^\epsilon, y^\epsilon)_{\epsilon>0}$ converge strongly in C^1 (at least along subsequences) and, then, in the second step, we prove that they converge to the unique solution of the averaged system (II.7) (which will imply that the whole sequence converges by a standard compactness argument).

The following lemma provides a proof of convergence of x^ϵ and y^ϵ.

Lemma 2.1. *Let $(x^\epsilon, y^\epsilon)_{\epsilon>0}$ the unique solution of (II.3)-(II.4)-(II.5). Then x^ϵ, y^ϵ are uniformly bounded in C^2 and therefore there exists a subsequence which is converging strongly in C^1 and such that $\ddot{x^\epsilon}$ is converging in L^∞ weak-$*$.*

Proof of Lemma. We first prove that $\dot{x^\epsilon}(t) \leq c$. To this aim, we define the positive function $\phi(t)$ as follows

$$\phi(t) = (\dot{x^\epsilon}(t) - c)^+ = \begin{cases} \dot{x^\epsilon}(t) - c & \text{if} \quad \dot{x^\epsilon}(t) - c > 0 \\ 0 & \text{otherwise,} \end{cases} \tag{II.9}$$

then multiply the both sides of equation (II.3) by $\phi(t)$

$$\ddot{x^\epsilon}(\dot{x^\epsilon}(t)-c)^+ = \frac{c-\dot{x^\epsilon}}{c}\tilde{g}\left(\frac{tc-x^\epsilon}{c\epsilon}, 1-\dot{x^\epsilon}/c, x^\epsilon, y^\epsilon\right)(\dot{x^\epsilon}(t)-c)^+ - k(t)\dot{x^\epsilon}\left(\dot{x^\epsilon}(t)-c\right)^+ .$$

The right-hand side of this equation is negative since $\tilde{g}(s,V,X,Y)$ is non negative if $Y \geq 0$, and $k(t) > 0$, therefore

$$\ddot{x^\epsilon}(t)(\dot{x^\epsilon}(t)-c)^+ \leq 0$$

which is equivalent to

$$\frac{1}{2}\frac{d}{dt}(\phi^2(t)) \leq 0 .$$

The function $\phi^2(t)$ is therefore a decreasing function. Furthermore, since $v_0 < c$, we have

$$\phi^2(t) \leq \phi^2(0) = [(v_0-c)^+]^2 = 0 ,$$

which yields the result.

Using the same method with $(\dot{x})^- = \max(-\dot{x}, 0)$, we can prove that $\dot{x}$ is a non-negative function.

Gathering these information, we obtain that, for any t

$$0 \leq x^\epsilon(t) \leq ct \ , \ 0 \leq \dot{x^\epsilon}(t) \leq c \ ,$$

and therefore the sequence $(x^\epsilon)_{\epsilon>0}$ is uniformly bounded and equicontinuous on $[0,T]$. Using these informations and the equations for the y^ϵ, we also see that the y^ϵ are also uniformly bounded in C^1 (and even in C^2) and coming back to the x^ϵ equation we see also that the x^ϵ are also uniformly bounded in C^2.

Consequently the Arzela-Ascoli compactness criterion ensures that there exists a subsequence $(x^{\epsilon_j}, y^{\epsilon_j})$ which converges in C^1. Moreover, since $\ddot{x^\epsilon}$ is bounded in L^∞, we can also extract a subsequence such that $\ddot{x^{\epsilon_j}}$ converges in the L^∞ weak-$*$ topology. □

We return now to the proof of Theorem 2.1. To simplify the exposure, we still denote by (x^ϵ, y^ϵ) the converging subsequence $(x^{\epsilon_j}, x^{\epsilon_j})$ and we denote by (x,y) the limit. By inserting the Definition (II.6) into Equation (II.3), we get

$$\ddot{x^\epsilon}(t) = (1-\dot{x^\epsilon}/c)\frac{\partial F}{\partial t}(\epsilon^{-1}(t-x^\epsilon/c), 1-\dot{x^\epsilon}/c, x^\epsilon, y^\epsilon) - k(t)\dot{x^\epsilon}(t)$$

therefore, using the notation $v^\epsilon = 1-\dot{x^\epsilon}/c$ and dropping most of the variables to simplify the expressions, we have

$$\ddot{x^\epsilon}(t) = \epsilon\frac{d}{dt}\left[F(\epsilon^{-1}(s-x^\epsilon/c), v^\epsilon, x^\epsilon, y^\epsilon)\right] - \epsilon\dot{v^\epsilon}\frac{\partial F}{\partial V} - \epsilon\dot{x^\epsilon}\frac{\partial F}{\partial X} - \epsilon\dot{y^\epsilon}\frac{\partial F}{\partial Y} - k\dot{x^\epsilon}$$

and then integrate the both sides of equation over $[0,t]$

$$\int_0^t \ddot{x}^\epsilon ds = \epsilon \int_0^t \frac{d}{ds}(F(\epsilon^{-1}(s-x^\epsilon/c), v^\epsilon, x^\epsilon, y^\epsilon))ds \\ - \epsilon \int_0^t (\dot{v^\epsilon}\frac{\partial F}{\partial V} + \dot{x}^\epsilon \frac{\partial F}{\partial X} + \dot{y}^\epsilon \frac{\partial F}{\partial Y})ds - \int_0^t k\dot{x}^\epsilon ds$$

which leads to

$$\dot{x}^\epsilon(t) - v_0 = \epsilon F(\epsilon^{-1}(t-x^\epsilon/c), 1-\dot{x}^\epsilon/c, x^\epsilon, y^\epsilon) \\ - \epsilon \int_0^t (\dot{v^\epsilon}\frac{\partial F}{\partial V} + \dot{x}^\epsilon \frac{\partial F}{\partial X} + \dot{y}^\epsilon \frac{\partial F}{\partial Y})ds - \int_0^t k\dot{x}^\epsilon ds$$

since $F(0,V,X,Y) = 0$ for any $V, X \in \mathbb{R}$ and $Y \in \mathbb{R}^K$.

Now we have to let ϵ tend to 0. First, since $\tilde{g}$ is periodic, it is standard to prove that

$$\epsilon F(\epsilon^{-1}t, V, X, Y) \to \bar{F}(V,X,Y)t \ ,$$

locally uniformly. Especially, it is easy to see that if $n \leq \epsilon^{-1}t < n+1$, therefore $\epsilon F(\epsilon^{-1}t, V, X, Y) \to \epsilon[n\bar{F}(V,X,Y) + O(1)]$.

In the same way, because of the definition of F and the regularity properties of $\tilde{g}$, for $\xi = V, X, Y$ we also have

$$\epsilon \frac{\partial F}{\partial \xi}(\epsilon^{-1}t, V, X, Y) \to \frac{\partial \bar{F}}{\partial \xi}(V,X,Y)t \quad \text{locally uniformly.}$$

As a consequence, since x^ϵ and y^ϵ are converging respectively to x and y in C^1, we have also

$$\epsilon F(\epsilon^{-1}(s-x^\epsilon(s)/c), v^\epsilon(s), x^\epsilon(s), y^\epsilon(s)) \to \bar{F}(v(s), x(s), y(s))(s-x(s)/c),$$

uniformly on $[0,T]$, where $v = 1 - \dot{x}/c$. And the same is true, replacing F by $\dfrac{\partial F}{\partial \xi}$ and $\bar{F}$ by $\dfrac{\partial \bar{F}}{\partial \xi}$.

From these properties, it is easy to deduce that

$$\epsilon \int_0^t (\dot{x}^\epsilon \frac{\partial F}{\partial X} + \dot{y}^\epsilon \frac{\partial F}{\partial Y})ds \to \int_0^t (s-x/c)(\dot{x}\frac{\partial \bar{F}}{\partial X} + \dot{y}\frac{\partial \bar{F}}{\partial Y})ds \text{ as } \epsilon \to 0 \ ,$$

for any $t \in [0,T]$.

On the other hand, $\dot{v^\epsilon} = -\ddot{x}^\epsilon/c$ converges in the L^∞ weak-$*$ topology to $\dot{v}$ and therefore

$$\epsilon \int_0^t \dot{v^\epsilon}\frac{\partial F}{\partial V}ds \to \int_0^t (s-x/c)\dot{v}\frac{\partial \bar{F}}{\partial V}ds \ ,$$

for any $t \in [0, T]$.

Gathering all these informations, we finally obtain

$$\begin{aligned}\dot{x}(t) - v_0 =&(t - x(t)/c)\bar{F}(1 - \dot{x}(t)/c, x(t), y(t)) \\ &- \int_0^t (s - x/c)(\dot{v}\frac{\partial \bar{F}}{\partial V}ds + \dot{x}\frac{\partial F}{\partial X} + \dot{y}\frac{\partial F}{\partial Y})ds \\ &- \int_0^t k(s)\dot{x}(s)ds \end{aligned} \tag{II.10}$$

The right-hand side being C^1 in t, we deduce that x is a C^2-function and derivating the both side of (II.10), we have the equation

$$\ddot{x}(t) = (1 - \dot{x}(t)/c)\bar{F}(1 - \dot{x}(t)/c, x(t), y(t)) - k(t)\dot{x}(t).$$

□

3 On the Effects of Intestinal Villi

As mentioned in the introduction, in the 1-d model of digestion presented in [8], we take into account the absorption effect by a simple absorption term through a Michaelis-Menten type nonlinearity and this can be assumed unreasonable when compared to the complexity of the involved phenomena. The same can be said for the enzymatic breakdown by the brush-border enzymes. Consequently the first aim of this section consists in giving some rigorous justification of these choices.

Our effort is therefore to find an appropriate system of equations describing the different effects of the structure and the spatial distribution of intestinal villi on these key phenomena of digestion. Therefore we introduce a 3-d toy model which takes into account the complex geometry of the small intestine as well as all these boundary effects, but this implies unavoidable simplifications on the transport process.

We start by a short presentation of the small intestine anatomy followed by introducing the three dimensional toy model of digestion.

A large number of villi and micro-villi are present on the surface of the small intestine. Their role is to enlarge the digestive and absorptive area in the small intestine. They increase the area of the small intestine at least 500 times ([31]). The absorptive surface of the villi contains the brush border enzymes which are responsible of the final step of degradation (surfacic degradation) for some nutrients. This increase is therefore a key issue in the process of nutrients degradation and absorption.([33]).

These finger like villi are covered by epithelial cells. They consist of absorptive, goblet and entero-endocrine cells. The epithelial cells are produced in crypts, they migrate and become mature from the crypts to the tips of the villi([34]). More precisely, the absorption rate is also proportional to the distance of each of the villi from its tip.

A microscopic observation of the small intestine surface is necessary in order to give realistic absorption and degradation shapes. The spatial aspect of absorption related to the distribution of villi and their absorption capacity is often neglected in modelling of digestion. In these models, absorption and degradation are modelled by a constant rate or a Michaelis-Menten process (see [8], Logan [15], ...).

As shown in figure (II.2) the size of the period is small compared to the size of the unfold small intestine which is around 18 meters. We consider, for the sake of simplicity, that the villi are distributed periodically in the inner surface of the small intestine.

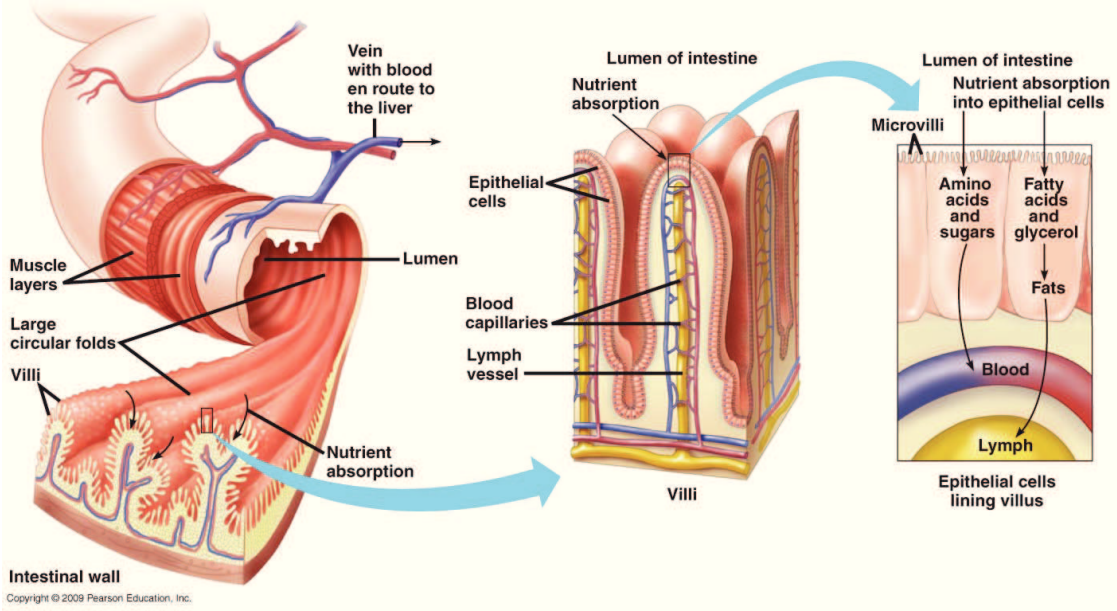

FIGURE II.2: The different scales on intestinal anatomy relevant to our model.

In this section, we seek a macroscopic description of digestion in the small intestine by taking into account all the effects of the presence of the villi in microscopic scale. Our approach is based on an asymptotic analysis, as ϵ goes to zero. The absorption rate of the limit problem is said to be the homogenized absorption rate.

3.1 Position of problem

The small intestine is assumed to be an axisymmetric cylindrical tube with a rapidly varying cross section. In order to describe it, we first introduce an axisymmetric, smooth domain Ω which is confined in a cylinder of radius $r > 0$. More precisely, we assume

$$\{(x_1, x_2, x_3) \in \mathbb{R}^3 \mid x_2 = x_3 = 0\} \subset \Omega \subset \{(x_1, x_2, x_3) \in \mathbb{R}^3 \mid x_2^2 + x_3^2 = r^2\}.$$

In addition, we assume that Ω is periodic in the x_1-direction (say 1-periodic), namely $(x_1 + 1, x_2, x_3) \in \Omega$ if $(x_1, x_2, x_3) \in \Omega$.

The small intestine is represented, for some $0 < \epsilon \ll 1$ by the domain Ω_ϵ given by

$$\Omega_\epsilon = \epsilon\Omega \cap \{x_1 \geq 0\} \tag{II.11}$$

The figure II.3 is a simple representation of this domain :

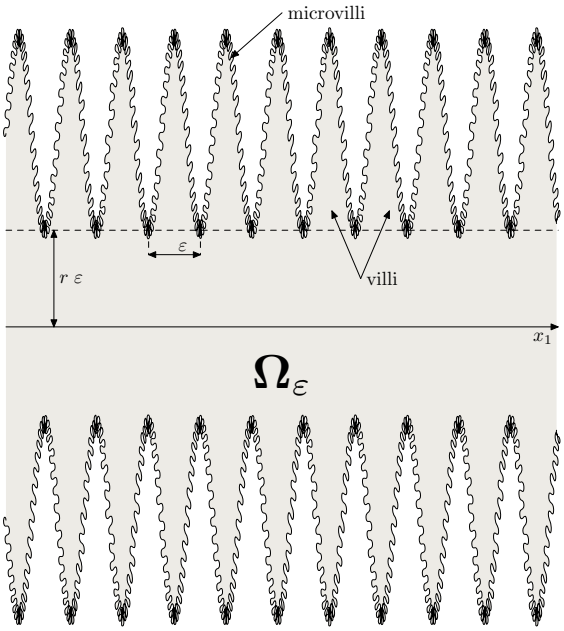

FIGURE II.3: A simple example of the domain Ω_ϵ. The oscillations on the villi represents the microvilli.

In this definition, the small intestine has an infinite length. However this assumption is not a real restriction, since we focus on the local absorption-degradation processes. Moreover, the $x_1 = 0$ part of the boundary corresponds to the pylorus and $\epsilon\partial\Omega$ to the villi. It is worth pointing out that Ω_ϵ is ϵ-periodic in the x_1 direction, the parameter ϵ characterizes the distance between the villi and thus it is natural to assume it to be very small.

A simple example of Ω_ϵ in cylindrical coordinates, can be the following

$$\Omega_\epsilon = \{(r, \theta, z) \text{ s.t } \mid r \mid \leq \epsilon + \epsilon\psi(z/\epsilon, \theta),\ z \geq 0,\ \theta \in [0, 2\pi]\}$$

where z plays here the role of x_1 and $\psi(z, \theta)$ is a 1-periodic function of z.

We introduce two functions $u^\epsilon, v^\epsilon : \Omega_\epsilon \times [0, T] \to \mathbb{R}$ for describing the evolution of the concentration of feedstuffs in the small intestine. For $x \in \Omega_\epsilon$ and $t \in [0, T]$, $v^\epsilon(x, t)$ denotes the concentration of the large feedstuffs molecules which are transformed into absorbable nutrients after different enzymatic reactions. The quantity $u^\epsilon(x, t)$ represents the concentration of produced nutrients at position x at each time t.

The evolution of substrates u^ϵ and v^ϵ in the intestinal lumen is due to (i) their diffusion by Fick's law, (ii) their propagation through intestinal lumen by a given velocity coming from the peristaltic waves and (iii) the enzymatic reactions which transform v^ϵ to u^ϵ both inside the intestinal lumen but also on the intestinal wall by the brush-border enzymes. When these reactions take place in the intestinal lumen, we call them volumic transformation, while we talk about surfacic transformation when they take place on the villi.

The rate of the volumic reactions depends on the concentration of feedstuffs and also enzymes activity at time t and at x, namely $\zeta(x, t)$, where $\zeta : [0, \infty) \times [0, T] \to \mathbb{R}$ is a continuous, positive and bounded function. There is a limitation in the transformation which is described by $\varphi : \mathbb{R} \to \mathbb{R}$, which is a bounded, increasing and Lipschitz continuous function such that $\varphi(s) = 0$ if $s \leq 0$. These assumptions on ζ and φ are denoted by (T1) in the sequel.

Taking into account the three above-mentioned phenomena, the equation for the evolution of concentration of the non-absorbable feedstuffs molecules in the intestinal lumen reads

$$\frac{\partial v^\epsilon}{\partial t} = \omega_\epsilon \Delta v^\epsilon - c(x_1, x/\epsilon, t) D v^\epsilon - \zeta(x_1, t)\varphi(v^\epsilon) \quad \text{in} \quad \Omega_\epsilon \times (0, T) \tag{II.12}$$

while for the absorbable nutrients, we have

$$\frac{\partial u^\epsilon}{\partial t} = \chi_\epsilon \Delta u^\epsilon - c(x_1, x/\epsilon, t) D u^\epsilon + \zeta(x_1, t)\varphi(v^\epsilon) \quad \text{in} \quad \Omega_\epsilon \times (0, T). \tag{II.13}$$

The first terms of the right-hand-sides of the above equations, where Δ denotes the usual Laplacian [2], are diffusion terms. The diffusion coefficients of large molecules of feedstuffs and small molecules of nutrients are denoted by ω_ϵ and χ_ϵ respectively.

2. If ϕ is a smooth function, $\Delta\phi = \dfrac{\partial^2\phi}{\partial x_1^2} + \dfrac{\partial^2\phi}{\partial x_2^2} + \dfrac{\partial^2\phi}{\partial x_3^2}$

It is shown that, for a fixed temperature, the diffusion coefficient d is inversely proportional to the molecular weight, to be more precise for a spherical molecule we have

$$d = \frac{kT}{3\mu}(\frac{\rho}{6\pi M})^{1/3}$$

in which k is Boltzmann constant, T is the intestinal temperature, μ the viscosity of the the intestinal liquid, ρ the molecule density and M the molecular mass. For fixed T and μ, this constant is very small because of the very small value of $kM^{-1/3}$ [33].

For reasons explained in section 3.3, we assume that

$$\omega_\epsilon := \epsilon\omega \quad \text{and} \quad \chi_\epsilon := \epsilon\chi \ ,$$

for some constants $\omega, \chi > 0$. Since the nutrients molecules are smaller than feedstuffs particles, we also have $\omega \leq \chi$. The second terms of the right-hand sides are transport terms. The C^1-function $c : [0, +\infty) \times \Omega \times [0, T] \to \mathbb{R}^3$ is modelling the velocity of substrates which comes from the peristaltic waves. The effect of the peristaltic waves is known to depend on the position in the small intestine and on time, this justifies the dependence of $c(x_1, X, t)$ on x_1 and t, while the dependence on $X = (X_1, X_2, X_3)$ takes into account the local effects at a lower scale.

A priori the diffusion of bolus is small compared to its velocity through the small intestine and therefore ω_ϵ and χ_ϵ are expected to be smaller than $c(x_1, X, t)$.

We assume the function c to satisfy the following properties :
(C1) The function $c(x_1, X, t)$ is a Lipschitz continuous function which is 1-periodic in X_1 and, if $e_1 = (1, 0, 0)$, then, for any $x_1 \in [0, +\infty)$, $X \in \Omega$ and $t \in [0, T]$,

$$c(x_1, X, t) \cdot e_1 \geq 0 \quad \text{and} \quad \int_P c(x_1, X, t)dX > 0 \ ,$$

where P is a period in Ω, say $P := \{X \in \Omega \ ; \ 0 \leq X_1 \leq 1\}$.

In addition to the regularity properties of c, this assumption means that the effect of the peristaltic waves is to move ahead the bolus in the small intestine.
(C2) For any $x_1 \in [0, +\infty)$, $X \in \Omega$ and $t \in [0, T]$, $\mathrm{div_X(c)} = 0$ where $\mathrm{div_X}$ denotes the divergence operator in the X-variable only.
This second assumption is justified by the incompressibility of the bolus at the microscopic level.
(C3) For any $x_1 \in [0, +\infty)$, $X \in \partial\Omega$ and $t \in [0, T]$, $c(x_1, X, t) \cdot N(X) = 0$, where $N(X)$ denotes the outward, unit normal to $\partial\Omega$ at X.

This last assumption means that the velocity vector is always tangent to the boundary. It is worth pointing out that, if $X = x/\epsilon$ then $N(X) = n(x)$, therefore it is true both for X

in Ω and for x in Ω_ϵ. As a consequence of this property, the nutrients reach the boundary only because of the diffusion effects.

Once they reach the boundary, the large particles of feedstuffs can change of chemical structure because of the presence of brush-border enzymes. As we already mentioned above, this effect is called surfacic degradation of feedstuffs and the result is the production of the smaller absorbable molecules of nutrients u^ϵ. We assume moreover that a portion $0 \leq \beta < 1$ of these nutrients is absorbed instantaneously while the remaining part ($\alpha := 1 - \beta$) diffuses in the small intestine. The surfacic degradation is modelled by the Neumann boundary condition

$$\omega \frac{\partial v^\epsilon}{\partial n} = -\varrho(x_1, X) v^\epsilon \quad \text{on } \partial\Omega_\epsilon \times (0, T) \tag{II.14}$$

where, ϱ is a continuous, positive and X_1-periodic function which represents the rate of surfacic degradation.

On the boundary of the small intestine, there are two main effects for the nutrients u^ϵ. We already describe the first one which is a production of nutrients by the surfacic degradation. The second one is the active and passive absorption of nutrients, namely their transport across the intestinal wall to the blood circulation. An active process requires the expenditure of energy, while a passive process results from the inherent, random movement of molecules [33]. These different categories of absorption as well as the production of u^ϵ from v^ϵ on the boundary construct the boundary condition of Equation (II.12)

$$\chi \frac{\partial u^\epsilon}{\partial n} = -\eta_p(x_1, x/\epsilon) u^\epsilon - \eta_a(x_1, x/\epsilon, t) g_a(u^\epsilon) + \frac{\alpha}{\omega} \varrho(x_1, x/\epsilon) v^\epsilon. \tag{II.15}$$

The functions η_p and η_a denote respectively the passive and active absorption rates. Both of them depend on the global position in the small intestine x_1 and the local one x/ϵ, by which we take into account the effect of the special physiology of the villi on the absorption rate which has been described at the beginning of this section. The dependence in time in the active absorption η_a, describes the presence of energy at time t. The function g_a governs the active absorption and depends on the nutrients categories. Typically, it is assumed to be the Michaelis Menten and therefore, it is a bounded, continuous, increasing function.

We formulate the key assumptions on the functions η_p, η_a and g_a
(T2) The functions $\eta_p(x_1, X), \eta_a(x_1, X, t)$ are bounded, continuous, positive, 1-periodic functions in X_1, and the function g_a is a bounded, continuous, increasing function with $g_a(s) = 0$ if $s \leq 0$. Moreover, there exists $\underline{\eta} > 0$ such that $\eta_p(x_1, X) \geq \underline{\eta}$ for any $x_1 \in [0, +\infty)$, $X \in \Omega$.

Finally, we complement the equations with the initial conditions

$$u^\epsilon(x, 0) = 0, \quad v^\epsilon(x, 0) = 0 \quad \text{in } \Omega_\epsilon, \tag{II.16}$$

which means that the small intestine is empty at time $t = 0$ and by a Dirichlet boundary condition at $x_1 = 0$, modelling the gastric emptying, namely

$$v^\epsilon(x,t) = v_0(t) \quad \text{for } x_1 = 0, t \in (0,T) \tag{II.17}$$
$$u^\epsilon(x,t) = u_0(t) \quad \text{for } x_1 = 0, t \in (0,T)\ , \tag{II.18}$$

where u_0 and v_0 are bounded continuous functions on $[0,T]$ with $u_0(0) = 0$ and $v_0(0) = 0$.

3.2 Formal asymptotic

In order to study the limit as $\epsilon \to 0$ of the system (II.12)-(II.18), we first argue formally : we consider the following expansions (called ansatz) for the solutions u^ϵ and v^ϵ

$$u^\epsilon(x,t) = u(x_1,t) + \epsilon u_1(x_1, \frac{x}{\epsilon}, t) + o(\epsilon) \tag{II.19}$$
$$v^\epsilon(x,t) = v(x_1,t) + \epsilon v_1(x_1, \frac{x}{\epsilon}, t) + o(\epsilon) \tag{II.20}$$

where $u_1(x_1, \frac{x}{\epsilon}, t)$ and $v_1(x_1, \frac{x}{\epsilon}, t)$ are 1-periodic functions in second variable.

From now on, in order to simplify the notations, we systematically denote by X the fast variable x/ϵ. On the other hand, the above system can be decoupled and we can first study the asymptotics of v^ϵ, namely only the initial-boundary value problem (II.12)-(II.14)-(II.16)-(II.17) and then use the result for studying the behavior of u^ϵ through (II.13)-(II.15)-(II.16)-(II.18). Since we use the same methods in both cases to obtain the homogenization results, we present the details only for the equation of nutrients u^ϵ while we only give the results for v^ϵ.

We first plug these expressions of v^ϵ and u^ϵ into (II.13), and then examine the higher order terms in ϵ. We find

$$\frac{\partial u}{\partial t} = \chi_\epsilon(\frac{\partial^2 u}{\partial x_1^2} + \frac{1}{\epsilon}\Delta_X u_1) - c(x_1,X,t)(\frac{\partial u}{\partial x_1}e_1 + D_X u_1) + \zeta(x_1,t)\varphi(v) + o(1) \tag{II.21}$$

At this stage, we notice that the relevant choice for observing the effects of villi is indeed $\chi_\epsilon = \epsilon\chi$, for some positive constant χ. With this choice, we obtain

$$\frac{\partial u}{\partial t} = \chi\Delta_X u_1 - c(x_1,X,t)(\frac{\partial u}{\partial x_1}e_1 + D_X u_1) + \zeta(x_1,t)\varphi(v) + o(1). \tag{II.22}$$

The equation for the first corrector u_1 (the "cell problem") is an equation in the fast variable X, i.e. for the functions $X \mapsto u_1(x_1,X,t)$, x_1, t playing the role of parameters. Setting

$$p := \frac{\partial u}{\partial x_1}(x_1,t)e_1 \quad , \quad \lambda := -\frac{\partial u}{\partial t}(x_1,t) \quad \text{and} \quad \delta := \zeta(x_1,t)\varphi(v),$$

and substituting p and λ in (II.22), we obtain the equation on Ω

$$-\chi\Delta u_1 + c(x_1, X, t)[p + D_X u_1] = \lambda + \delta \quad \text{in } \Omega. \tag{II.23}$$

We argue in the same way for the boundary condition : plugging (II.19) and (II.20) into $(II.15)$, we obtain

$$\chi(\frac{\partial u}{\partial x_1}e_1 + D_X u_1).n = -\left(\eta_p(x_1, X)u + \eta_a(x_1, X, t)g_a(u) - \frac{\alpha}{\omega}\varrho(x_1, X)v\right) + o(1)\ . \tag{II.24}$$

Using the introduced notations and recalling that $N(X) = n(x)$, the above equation gives

$$(p+D_X u_1).N = -\frac{1}{\chi}\left(\eta_p(x_1, X)u + \eta_a(x_1, X, t)g_a(u) - \frac{\alpha}{\omega}\varrho(x_1, X)v\right)+o(1)\ . \tag{II.25}$$

Introducing the notations $\mu := u(x_1, t)$ and $\nu = v(x_1, t)$ and

$$\Theta(x_1, X, t, u, v) := \eta_p(x_1, X)u + \eta_a(x_1, X, t)g_a(u) - \frac{\alpha}{\omega}\varrho(x_1, X)v\ ,$$

the complete cell problem reads

$$\begin{cases} -\chi\Delta u_1 + c(x_1, X, t)[p + D_X u_1] = \lambda + \delta \ \text{ in } \Omega \\ \quad (p + D_X u_1) \cdot N = -\dfrac{1}{\chi}\Theta(x_1, X, t, \mu, \nu) \ \text{ on } \partial\Omega \end{cases} \tag{II.26}$$

We assume that this problem has indeed a smooth solution u_1 which is 1-periodic in X_1. Recalling that Ω is 1 periodic in the X_1 direction and integrating (II.26) over a period P (remarking also that $\Delta_X u_1 = \Delta_X(u_1 + p \cdot X)$), we obtain

$$(\lambda + \delta)|P| = \chi \int_P -\Delta_X(u_1 + p \cdot X)dX + \int_P c(x_1, X, t)[p + D_X u_1])dX \tag{II.27}$$

where $|P|$ denotes the Lebesgue measure of P. By using Green Formula

$$-\chi \int_P \Delta_X(u_1 + p \cdot X)dX = -\chi \int_{\partial P} (D_X u_1 + p).\tilde{N}d\sigma$$

where $\tilde{N}$ denotes the outward, unit normal to ∂P and where

$$\partial P = (\partial P \cap \partial\Omega) \cup (\partial P \cap \Omega)\ .$$

We first point out that, because of the periodicity of u_1 and the opposite orientation of the normal vector on both side of the cell

$$\chi \int_{(\partial P \cap \Omega)} (D_X u_1 + p) \cdot \tilde{N}d\sigma = 0. \tag{II.28}$$

On the other hand, recalling the boundary condition of (II.26)

$$-\chi \int_{\partial P \cap \partial \Omega} (D_X u_1 + p).\tilde{N} d\sigma = \int_{\partial P \cap \partial \Omega} \Theta(x_1, X, t, \mu, \nu) d\sigma.$$

Next we consider the c-term : by integration by parts

$$\int_P c(x_1, X, t) D_X u_1 dX = \int_{\partial P} u_1 c(x_1, X, t).\tilde{N} d\sigma - \int_P u_1 \mathrm{div_X(c)dX}.$$

Because of **(C2)**, the last integral of the right-hand side vanishes, while, for the first one, we use similar argument as above : because of the periodicity properties of the velocity function c, the integral over $\partial P \cap \Omega$ is 0 (the same reasons as for (II.28)) and by **(C3)**, it is also the case for the integral over $\partial P \cap \partial\Omega$.

Gathering these informations, inserting them in (II.27) and recalling the definition of Θ, one gets

$$\begin{aligned}(\lambda + \delta)|P| = \int_{\partial P \cap \partial \Omega} [\eta_p(x_1, X)\mu + \eta_a(x_1, X, t) g_a(\mu) - \frac{\alpha}{\omega} \varrho(x_1, X)\nu] d\sigma \\ + p \cdot \int_P c(x_1, X, t) dX. \end{aligned} \tag{II.29}$$

In order to obtain the homogenized equation, we introduce

$$\begin{aligned} \bar{c}(x_1, t) &= \frac{1}{|P|} \int_P c(x_1, X, t) dX, \\ \bar{\eta}_p(x_1) &= \frac{1}{|\partial P \cap \partial \Omega|} \int_{\partial P \cap \partial \Omega} \eta_p(x_1, X) d\sigma \\ \bar{\eta}_a(x_1, t) &= \frac{1}{|\partial P \cap \partial \Omega|} \int_{\partial P \cap \partial \Omega} \eta_a(x_1, X, t) d\sigma \\ \bar{\varrho}(x_1) &= \frac{1}{|\partial P \cap \partial \Omega|} \int_{\partial P \cap \partial \Omega} \varrho(x_1, X) d\sigma \end{aligned} \tag{II.30}$$

where $|\partial P \cap \partial\Omega|$ denotes the area of the surface $\partial P \cap \partial\Omega$. With the notation

$$\bar{\Theta}(x_1, t, u, v) := \bar{\eta}_p(x_1, X)u + \bar{\eta}_a(x_1, X, t) g_a(u) + \frac{\alpha}{\omega} \bar{\varrho}(x_1, X) v \ ,$$

$$R(P) := \frac{|\partial P \cap \partial \Omega|}{|P|} \ ,$$

we get

$$\lambda = R(P) \bar{\Theta}(x_1, t, \mu, \nu) + \bar{c}(x_1, t) \cdot p - \delta, \tag{II.31}$$

The one dimensional averaged equation of transport and absorption of nutrients is thus obtained by inserting the value of λ and p in the equation (II.31)

$$\frac{\partial u}{\partial t} + \bar{c}(x_1,t)\cdot e_1 \frac{\partial u}{\partial x_1} = \zeta(x_1,t)\varphi(v) - R(P)\bar{\Theta}(x_1,t,u,v) \qquad \text{(II.32)}$$

The term $R(P)\bar{\Theta}(x_1,t,u,v)$ represents the global result of the different phenomena on the boundary of the small intestine : production of nutrients by surfacic degradation, active and passive absorption. The interesting feature in this term comes from the coefficient $R(P)$ which measures the ratio between the large surface of the villi compared to the relatively small volume of each cell. It therefore describes the effect of the geometry of the villi on the absorption and degradation processes.

The term $R(P)[\bar{\eta}_p(x_1)u + \bar{\eta}_a(x_1,t)g(u)]$ gives an averaged value of absorption by intestinal wall, which takes into account the effect of villi folds as well as the differences between passive and active absorption.

In the same way as for the nutrients u^ϵ, we may obtain the one dimensional homogenized equation for feedstuffs v^ϵ

$$\frac{\partial v}{\partial t} + \bar{c}(x_1,t)\cdot e_1 \frac{\partial v}{\partial x_1} = -\zeta(x_1,t)\varphi(v) - R(P)\frac{1}{\omega}\bar{\varrho}(x_1)v. \qquad \text{(II.33)}$$

In order to compare the homogenized equations (II.32)-(II.33) with the models presented in [8], we recall that, roughly speaking, in these models, the bolus is identified as a cylinder of fixed length and variable radius r, composed of a single feedstuff A which is transformed into an absorbable nutrient B through different types of enzymatic degradations. In fact, the main model is more sophisticated since A and B can appear under several forms (typically for A a solubilized and a non-solubilized form).

Two degradation mechanisms are taken into account : a "volumic" one taking place inside the bolus and resulting from the action of pancreatic and gastric enzymes and a "surfacic" one taking place on the villi and resulting from the action of the brush-border enzymes. Then, once the absorbable nutrient B reaches the surface of bolus, hence the intestinal wall, the absorption is ensured by a Michaelis- Menten mechanism. Therefore, even if the above 3-d model is very simplified, the functions v and A have the same nature and represent the large particles of feedstuffs, as well as the functions u and B represent the absorbable nutrients. Furthermore the 3-d model described the same phenomena, at least on the boundary.

Therefore, as we already mentioned it in the introduction, the above homogenization process equations (II.32)-(II.33) justifies the rather simple form of the equations presented in [8] : as long as we are just interested in "macroscopic" phenomena, it is reasonnable to describe the effects of the complex geometry of the villi, the different types of degradation and the absorption process by these odes.

Remark 3.1. *In the above analysis, the effects of villi is summarized and measured by the (a priori large) $R(P)$-coefficient which described the consequences of their particular finger-like geometry. It is worth pointing out that this type of analysis can be used as well to understand the effects of villi in the intestinal tract but also the effects of micro-villi inside the villi.*

3.3 The rigorous result and proof

We are now in position to state the rigorous result.

Theorem 3.1. *Assume that Ω is a C^2-domain satisfying the properties described in Section 3.1, that* **(C1)-(C3)**, **(T1)-(T2)** *holds and that u_0, v_0 are continuous functions such that $u_0(0) = v_0(0) = 0$. Then the sequences $(u^\epsilon, v^\epsilon)_\epsilon$ converge locally uniformly, as $\epsilon \to 0$, to the unique (viscosity) solution (u, v) of the system*

$$\begin{cases} \dfrac{\partial u}{\partial t} + \bar{c}(x_1,t)\cdot e_1 \dfrac{\partial u}{\partial x_1} = \zeta(x_1,t)\varphi(v) - R(P)\bar{\Theta}(x_1,t,u,v) \ \text{ in } Q_T \\ \dfrac{\partial v}{\partial t} + \bar{c}(x_1,t)\cdot e_1 \dfrac{\partial v}{\partial x_1} = -\zeta(x_1,t)\varphi(v) - R(P)\dfrac{1}{\omega}\bar{\varrho}(x_1)v \ \text{ in } Q_T \\ \quad u(0,t) = u_0(t) \ \text{ and } \ v(0,t) = v_0(t) \qquad \text{on } \ \partial Q_T \\ u(x_1,0) = v(x_1,0) = 0 \qquad \text{in } [0,+\infty) \end{cases} \tag{II.34}$$

where $Q_T = (0,+\infty)\times(0,T)$ and $\partial Q_T = \{x_1 = 0, t \in (0,T)\}$.

The averaged problem (II.34) can be seen as a simplified version of the more complicated initial-boundary value problem (II.12)-(II.18) : it is clearly easier to compute the solution of (II.34) than to take into account the complex geometry and boundary condition of (II.12)-(II.18).

Proof of Theorem 3.1. Before providing the proof, we make some remarks about the existence and uniqueness of u^ϵ and v^ϵ. The system II.12)-(II.18) is in fact decoupled and therefore we prove (by similar methods) the existence and uniqueness of v^ϵ and then of u^ϵ.

The initial-boundary value problem (II.12)-(II.14)-(II.16)-(II.17) is a classical parabolic problem with Dirichlet and Neumann boundary conditions : it therefore admits smooth solutions. If one does not insist on proving the existence of smooth solutions, the existence and uniqueness of a viscosity solution of this problem can also be obtained by easier viscosity solutions arguments, using Perron's method (cf. [35], [36]) and comparison results ([37], [36]). Of course, the result for (II.13)-(II.15)-(II.16)-(II.18) follows from the same arguments.

Applying the Maximum Principle (or a comparison result for viscosity solutions), it is easy to prove that $0 \leq v^\epsilon(x,t) \leq ||v_0||_\infty$ in $\overline{\Omega}_\epsilon \times [0,T]$ since 0 and $||v_0||_\infty$ are respectively subsolution and supersolution of (II.13)-(II.15)-(II.16)-(II.18) . In particular, the v^ϵ 's are uniformly bounded. For the u^ϵ, the situation is unfortunately a little bit more complicated : since 0 is a subsolution of (II.13)-(II.15)-(II.16)-(II.18), we have $u^\epsilon(x,t) \geq 0$ on $\overline{\Omega}_\epsilon \times [0,T]$ but it is not obvious at all to get an upper bound. For the time being, we assume that the u^ϵ 's are uniformly bounded and we will come back on this point at the end of the proof.

We provide the full convergence proof only in the case of the u^ϵ's, the one for the v^ϵ being obtained by similar and even simpler argument. In this proof, because of the decoupling of our system, we assume that we already know that the v^ϵ's are converging uniformly.

In order to prove the convergence of u^ϵ towards u, we use the standard method in such problems : we combine the half-relaxed limit method [38, 36] with the Perturbed Test-Function method introduced by L. C. Evans [27]. It is worth pointing anyway that the non-classical feature in our result and proof comes from the 3-d to 1-d passage to the limit and the change in the nature of the problem.

To this end, we introduce

$$\bar{u}(x,t) = \limsup_{\substack{\epsilon \to 0, y \to x \\ s \to t}} u^\epsilon(y,s) \quad , \quad \underline{u}(x,t) = \liminf_{\substack{\epsilon \to 0, y \to x \\ s \to t}} u^\epsilon(y,s) \ .$$

We have to prove that $\bar{u}$ is a subsolution of $(II.34)$ and $\underline{u}$ is a supersolution of $(II.34)$; since the proofs for the sub and supersolution cases are similar, we only present the arguments for the subsolution case.

Let $\phi : [0,+\infty) \times [0,T] \to \mathbb{R}$ be a smooth test-function and (x_1^0, t_0) be a strict maximum point of $\bar{u} - \phi$. In order to prove that $\bar{u}$ is a subsolution of $(II.34)$, we first consider the case when $x_1^0 > 0, t_0 > 0$ where we have to prove

$$\frac{\partial \phi}{\partial t}(x_1^0,t_0) + \bar{c}(x_1^0,t_0) \cdot e_1 \frac{\partial \phi}{\partial x_1}(x_1^0,t_0) \leq \\ \zeta(x_1^0,t_0)\phi(v) - R(P)\bar{\Theta}(x_1^0,t_0,u(x_1^0,t_0),v(x_1^0,t_0)) \qquad \text{(II.35)}$$

To apply the perturbed test-function method, we need the

Lemma 3.1. *The cell problem (II.26) has a X_1-periodic solution u_1 if and only if the parameters $\lambda, p, \mu, \nu, \delta, x_1, t$ satisfy Equation (II.31). Moreover this solution is unique up to an additive constant.*

Démonstration. The proof is standard and relies on the Fredholm alternative. By **(C2)**, the operator $\mathcal{L} := -\chi\Delta - c \cdot D$ together with Neumann boundary conditions, is self-adjoint

and the Strong Maximum Principle shows that the kernel of this operator only contains the constant functions. On the other hand, the computations of the previous subsection ensure that the right hand side of equation (II.26) (including the boundary condition) is orthogonal to the constant functions, i.e. the kernel of $\mathcal{L}$, if and only if Equation (II.31) holds. Therefore this condition implies the existence of a solution of (II.26), which is C^2 by using standard elliptic regularity. This solution is of course unique up to an additive constant because of the structure of the kernel. □

We pick some constant $0 < \gamma \ll 1$. In view of Lemma 3.1, for the choice of the parameters x_1^0, t_0, $\delta := \zeta(x_1^0, t_0)\varphi(v(x_1^0, t_0))$

$$\nu = v(x_1^0, t_0)\ ,\ \mu = u(x_1^0, t_0) - \gamma\ ,\ p = \frac{\partial \phi}{\partial x_1}(x_1^0, t_0)e_1 \tag{II.36}$$

and if we choose λ given by Equation (II.31), there exists a smooth solution $u_1(X)$ of (II.26) associated to these parameters.

We use this function to introduce the perturbed test-function ϕ^ϵ

$$\phi^\epsilon(x,t) = \phi(x_1,t) + \epsilon u_1(\frac{x}{\epsilon})\ .$$

By standard results ([38], p.88), for ϵ small enough, there exists a maximum point (x^ϵ, t^ϵ) of $u^\epsilon - \phi^\epsilon$ near $((x_1^0, 0, 0), t_0)$. Moreover

$$x^\epsilon \to (x_1^0, 0, 0), \quad t^\epsilon \to t_0 \quad \text{as} \quad \epsilon \to 0 \tag{II.37}$$

$$u^\epsilon(x^\epsilon, t^\epsilon) \to \bar{u}(x_1^0, t_0) \quad \text{as} \quad \epsilon \to 0 \tag{II.38}$$

First, we prove that the maximum point (x^ϵ, t^ϵ) can not be on the boundary for ϵ small enough. Otherwise, if $(x^\epsilon, t^\epsilon) \in \partial\Omega_\epsilon \times (0, T)$, then, by the maximum point property on the boundary

$$\frac{\partial}{\partial n}(u^\epsilon(x^\epsilon, t^\epsilon) - \phi(x_1^\epsilon, t^\epsilon) - \epsilon u_1(X^\epsilon)) \geq 0$$

where $X^\epsilon = x^\epsilon/\epsilon$, thus

$$\frac{\partial u^\epsilon}{\partial n}(x^\epsilon, t^\epsilon) - [\frac{\partial \phi}{\partial x_1}(x_1^\epsilon, t^\epsilon).e_1 + D_X u_1(X^\epsilon)].n \geq 0.$$

Using the smoothness of ϕ and recalling that $n(x^\epsilon) = N(X^\epsilon)$, we can write this inequality as

$$\frac{\partial u^\epsilon}{\partial n}(x^\epsilon, t^\epsilon) - [p + D_X u_1(X^\epsilon)] \cdot N \geq o(1), \tag{II.39}$$

where, here and below, $o(1)$ denotes a quantity which goes to 0 as ϵ tends to 0.

Recalling Equation (II.15) permits to obtain

$$-\frac{1}{\chi}\Theta\left(x_1^\epsilon, X^\epsilon, t^\epsilon, u^\epsilon(x_1^\epsilon, t^\epsilon), v^\epsilon(x_1^\epsilon, t^\epsilon)\right) - \Big(p + D_X u_1(X^\epsilon)\Big) \cdot N \geq o(1). \tag{II.40}$$

Because of (II.37)-(II.38) and the continuity properties of the functions η_p, η_a, ϱ and g_a and because of the convergence of v^ϵ, Equation (II.40) gives

$$-\Theta\left(x_1^0, X^\epsilon, t_0, \bar{u}(x_1^0, t^0), v(x_1^0, t^0))\right) - \chi\Big(p + D_X u_1(X^\epsilon)\Big) \cdot N \geq o(1).$$

Now we replace $\bar{u}(x_1^0, t^0)$ by $\mu + \gamma$

$$\Theta\left(x_1^0, X^\epsilon, t_0, \mu + \gamma, v(x_1^0, t^0))\right) - \chi\Big(p + D_X u_1(X^\epsilon)\Big) \cdot N \geq o(1).$$

Because of the properties of η_p, η_a, ϱ and g_a, $\Theta(x_1, X, t, u, v)$ is a strictly increasing function in u (uniformly wrt the other parameters) ; by using (II.26) together with (T2), we obtain

$$-\underline{\eta}\gamma \geq -\Theta\left(x_1^0, X^\epsilon, t_0, \mu + \gamma, v(x_1^0, t^0))\right) + \Theta\left(x_1^0, X^\epsilon, t_0, \mu, v(x_1^0, t^0))\right) \geq o(1) \tag{II.41}$$

which yields the contradiction.

Therefore the maximum point (x^ϵ, t^ϵ) of $u_\epsilon - \phi_\epsilon$ is in $\Omega_\epsilon \times (0, T)$. Since u_ϵ is a solution of (II.13), classical properties yield to the inequality

$$\begin{aligned}\frac{\partial \phi}{\partial t}(x_1^\epsilon, t^\epsilon) - \chi \Delta_X u_1(X^\epsilon) + c(x^\epsilon, X^\epsilon, t^\epsilon)\left(\frac{\partial \phi}{\partial x_1}(x_1^\epsilon, t^\epsilon) e_1 + D_X u_1(X^\epsilon)\right) \\ - \zeta(x_1^\epsilon, t^\epsilon)\varphi(v) \leq o(1).\end{aligned} \tag{II.42}$$

For ϵ small enough, using (II.37) and the regularity of ϕ imply

$$\frac{\partial \phi}{\partial t}(x_1^0, t^0) - \chi \Delta_X u_1(X^\epsilon) + c(x_1^0, X^\epsilon, t_0)(p + D_X u_1(X^\epsilon)) - \delta \leq o(1). \tag{II.43}$$

Furthermore, by Equation (II.26),

$$\lambda = -\chi \Delta u_1 + c(x_1^0, X^\epsilon, t_0)(p + D_X u_1) - \delta$$

which yields to the inequality

$$\frac{\partial \phi}{\partial t}(x_1^0, t_0) + \lambda \leq o(1).$$

As we already mentioned it above, this inequality is equivalent to the inequality (II.35) by just inserting the value of λ from Lemma 3.1 into the above equation and letting ϵ tend to 0. And the proof of this first case is complete.

We should now consider the cases when the maximum point is achieved either for $t = 0$ or at $x_1 = 0$ to complete the proof.

For the initial condition ($t = 0$), a combination of the above proof and classical arguments shows that we have the viscosity inequality

$$\min\{\frac{\partial \bar{u}}{\partial t} + \bar{c}(0,t) \cdot e_1 \frac{\partial \bar{u}}{\partial x_1} - \zeta(0,t)\varphi(v) + R(P)\Theta(x_1,t,u,v), \bar{u}\} \leq 0\,,$$

if $x_1 > 0$, while, for $x_1 = 0, t > 0$, one has

$$\min\{\frac{\partial \bar{u}}{\partial t} + \bar{c}(x_1,t) \cdot e_1 \frac{\partial \bar{u}}{\partial x_1} - \zeta(x_1,t)\varphi(v) + R(P)\Theta(x_1,t,u,v)), \bar{u} - u_0(t)\} \leq 0\,,$$

and for the case $x_1 = 0, t = 0$ –which is a priori a particular case–, since $u_0(0) = 0$, we can still use one of these inequalities which are the same.

It is proved (cf. ([38]p.99)[36]) that, if $\bar{u}$ is a subsolution of (II.34), then the above initial condition in viscosity sense reduces in fact to a classical one

$$\bar{u}(x_1^0, 0) \leq 0 \quad \text{on } [0, +\infty).$$

Since $\bar{c}(x_1,t) \cdot e_1 > 0$, the generalized Dirichlet condition reduces also to a classical one (cf. [38](cor 4.1 in p.169)), namely

$$\bar{u}(0,t) \leq u_0(t) \quad \text{on } [0,T),$$

as a consequence of the fact that the characteristic are pointing outward the domain on the boundary.

To conclude the proof, we invoke a (strong) comparison result for (II.34) : such result is classical and it yields $\bar{u} \leq \underline{u}$ on $[0, +\infty) \times [0,T]$, implying the desired convergence result.

It remains to prove that the u^ϵ's are indeed uniformly bounded. To this aim, we recall that Ω is a C^2-domain and therefore there exists a x_1-periodic, C^2-function $d : \bar{\Omega} \to [0, \infty)$ such that

$$Dd(x) \cdot N \leq -1 \quad \text{on} \quad \partial\Omega.$$

Because of the particular form of Ω, the function d, as well as its first and second derivatives, are also bounded functions.

Now, we introduce the functions $w^\epsilon : \bar{\Omega}_\epsilon \times [0,T] \to [0,\infty)$ given by

$$w^\epsilon(x,t) = k_1 + k_2 t + k_3(\epsilon||d||_\infty - \epsilon d(x/\epsilon))\,,$$

for some constants $k_1, k_2, k_3 \geq 0$. We first plug these functions into the boundary condition (II.15) : using that the v^ϵ's are bounded and that the absorption terms are positive, the supersolution condition is satisfied if we choose k_3 large enough. Then we consider Equation (II.13) : since d has bounded first and second derivatives, the supersolution condition is also satisfied by choosing k_2 large enough. Finally we choose k_1 large enough to treat the boundary condition (II.17).

Applying the Maximum Principle (or a comparison result for viscosity solutions) gives $u^\epsilon(x,t) \leq w^\epsilon(x,t)$ in $\overline{\Omega}_\epsilon \times [0,T]$ and the proof is complete. □

Chapitre III

Digestion Modelling in the Small Intestine : Impact of Dietary Fibre

In this work, we continue the modelling of the digestion in the small intestine, started in a previous article, by investigating the effects of dietary fibre. We recall that this model aims at taking into account the three main phenomena of the digestion, namely the transit of the bolus, the degradation of feedstuffs and the absorption through the intestinal wall. In order to study the role of dietary fibre on digestion, we model their two principal physiochemical characteristics which interact with the function of the small intestine, i.e. viscosity and water holding capacity. This leads us to consider some features of digestion which have not been taken into account previously, in particular the interrelationship between the evolution of dry matter and water in the bolus. The numerical results are in agreement with the positive effect of insoluble dietary fibre on the velocity of bolus along the small intestine and on its degradation. These results highlight the negative effect of soluble dietary fibre on digestion. Although, this model is generic and contains a large number of parameters, to our knowledge, it is among the first qualitative dynamical modelling of fibre influence on intestinal digestion [1].

1. Ce chapitre fait l'objet d'un preprint accessible en ligne sur le serveur HAL de CNRS,
Digestion modelling in the small intestine : impact of dietary fibre,
Masoomeh Taghipoor and Guy Barles and Christine Georgelin and Jean-René Licois and Philippe Lescoat.

1 Introduction

Digestion in the small intestine can be described through three main phenomena : transit of the bolus along the small intestine, degradation of macromolecules into smaller ones and absorption through intestinal wall. Taking into account these phenomena, the authors have presented in [8] a generic model of digestion in which the bolus include only one category of macromolecules (carbohydrates, proteins or lipids) and water.

However mixing these nutrients influences the digestion process through interactions between molecules. In order to improve this model and to make it more realistic, we should consider the effects of such interactions, and we have decided to do so by first including dietary fibre in the bolus because of their significant role on the digestion. One of the key properties of fibre is its water holding capacity and this leads us to investigate the role of water in the digestion processes. To do so, we distinguish dry matter and water in each substrate, we model water kinetic in correlation with the dry matter one and we take into account the impact of water in all the aspects of digestion.

To be more precise on our approach, we first describe the main underlying assumptions which guide our modelling, then we show how they are translated into equations and finally numerical tests are performed for examining the effects of several hypothesis. In addition, we point out known or assumed mechanisms relating dietary fibre and digestion process.

This paper is organized as follows : physiochemical characteristics of soluble and insoluble dietary fibre are introduced in Section 2. In Section 3, main assumptions of the model are presented. Section 4 is devoted to the description of the composition of bolus, the chemical transformations of macromolecules and all the notations. Digestion in the presence of dietary fibre includes the modification of transport as well as degradation and absorption equations as described in Section 5. Section 6 is a comparison of the numerical results considered as *in silico* experiments. Finally, in Section 7, the model is discussed and perspectives are proposed.

2 Biological Background on Water and Dietary Fibre

Digestion modelling requires the knowledges of the physiochemical properties of macromolecules concerned by this phenomenon as well as mechanical and biochemical reactions observed for their degradation.

Dietary fibre (DF) is usually defined as the sum of plant non-starch polysaccharides and lignin that are not hydrolysed by the enzymes secreted by the non-ruminant diges-

tive system, but that can be partially digested by microflora in the gut. A main effect of fibre is to regulate intestinal degradation and absorption of nutrients as well as their transit along the gut. Physiochemical characteristics of fibre include viscosity, hydration, fermentability (mostly in the large intestine), adsorption or entrapment of nutrients and bulking effect. Each of these characteristics affects meaningfully the function of the gastrointestinal tract [39, 40]. These characteristics depend on the polysaccharides chemistry. One way to classify dietary fibre is based on their water solubility. Insoluble dietary fibre include cellulose, some hemicelluloses and lignin. The other is soluble dietary fibre such as viscous fibre which includes beta-glucans, pectins, gums, mucilages and some hemicelluloses [41, 42].

For monogastrics, most available nutrients are degraded and absorbed in the small intestine. At the beginning of duodenum the bolus consists of partially degraded feedstuffs and water. Once in the small intestine, mechanical and chemical digestion of feedstuffs make the nutrients available to the organism. Enzymatic hydrolysis is the most important chemical reaction in digestion, which takes place in aqueous solution. Enough water is required for an efficient digestion process eventhough water/nutrient ratio are not precisely known. Furthermore, classification of dietary fibre through their water solubility and the impact of Water Holding Capacity (WHC) of DF on digestion reveals the key-role of water on digestion. WHC is defined by B. Shneeman [40] as the ability of fibre source to swell when mixed with water and to hold water within its matrix.

Soluble dietary fibre

Soluble DF are believed to impact significantly digestion and absorption as well as bolus transport in the small intestine. The main physiochemical properties of soluble DF are viscosity, water holding capacity (WHC) and organic compound entrapment [43]. Soluble DF, because of its high viscosity, is generally associated with slow transit through the stomach and increasing of the small intestinal transit time [44].

Insoluble dietary fibre

Insoluble DF acts primarily in the large intestine where, due to its WHC, increases faecal bulk, dilutes colonic contents and decreases mouth-to-anus transit time [43]. However, its effects on digestion and transit in the small intestine can not be neglected since insoluble DF affects the transit time in the small intestine through its laxative property. Recent studies have shown that the inclusion of a moderate level of dietary fibre improves the digestibility in chicks [45]. Therefore to obtain an optimal efficiency in nutrient utilization, Burhalter et al. [46] proposed to increase the ratio of insoluble to soluble DF. Moreover, the use of insoluble fibre in commercial broiler chicks improves the intestine

morphological parameters and result in a better performance assumed to be connected to more efficient digestion and absorption processes [47]. Two hypothesis are proposed in order to study the influence of insoluble DF on nutrients digestibility in the small intestine : (i) insoluble DF increases the retention time in the stomach changing the nutrient profile of the bolus at the entry of the small intestine which could lead to a higher digestion and absorption. (ii) Physical characteristics of insoluble DF change the digestion process mostly through their capacity of swelling water and nutrients. These both hypothesis are either tested in the *in silico* experiments (cf. Section 6.1) or included in the equations (cf. Section 5).

Water

To have a better understanding of the role of dietary fibre, it is therefore required to study more precisely the evolution of water during digestion in the small intestine. For example, depending on the bolus composition, water absorption through intestinal wall or its secretion into the small intestine lumen could be observed. However, the evolution of water amount in the small intestine depends also on other components' kinetics within the bolus as described by (Reaction 1), (Reaction 2) and (Reaction 3) in Section 4.

3 Key Model Assumptions

In this section, the key assumptions for the model are presented.

H1 : *Each component of the bolus (macromolecules, partially degraded macromolecules, nutrients and fibre) is represented mathematically as a portion of dry matter and a characteristic proportion of water.*

For example, "starch in a bolus" includes both dry starch and water used to maintain starch molecules in aqueous solution. The same is observed for the "disaccharides in a bolus" and "glucose in a bolus" combining smaller molecules resulting from starch hydrolysis associated with a specific level of water. In other words, a component C of bolus is represented as $C^{dm} + W_C$ where C^{dm} denotes the dry matter of C and W_C is the necessary amount of water to maintain it in a solution state. Moreover, we have assumed that the mass of W_C is proportional to the mass of C^{dm}, i.e. equal to $c\,C^{dm}$ for some characteristic number $c \geq 0$ whic represents the necessary amount of water proportion to maintain C in solubilized phase. Despite the presence of water in the bolus, a little amount of non-solubilized dry matter may be included in bolus, which is (of course) associated with $c = 0$.

H2 : *Without DF, the bolus contains a single macromolecule and water. It is represented by a homogeneous cylinder with the constant length ℓ. Including insoluble DF transforms this homogeneous bolus into an heterogeneous one by modifying the*

concentrations of feedstuffs and nutrients.

A bolus in the small intestine is a viscous solution of dry matter and water : we assume that its volume is very close to the volume occupied by the water in the bolus. In other words, our assumption is that DM does not fill any volume (e.g. : solubilized sugar + water does fill the same volume as the water alone). Once the volume is known, [H2] allows to compute the radius of the bolus $r(t)$, which impacts its movement along the small intestine. For a bolus with constant mass at the beginning of duodenum, [H2] influences the degradation by increasing the concentration of nutrients in the homogeneous part of bolus. Indeed the space occupied by insoluble dietary fibre is unavailable for the other macromolecules.

H3 : *Digestion in the small intestine is due to volumic and surfacic transformations. Volumic degradation is the enzymatic hydrolysis of bolus components by pancreatic and exogenous enzymes inside the bolus while the surfacic one is the degradation by brush border enzymes on the internal wall of small intestine.*

Some additional facts should be pointed out : water facilitates the contact of the macromolecules with the brush border enzymes, enhancing the surfacic degradation. Increasing the water to dry matter ratio dilutes the bolus and decreases the volumic degradation. Both of these reactions are proportional to the mass ratio of concerned substrates.

H4 : *The bolus movement along the small intestine is due to peristaltic waves. The efficiency of these waves are proportional to the radius of bolus, and inversely proportional to the distance from the pylorus.*

We use, in this article, the model of transport with an averaged velocity function as presented in [26]. The movement of the bolus in the model by this equation is due to a homogenized acceleration caused by the average effect of the peristaltic waves. Of course, there would no difficulty to come back to the model which takes into account all the frequent peristaltic waves.

H5 : *The water in the bolus which is not hold by the macromolecules and DF through WHC i.e. "available water", decreases the viscosity of the bolus and facilitates its movement. Due to osmotic type equilibrium, the concentration of this "available water" tends to reach a fixed ratio.*

In other words, "Available water" reduces the friction caused by the bolus contact with the intestinal wall.

H6 : *Dietary fibre modifies the bolus evolution through its WHC by holding the water in its matrix, and therefore modifying the volume of the bolus. Soluble DF decreases the efficiency of peristaltic waves.*

By their WHC, dietary fibre holds a significant quantity of water in the bolus and therefore keep the volume and the radius of the bolus higher. It is worth pointing out that soluble dietary fibre change the consistence of the bolus in the sense of making it more jelly, implying the decreases of efficiency of peristaltic waves.

4 Physiological Aspects and Bolus Composition

Different steps of mechanical and chemical transformations are detailed below. We present also the composition of the bolus and their interactions.

- **Non degradable substrate** A_{nd} **:** The quantity A_{nd} represents the mass of macromolecules which is not degradable by endogenous enzymes of the digestive tract.
- **Non solubilized substrate** A_{ns} **:** The quantity A_{ns} represents the mass of macromolecules which is not accessible to enzymatic hydrolysis. In presence of a sufficient quantity of water, A_{ns} is transformed into A_s.
- **Solubilized substrate** A_s^{dm} **:** The quantity A_s^{dm} is the mass of dry substrate in solution state. It is called solubilized substrate and it is assumed that one unit of A_s^{dm} requires W_s units of water to remain solubilized. Recalling [H1], W_s represents the required mass of water to solubilize A_s^{dm}. This quantity depends on the properties of each macromolecules. The mass of W_s is assumed to be equal to the mass of αA_s^{dm} where α represents the ratio of water associated with A_s^{dm}. For simplification purposes, the mix of A_s^{dm} and water is represented by A_s .
- **Intermediate substrate** B_{int}^{dm} **:** The quantity B_{int}^{dm} is the mass of dry intermediate substrate obtained from the degradation of A_s by volumic transformation [H3]. It is solubilized and W_{int} represents the required amount of water to maintain solubilization. The mass of W_{int} is assumed to be equal to the mass of βB_{int}^{dm} where β represents the ratio of water associated with B_{int}^{dm}. For $B_{int} = B_{int}^{dm} + W_{int}$, volumic transformation is represented as

  $$A_s + enzymes \rightarrow B_{int} + (W_s - W_{int}) \qquad \text{(Reaction 1)}$$

  Depending on the value of W_s and W_{int}, the amount of $W_s - W_{int}$ of water can be released or hold in the bolus.
- **Absorbable nutrients** B_{abs}^{dm} **:** The quantity B_{abs}^{dm} is the mass of dry absorbable nutrients obtained from surfacic reactions (cf. [H3]). For $B_{abs} = B_{abs}^{dm} + W_{abs}$, the surfacic transformation is defined as

  $$A_s + enzymes \rightarrow B_{abs} + (W_s - W_{abs}) \qquad \text{(Reaction 2)}$$

  $$B_{int} + enzymes \rightarrow B_{abs} + (W_{int} - W_{abs}) \qquad \text{(Reaction 3)}$$

  W_{abs} is the required amount of water to maintain solubilization and its mass is assumed to be equal to $\gamma\, B_{abs}^{dm}$ where γ represents the ratio of water associated with the B_{abs}^{dm}.
- **Soluble and insoluble dietary fibre :** F_{sol}^{dm} and F_{insol}^{dm} represent the soluble and non-soluble dry dietary fibre respectively. The main property of dietary fibre presented in Section 1 and hypothesis [H5] is its water holding capacity.

  $$F_{sol} = W_{sol} + F_{sol}^{dm}$$

$$F_{insol} = W_{insol} + F^{dm}_{insol}$$

where the mass of W_{sol} (W_{insol}) is assumed to be equal to $\lambda_s F^{dm}_{sol}$ ($\lambda_i F^{dm}_{insol}$) for λ_s and λ_i which represent the ratio of water associated with F^{dm}_{sol} and F^{dm}_{insol} respectively . As described in Section 1, DF is not degradable by endogenous enzymes of the small intestine.
The following diagram shows the different transformations inside the bolus.

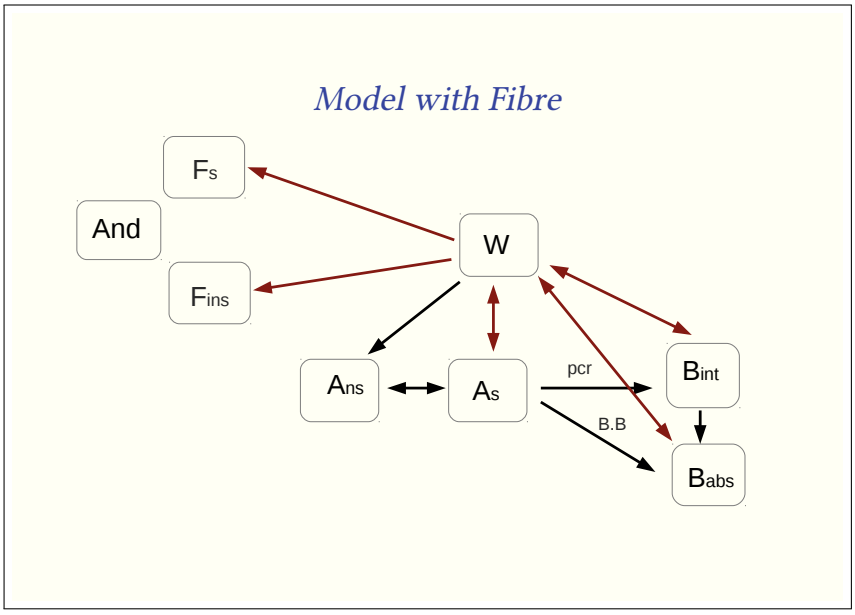

FIGURE III.1: Physical and chemical transformations inside the bolus and included in the model are represented in this scheme. “B.B“ stands for brush border enzymes and “pcr” stands for pancreatic ones.

- **Dry Matter :** Total amount of Dry Matter substrate in the bolus is therefore

$$DM = A_{nd} + A_{ns} + A^{dm}_s + B^{dm}_{int} + B^{dm}_{abs} + F^{dm}_{sol} + F^{dm}_{insol}.$$

- **Water :** Impact of dietary fibre on digestion is closely linked to their WHC capacity. Though, water evolution in the bolus has to be described to understand effects of DF on digestion.
  Total water W_{tot} in the bolus comes from three main sources
  (i) W_{feed} : water incorporated naturally in feedstuffs (e.g. : one gram of wheat contains 12 $\%$ of water). The amount of W_{feed} coming out of the stomach is assumed to be proportional to the ingested dry matter DM, $W_{feed} = K_{feed} \cdot DM$.
  (ii) W_{sec} : Water included in the endogenous secretions of saliva and stomach which is also assumed to be proportional to the ingested dry matter, $W_{sec} = K_{sec} \cdot DM$.
  (iii) W_{drink} : Drunk water is assumed to be independent to the quantity of DM.

Total water included in the bolus is therefore defined as the sum of W_{feed}, W_{sec} and W_{drink}

$$W_{tot} = W_{feed} + W_{sec} + W_{drink}.$$

Thereby, "available water", W, as presented in [H6], is defined as the difference between W_{tot} and the water associated with DM for maintaining the solution state. In term of mass, the quantity of "available water" in the bolus at each time is

$$W = W_{tot} - W_s - W_{int} - W_{abs} - W_{sol} - W_{insol} \ .$$

- **Mass of bolus** M **:** The total mass of bolus, M, is given by $M = DM + W_{tot}$.
- **Volume of bolus** V **:** To define the bolus volume, as explained in [H2], the volume of each substrate in solution is assumed to be the same as the volume filled by water associated with that substrate, i.e. the volume of A_s is equal to W_s/ρ_w, where $\rho_w = 1$ is the water density. The volume of bolus is therefore represented as

$$V = W_{tot} = \pi r^2 \ell \rho_w = \pi r^2 \ell.$$

Since the length of the bolus is assumed to be fixed, the volume evolution leads to compute the radius $r(t)$ of bolus at each time. Consequently its surface is written as $S = 2\pi r \ell$.
In the following section, the different properties of dietary fibre on the model of digestion are taken into account.

5 Model Equations

To include WHC property of soluble DF in the digestion model, the mix of F_{sol}^{dm} and W_{sol} is assumed to form a viscous gel in the bolus. Therefore in our model the mass of "available water" in the bolus is reduced. Moreover, viscous fibre enhances motility but decreases transit rate, since it resists propulsive contractions [48]. This resistance to peristaltic waves is described through a new notion called efficient radius of bolus called r_{sol}. As described in [H2], the volume filled by soluble DF is $W_{sol} = \lambda_s F_{sol}$, then

Definition 5.1. *The efficient radius of bolus is defined as*

$$r_{sol} = \sqrt{(W_{tot} - W_{sol})/2\pi\ell}.$$

In the same way, the efficient surface of bolus is described as $S_{sol} = 2\pi r_{sol}\ell$.

This definition is used to describe the decrease of the surfacic degradation and absorption caused by soluble DF in the model.

One of the hypothesis in the first model of digestion in [8] is the bolus homogeneity. The mass concentration of each component of the bolus is assumed to be its mass divided

by the total mass M of the bolus. To model the digestion in presence of insoluble DF, new notions are defined because of heterogeneity of bolus as described in [H2]. The volume filled by insoluble DF (the mix of F^{dm}_{insol} and W_{insol}), is assumed to be unavailable to the macromolecules of feedstuffs in the bolus. In the digestion model, this hypothesis is taken into account by the following definition.

Definition 5.2. *The apparent concentration of different substrates in the bolus is represented as*

$$[A^{dm}_s] = \frac{A^{dm}_s}{M - F_{insol}}, \quad [B^{dm}_{int}] = \frac{B^{dm}_{int}}{M - F_{insol}}, [B^{dm}_{abs}] = \frac{B^{dm}_{abs}}{M - F_{insol}}$$

$$[A_{ns}] = \frac{A_{ns}}{M - F_{insol}}, \quad [W] = \frac{W}{M - F_{insol}}, \quad [A_{nd}] = \frac{A_{nd}}{M - F_{insol}}$$

The degradation of macromolecules A_s and B_{int} as well as the absorption of the nutrients B_{abs} are affected by WHC property of the insoluble DF through this definition. Figure III.2 shows the regions of bolus which are filled by insoluble DF and therefore unreachable by the macromolecules and nutrients.

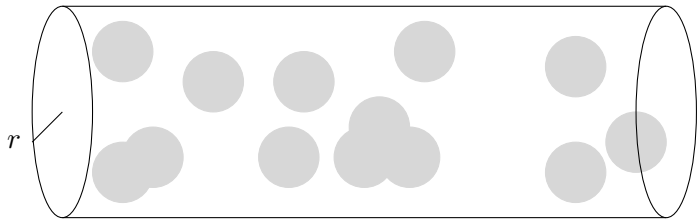

FIGURE III.2: The distribution of insoluble fibre in the bolus as assumed in the model. The apparent volume V_{app} (see Definition 5.3) is the white part of the cylinder.

Integrating the insoluble DF in the bolus changes also the region reachable to volumic degradation (see Figure III.2). According to hypothesis [H2], W_{insol} is the volume filled by insoluble fibre.

Definition 5.3. *The apparent volume of bolus V_{app} is therefore defined as*

$$V_{app} = W_{tot} - W_{insol}.$$

The above considerations are taken into account in the following steps of digestion described below.

5.1 Transport of bolus

The averaged equation of transport of bolus introduced in [26] reads

$$\frac{d^2x}{dt^2} = \tau(1 - c^{-1}\frac{dx}{dt})\frac{c_0 + c_1 r}{a + bx} - \frac{K_{visco}}{[W]}\frac{dx}{dt},$$

where τ is the mean effect of the pulses by unit of time, c is mean velocity of peristaltic waves, x the position in the small intestine. Taking into account the properties of dietary fibre, this equation changes to

$$\frac{d^2x}{dt^2} = \tau(1 - c^{-1}\frac{dx}{dt})\frac{c_0 + c_1 r_{sol}}{a + bx} - \frac{K_{visco}}{[W]}\frac{dx}{dt}. \tag{III.1}$$

The bolus movement described by this equation depends on its position in the small intestine and on its efficient radius. Moreover, the acceleration is slowed down by a viscosity term which depends on the available water.

5.2 Volumic transformation

Volumic transformation presented by (Reaction 1) in Section 4 is the degradation of A_s^{dm} due to pancreatic and exogenous enzymes resulting in production of B_{int}^{dm}. Evolution of A_s^{dm} by this transformation is represented by

$$\frac{dA_s^{dm}}{dt} = -k_{vol}(x)[A_s^{dm}]V_{app}$$

where $k_{vol}(x)$ takes into account the enzymatic activity which is a function of bolus position at each time t. The term $[A_s^{dm}]V_{app}$ describes the dependence of volumic degradation on the concentration of A_s^{dm} at each unit of apparent volume i.e. the volume filled by the insoluble DF is not accessible to the enzymes and macromolecules.

Consequently, integrating the insoluble fibre in the bolus influences the volumic transformation by increasing the substrates concentration via the Definition 5.2 and by changing the volume and using V_{app} introduced in Definition 5.3.

As described in Section 5.1, integrating the soluble fibre modifies the velocity of bolus along the small intestine and therefore the distance travelled at each time $x(t)$. Consequently, it influences the volumic degradation through the function $k_{vol}(x(t))$.

This reaction takes place in a solution and each unit of A_s^{dm} degraded by this equation causes the release of "available water" $W_s = \alpha A_s^{dm}$.

The volumic production of intermediate substrate B_{int}^{dm} is the result of degradation of A_s^{dm}

$$\frac{dB_{int}^{dm}}{dt} = k_{vol}(x)[A_s^{dm}]V_{app}.$$

Each unit of produced B_{int}^{dm} requires and uses $W_{int} = \beta B_{int}^{dm}$ to maintain the solution state. According to (Reaction 1), the result of volumic transformation is the consumption or release of "available water" W. Thereby, volumic evolution of water is represented as

$$\frac{dW}{dt} = \tilde{k}_{vol}(x)[A_s^{dm}]V_{app}\ , \tag{III.2}$$

where $\tilde{k}_{vol} = (\alpha - \beta)k_{vol}$.

Soluble fibre can be hydrolysed by exogenous enzymes e_{exo} (cellulase, hemicellulases, ...) ingested by food

$$F_{sol} + e_{exo} \rightarrow B_{int} + (W_{ol} - W_{int}). \tag{Reaction 4}$$

Hydrolysis of F_{sol} by exogenous enzymes follows the same evolution as the volumic transformation of A_s^{dm}

$$\frac{dF_{sol}^{dm}}{dt} = -k_s e_{exo} \tilde{ph}(x)[F_{sol}^{dm}]V_{app}$$

where $[F_{sol}^{dm}] = F_{sol}/(M - F_{insol})$ and $\tilde{ph}(x)$ is the exogenous enzyme activity along the small intestine. This reaction produces the intermediate substrate B_{int}^{dm}

$$\frac{dB_{int}^{dm}}{dt} = k_s e_{exo} \tilde{ph}(x)[F_{sol}^{dm}]V_{app}.$$

The amount $(W_{sol} - W_{int})$ is released by (Reaction 4) and modifies the evolution of water

$$\frac{dW}{dt} = ... + \tilde{k}_s e_{exo} \tilde{ph}(x)[F_{sol}^{dm}]V_{app} \tag{III.3}$$

where $\tilde{k}_s = (\lambda_s - \beta)k_s$.

5.3 Surfacic transformation

Surfacic degradation is the last step of transformation of macromolecules in the small intestine. The produced nutrients by this degradation are then absorbed through intestinal wall. Surfacic degradation depends on the fraction of A_s on the surface of the bolus represented by $[A_s]S_{sol}$ therefore

$$\frac{dA_s^{dm}}{dt} = -k_{surf}[A_s][W]S_{sol}$$

where k_{surf} stands for the rate of surfacic degradation of A_s and the efficient surface S_{sol} has been defined by Definition 5.1. Moreover, it is assumed that the brush-border enzymes are always in excess in the small intestine. Surfacic degradation of B_{int}^{dm} follows the same process as for A_s^{dm}. Therefore for $[B_{int}]$ defined by Definition 5.2, we have

$$\frac{dB_{int}^{dm}}{dt} = -\tilde{k}_{surf}[B_{int}][W]S_{sol}.$$

where k_{surf} stands for the rate of surfacic degradation of B_{int}. Evolution of water in the bolus is influenced by the surfacic degradation, i.e. the quantity of water consumed (or released) by (Reaction 2). Therefore the surfacic evolution of water is

$$\frac{dW}{dt} = ... + \Big((\beta-\gamma)\tilde{k}_{surf}[B_{int}] + (\alpha-\gamma)k_{surf}[A_s]\Big)[W]S_{sol}. \tag{III.4}$$

5.4 The equilibrium between A_s and A_{ns}

Modifications of feedstuffs in the stomach by the enzymes and water change most of the A_{ns} into $A_s = A_s^{dm} + W_s$ and makes them accessible to intestinal enzymes.

However, for some feedstuffs, the bolus may contain A_{ns} at the beginning of small intestine. In this case, the digestion of bolus contains also the transformation of A_{ns} into A_s. Mixing with bile acid for lipids and producing the micelles, denaturing for the proteins and adding water and solubilization for the dry starch are examples of the transformation of A_{ns} into A_s in the small intestine.

The solubilization of A_{ns} which takes place in the presence of enough quantity of W and results in the production of A_s, is a phenomenon taken into account in the model. Solubilization is reversible and lack of water may cause production of A_{ns} releasing W in the bolus.

Thereby, the balance is assumed to be reached when

$$A_s = \mu([W])A_{ns}$$

for μ which is an increasing function of $[W]$. If k_{equi} stands for the rate of turning back to equilibrium then the dynamical equilibrium may be defined

$$\frac{dA_{ns}}{dt} = -k_{equi}\big(\mu([W])A_{ns} - A_s\big) \tag{III.5}$$

and therefore

$$\frac{dA_s^{dm}}{dt} = k_{equi}\big(\mu([W])A_{ns} - A_s\big).$$

The variation of water quantity caused by the equilibrium may be represented as

$$\frac{dW}{dt} = ... + \alpha k_{equi}\big(\mu([W])A_{ns} - A_s\big). \tag{III.6}$$

5.5 Pancreatic and biliary secretions

Pancreatic and biliary secretions consist of a solution of nutrients and enzymes which do not contain available water W. In fact, water included in this solution is assumed to be associated with nutrients and enzymes to keep them solubilized. Modelling details on these secretions could be seen in [8]. Adding dietary fibre increases the quantity of pancreatic secretions. However this point is not yet included in the model.

5.6 Absorption through intestinal wall

Absorption of nutrients through intestinal wall depends on their concentration on the inner surface of intestinal wall

$$\frac{dB_{abs}^{dm}}{dt} = ... - k_{abs}[B_{abs}^{dm}]S_{sol}$$

The passage of nutrient through intestinal wall releases the associated water, thus

$$\frac{dW}{dt} = ... + \gamma k_{abs}[B_{abs}^{dm}]S_{sol} \tag{III.7}$$

where k_{abs} represents the rate of absorption through intestinal wall.

5.7 Water equilibrium

Water equilibrium was already taken into account in [8]. The assumption was that $[W]$ tends to reach a fixed ratio (10%), suggesting the equation

$$\frac{d[W]}{dt} = -k_w([W] - 0.1) \tag{III.8}$$

where $[W] = W(t)/M(t)$, $M(t)$ representing the bolus mass. The superposition of the equations (III.2), (III.3), (III.4), (III.6), (III.7) and (III.8) provides the equation describing the evolution of W along the small intestine.

The evolution of bolus mass is represented as

$$\frac{dM}{dt} = (\alpha+1)\frac{dA_s^{dm}}{dt} + (\beta+1)\frac{dB_{int}^{dm}}{dt} + (\gamma+1)\frac{dB_{abs}^{dm}}{dt} + (\lambda_{sol}+1)\frac{dF_{sol}^{dm}}{dt} + \frac{dA_{ns}}{dt} + \frac{dW}{dt},$$

each term of the above equation is replaced by its expression, therefore we obtain

$$\frac{dM}{dt} = \frac{M}{M-W}(-k_w(W - 0.1M) - k_{abs}[B_{abs}^{dm}]S_{sol}). \tag{III.9}$$

The variation of bolus volume depends on the absorption or secretion of "available water" and endogenous secretions in the small intestine i.e.

$$\frac{dV}{dt} = \frac{dW}{dt}, \tag{III.10}$$

therefore

$$\frac{dV}{dt} = -k_w(W - 0.1M) + \text{Secretions.}$$

6 Numerical Simulations

A thorough examination of the effects of the different parameters of the model on transport, degradation and absorption is carried out by Scilab software. In these *in silico* experiences, the presence of dietary fibre F_{sol} and F_{insol} in the bolus, the variation of the initial values of bolus and the sensitivity of the model on the parameters α, β and γ (cf. Section 4) are investigated.

The mass of the bolus at the entry of the small intestine is assumed to be fixed in all our following experiences. The bolus at the entry of the small intestine contains A_{nd}, A_{ns}, A_s, B_{int}, B_{abs} and W. When studying the influence of dietary fibre on digestion, the non degradable substrate A_{nd} is replaced by F_{sol} or F_{insol}.

6.1 Influence of dietary fibre on intestinal absorption

As described in Section 1, the positive effect of insoluble DF in digestion may be due to two main reasons : (i) modification of the composition of bolus due to the increase of retention time in the stomach, (ii) modification of the bolus physical characteristics.

The effects of these two cases on the digestion model are studied in this section.

Influence of the modification of the bolus in the stomach

Including insoluble DF in the bolus delays gastric emptying. The direct effect of this phenomenon is to increase the solubilization in the bolus and to start partially the degradation. We studied the effects of such a change in the initial conditions for our model. To this aim, two numerical experiences are carried out : (a) the increase in the ratio of A_s to A_{ns} and (b) the increase in the ratio of B_{int} to A_s when $A_{ns} = 0$.

(a) Our first experience consists in increasing the ratio of A_s to A_{ns} in the bolus at the entry of the small intestine. The value of absorbed dry nutrients at the end of the small intestine does not vary meaningfully. Table III.1 shows the absorbed dry nutrients to DM ratio at the end of ileum $x = 17$ for different for the different A_s^{dm} to DM ratio at the beginning of the small intestine. Despite the variations in

$x = 0$		End of the small intestine $x = 17$
$A_s^{dm}.DM^{-1}$ (%)	$A_{ns}.DM^{-1}$ (%)	Absorbed dry nutrients to DM ratio (%)
0	85	56
42	42	57
85	0	58

TABLE III.1: The proportion of absorbed nutrients to DM for different scenarios of solubilization in the bolus at the entry of duodenum.

the ratio of A_s to A_{ns}, the equilibrium between A_s and A_{ns} defined by Equation (III.5) is reached quickly (see Figure III.3). The sensitivity analysis shows also that the value of absorbed dry nutrients is almost independent to the variations in the ratio of A_s to A_{ns}. However, this results depend on the choice of equilibrium rate k_{equi}, a small value of k_{equi} may decrease the difference between the final values of absorbed nutrients.

(b) In the second experience, the modification in the stomach is assumed to result in the transformation of all A_{ns} in the bolus into A_s and additionally the production of B_{int}. Variations in the ratio of A_s to B_{int} inside the bolus at the entry of the small intestine are tested. Table III.2 shows the variation of absorbed dry nutrients at the end of the small intestine as a function of the initial value of B_{int}.
Numerical results shows the increase in absorbed dry nutrients when the ratio of B_{int} to A_s is increased.

$x = 0$		End of the small intestine $x = 17$
$B_{int}^{dm}.DM^{-1}$ (%)	$A_s.DM^{-1}$ (%)	Absorbed dry nutrients to DM ratio (%)
0	85	57
42	42	61
85	0	64

TABLE III.2: The relation between the absorbed dry nutrients at the end of digestion and the different initial values of B_{int}^{dm}.

Direct effect of DF on the function of the small intestine

Besides the modification of the bolus in the stomach, presence of insoluble DF changes also the physiochemical characteristics of bolus (Section 5).

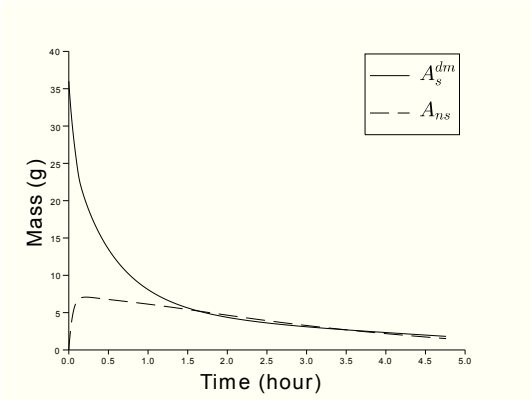

(a) $A_s^{dm} = 36$, $A_{ns} = 0$

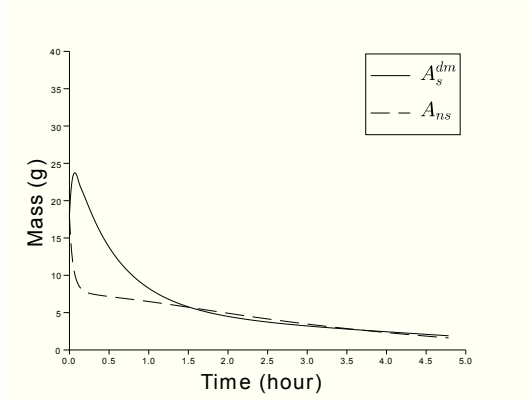

(b) $A_s^{dm} = 18$, $A_{ns} = 18$

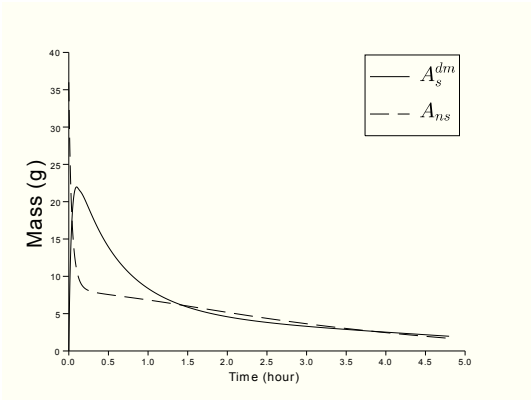

(c) $A_s^{dm} = 0$, $A_{ns} = 36$

FIGURE III.3: The equilibrium $A_s^{dm} - A_{ns}$ is reached quickly for different initial value of A_s.

To observe the effect of DF in the model of digestion, value of insoluble and soluble DF was increased from $1\ g$ to $5\ g$ in a bolus of $120\ g$.

Figure III.4 shows that the presence of insoluble DF promotes intestinal absorption, however this increase in absorbed dry nutrients is not meaningful. The results in this figure, show that the increasing of the value of soluble DF decreases the quantity of absorbed dry nutrients and increases the final total mass.

Therefore, numerical simulation shows that the positive effect of insoluble DF on the amount of absorbed dry nutrients is mainly due to the modification of the bolus in the stomach. However, the effect of the interaction of bolus with the small intestine as described in Figure III.4 may not be neglected.

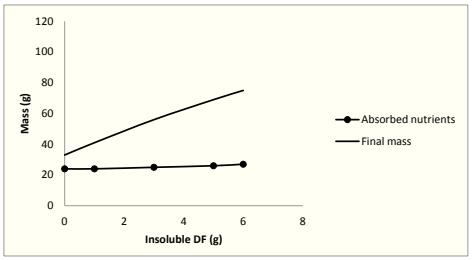

(a) Aborption versus F_{ins}

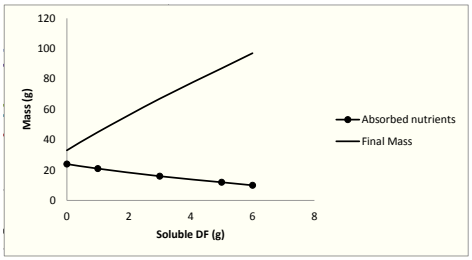

(b) Aborption versus F_s

FIGURE III.4: Change in the final mass of bolus and absorbed dry nutrients for different amount of DF in the bolus at the entry of duodenum.

Time of intestinal transit in the presence of DF

Numerical results of transit time in presence of DF are presente in Table III.3.

These results show that integrating insoluble DF in the bolus decreases the time of intestinal transit from $5\,h$ for a bolus of $120\,g$ without insoluble DF to $3,9\,h$ for a bolus of the same mass which contains $5\,g$ of DF. These results are consistent with published values. The experiences done by Wilfart et al. [13] have shown that increasing dietary fibre content reduced or tended to reduce the mean retention time in the small intestine.

These results show that integrating soluble DF in the bolus increases the intestinal digestion time from $5\,h$ to $6,7\,h$ illustrating the effect of viscosity due to soluble DF on transit time.

$x = 0$	Intestinal transit time (hour)	
$F \cdot DM^{-1}$ (%)	bolus containing F_{insol}	bolus containing F_{sol}
0	5	5
2	$4,7$	$5,4$
7	$4,3$	$5,9$
11	4	$6,5$
14	$3,9$	$6,7$

TABLE III.3: Intestinal transit time for the different quantities of $F = F_{sol}$ or F_{insol} in the bolus at the entry of duodenum

6.2 Water associated to dry matter

To study the influence of the quantity of associated water on digestion, variation of the values of α, β and γ have been tested. We observe their influence on digestion and specifically on the absorbed dry nutrients and A_s-A_{ns} equilibrium. Two main simulations are carried out : an uniform water content for A_s, B_{int} and B_{abs} i.e. $\alpha = \beta = \gamma$ and a a non uniform one.

The objective of these experiences is to understand how the different values of α, β and γ influence the digestion in our modelling.

a. Uniform water content for A_s, B_{int} and B_{abs}

The value of $\alpha = \beta = \gamma$ varied from 1 to 4 in the model presented in section 5. Our objective is to observe its effect on the value of absorbed dry nutrients as well as on the final mass of bolus.

Numerical results presented in Figure III.5 show the negative effect of this increase on the absorbed dry nutrients. Increasing the quantity of water (α, β and γ) associated with the dry feedstuffs (A_s^{dm}, B_{int}^{m} and B_{abs}^{dm}) in our model, dilutes the bolus and decreases the volumic degradation, it decreases also the quantity of dry nutrients in contact with the internal surface of the bolus. These results seems to be consistent with the reality, in fact,

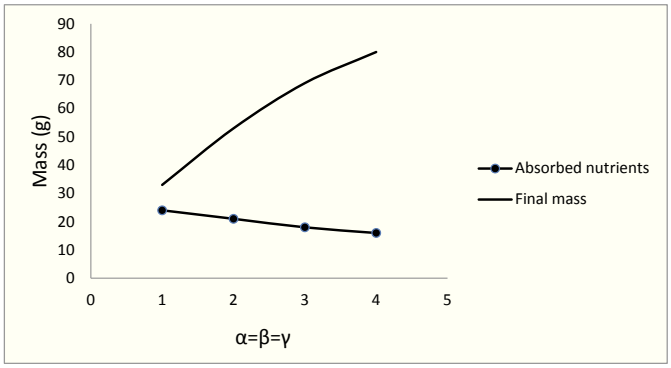

FIGURE III.5: Dependence of the absorbed dry nutrients and the final mass of bolus at the end of the small intestine on the value of α, β and γ.

the more water is presented in the bolus, the less (pancreatic and brush border) enzymes

and molecules are in contact.

We are also interested by the effect of these variations on the $A_s^{dm} - A_{ns}$ equilibrium defined by Equation (III.5). The results are shown in Figure III.6. The equilibrium is almost reached in the four experiences, however the choice of k_{equi} can change the necessary time to reach the equilibrium. A significant production of A_{ns} is observed in Figure III.6.d because of the lack of the available water at the beginning of the small intestine.

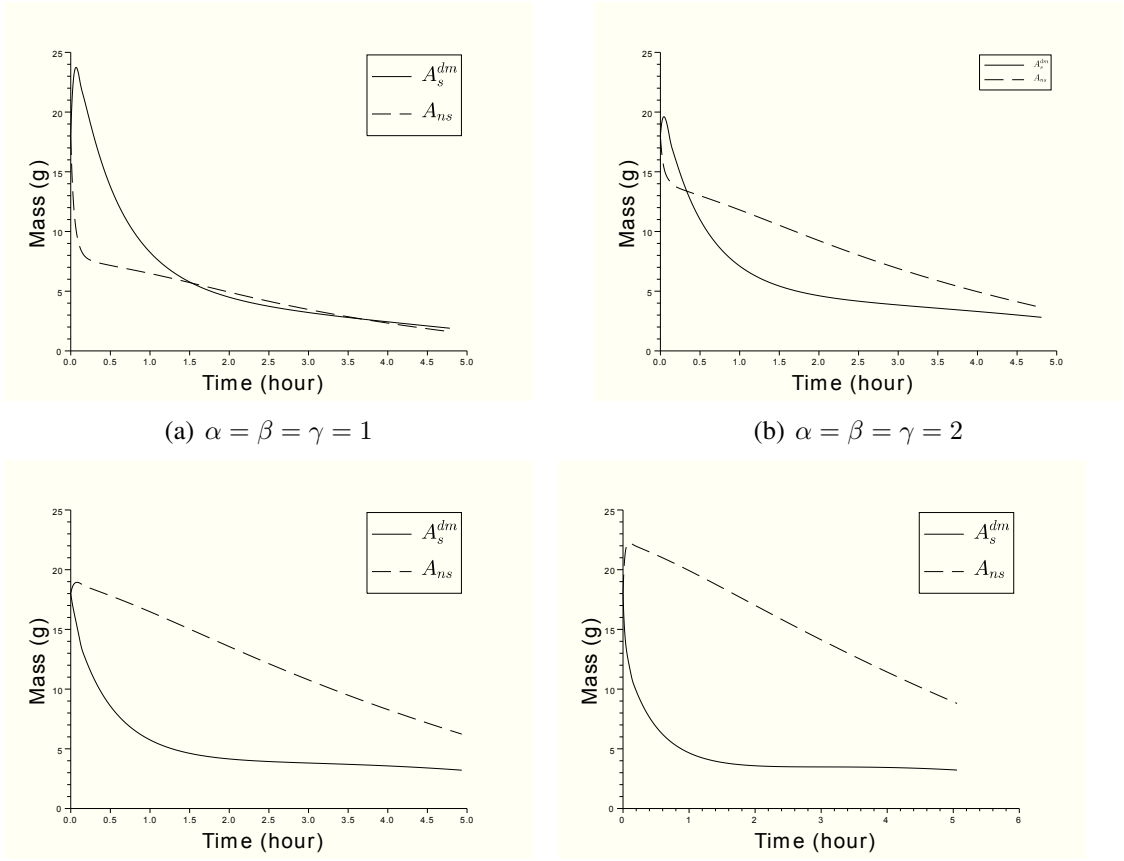

(a) $\alpha = \beta = \gamma = 1$ (b) $\alpha = \beta = \gamma = 2$

(c) $\alpha = \beta = \gamma = 3$ (d) $\alpha = \beta = \gamma = 4$

FIGURE III.6: The evolution of the equilibrium $A_s^{dm} - A_{ns}$ depends strongly on the quantity of α, β and γ.

b. Non-uniform water content for A_s, B_{int} and B_{abs}

In the second experience, the quantity of absorbed dry nutrients at the end of the small intestine and the numerical results of A_s-A_{ns} equilibrium for different values of α, β and γ were observed. The choice of the values of A_s, B_{int} and B_{abs} is based on the hypothesis that the value of β is always between the values of α and γ because of the molecule

size of B_{int}^{dm}. Even if the longest transit time was observed for $\alpha < \beta < \gamma$, it shows the

	Absorbed dry nutrients to DM ratio (%)	Retention time in the small intestine (h)
$\alpha = 1$, $\beta = 2$, $\gamma = 3$	45	$5,2$
$\alpha = 2\,\beta = 2$, $\gamma = 2$	50	$4,9$
$\alpha = 3$, $\beta = 2$, $\gamma = 1$	54	$4,6$

TABLE III.4: Transit time and absorbed dry nutrients at the end of the small intestine depend on the values of α, β and γ.

lowest level of dry absorbed nutrients. This stresses the key-role of "available water" W on digestion.

$A_s - A_{ns}$ equilibrium is observed in two cases :

(i) Firstly, it was assumed that $\alpha > \beta > \gamma$. There is a little production of A_{ns} from A_s (desoubilization) because of the lack of water at the entry of the small intestine followed by the degradation of A_s.

(ii) Secondly, it was assumed that $\alpha < \beta < \gamma$. There is a rapid solubilization of A_{ns} followed by degradation of A_s into B_{int}. The released water by degradation of A_s is not sufficient to maintain the solution state of B_{int} since $\alpha < \beta$. The required water is provided by the transformation of A_s into A_{ns} as it can be seen in the Figure III.7.

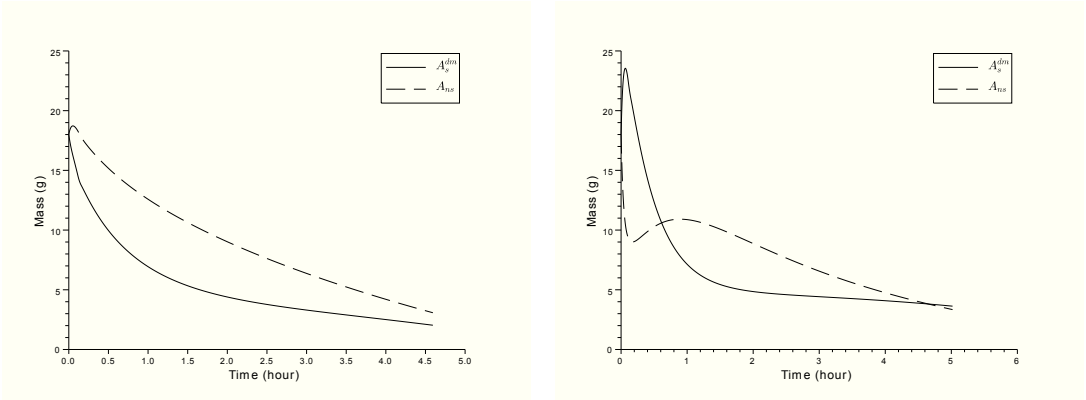

(a) $\alpha > \beta > \gamma$ (b) $\alpha < \beta < \gamma$

FIGURE III.7: The equilibrium $A_s^{dm} - A_{ns}$ for different quantity of α, β and γ.

6.3 The variation of the water ratio inside the bolus

We are interested by the change in the ratio of W inside the bolus and its influence on the absorption in the small intestine. For the sake of simplicity, it was assumed that $W_{feed} = W_{sec} = 0$.

In order to study this effect, the value of dry matter in the bolus is assumed fixed at $42\,g$ while the value of water increases in each experience.

In the numerical simulations, the ratio of water included in the bolus represented 55%, 60% and 66% of bolus. The *ratio of absorbed dry nutrients to the total absorption (water and nutrients)* is collected. Results are presented in Table III.5. The numerical results of

$(\%)$ Amount of water at $x = 0$ inside bolus	$(\%)$ Ratio of absorbed dry nutrients at $x = 17$	(g) Mass of Absorbed dry nutrients	Transit time (hour)
50	50	25	$5,7$
60	35	26	$5,2$
66	28	27	$4,5$

TABLE III.5: Dependence of absorbed dry nutrients to the water ratio. DM stands for the amount of dry matter in the bolus at the entry of bolus.

Table III.5 shows that increasing the value of water in the bolus decreases the *ratio of absorbed dry nutrient to the total absorbed matter (water+dry nutrients)*, even though the value of absorbed dry nutrients increases.

In fact, in our model, at the end of each experience the value of W_t is approximatively 55% of the total mass of bolus and this equilibrium is achieved almost quickly (because of the choice of k_w). Therefore, increasing the value of water in this model does not have a meaningful effect on the final absorption and the slight increase in the absorbed mass of dry nutrients is due to the change of the volume of bolus in each experience which promotes the access of nutrients to intestinal wall for absorption, although this increase dilutes the bolus and decreases the volumic degradation. Here again, this is the direct result the choice of the parameters (rate of surfacic (k_{surf}) and volumic (k_{vol}) degradation).

7 Discussion

In this paper, we have continued the modelling of the digestion in the small intestine started in [8]. The objective was to obtain a more realistic model of digestion process by including new phenomena and completing the others : DM and water are treated sep-

arately, water evolution is influenced by the degradation of other molecules, the effects of DF on the digestion are taken into account which is also a first step toward a non-homogeneous model with different types of feedstuffs.

The advantages and the defects of this model as well as the perspectives are outlined in the following paragraphs.

One of the main aspect of this model remains its genericity, we have tried to identify and model the main generic phenomena of digestion and ignored or implicitly taken into account in the parameters the ones which required the specific properties of feedstuffs' molecules (effects on gastric emptying, on viscosity,...etc.). The different steps of digestion (equilibrium between A_{ns} and A_s, successive transformation of A_s into B_{int} and B_{abs}), the effects of physical characteristic of bolus (surface and volume) on its degradation and transit, the interaction between DF and feedstuffs molecules (among others) have been considered while some other phenomena like the separation between the enzyme activities of different feedstuffs' molecules, dependence of the enzyme activity with respect to the dilution of bolus, the different substrates density, the impact of DF on initial condition (and others) have been ignored.

To our point of view, we obtained a more realistic model by integrating these new phenomena in the model of digestion. In particular, the WHC of dietary fibre which in turn interferes the digestion of other feedstuffs molecules, leads us to introduce the separation between DM and water and consider all the effects of water.

However, some other phenomena are still ignored either because of the lack of information concerning their effects or because of their supposed little impact on digestion at this scale. Of course, It would be interesting to include in the model the phenomena like interaction between different categories of feedstuffs and then define the specific enzyme activity for different cases to exploit their potential to impact the digestion. The future development of the model will be based on these new objectives.

Modelling the influence of soluble and insoluble DF on the initial condition and on degradation of other feedstuffs' molecules as well as on the movement of bolus (Experience 6.1) is the first try to model a more realistic non-homogeneous bolus. DF have normally a high WHC which increases the volume of aqueous phase in the bolus and therefore dilutes the solution of nutrients and enzymes [49]. This is known to influence the volumic and surfacic reactions. However, these effects depend highly to the choice of W_{sol} and W_{insol}. Another aspect of the model is the water equilibrium and its impact on absorption, here again the choice of parameters (W_{as}, W_{int} and W_{abs}) plays significant role on the final results of digestion.

On the other hand, Experience 6.3 reveals the role of other parameters of model (k_w, k_{equi}, k_{surf}, k_{vol}). As it has been described in this experience, the change of water absorption rate k_w, can change (even inverse) the numerical results. However, it is worth

pointing that the choice of the model parameters are based on the observed behaviours (literature), the results are therefore consistent qualitatively with the reality (positive influence of insoluble DF on digestion, negative effect of soluble DF, ...).

Taking into account these new phenomena requires the introduction of new parameters which can be identified with the help of existing experimental data. To the best of our knowledge, some of these parameters like the water associated to dry nutrients (W_{sol} , W_{insol}, W_{as}, W_{int} and W_{abs}) are introduced for the first time and they should be identified

One of the advantages of this model is its capacity to be reduced and to be adapt to the new experiences which makes the parameters identification possible. Reduction consists in the decreasing the number of equations of system or the number of parameters without affecting its genericity (e.g. a bolus which does not contain the DF, results in a more simplified digestion process which in turn caused decreasing the equations (parameters) involved in the digestion model).

It is also worth pointing that the value of most of the parameters depends to the special category of feedstuffs. The close collaborations between biologists and mathematicians is therefore required to identify these new parameters (literature data in biology, define the new experimentations, ...). This reveals one of the main interest of modelling which is to ask the precise questions about the modeled phenomenon. In fact, this approach allows to use all the existing data and limit the new animal experimentation to the special cases (when the existing data are not sufficient).

8 Appendix

8.1 The Model equations

◇ Equation of transport

$$\frac{d^2x}{dt^2} = \tau(1 - C^{-1}\frac{dx}{dt})\frac{c_0 + c_1 r_{sol}}{a + bx} - \frac{K_{visco}}{[W]}\frac{dx}{dt}.$$

◇ Non solubilized substrate A_{ns}

$$\frac{dA_{ns}}{dt} = -k_{equi}\big(\mu([W])A_{ns} - A_s\big)$$

◇ Soluble DF F_{sol}

$$\frac{dF_{sol}^{dm}}{dt} = -k_s e_{exo}\tilde{ph}(x)[F_{sol}^{dm}]V_{app}$$

◇ Solubilized substrate A_s^{dm}

$$\frac{dA_s^{dm}}{dt} = -k_{vol}(x)[A_s^{dm}]V_{app} - k_{surf}[A_s][W]S_{sol} + k_{equi}\big(\mu([W])A_{ns} - A_s\big) + \text{secretions}$$

◇ Intermediate substrate B_{int}^{dm}

$$\frac{dB_{int}^{dm}}{dt} = k_{vol}(t)[A_s^{dm}]V_{app} + k_s e_{exo}\tilde{ph}(x)[F_{sol}^{dm}]V_{app} - \tilde{k}_{surf}[B_{int}][W]S_{sol} + \text{secretions}$$

◇ Absorbable nutrients B_{abs}^{dm}

$$\frac{dB_{abs}^{dm}}{dt} = \Big(\tilde{k}_{surf}[B_{int}] + k_{surf}[A_s]\Big)[W]S_{sol} - k_{abs}[B_{abs}^{dm}]S_{sol}$$

◇ Exogenous enzymes $e(t)$

$$\frac{de}{dt} = -k_e e$$

◇ Free Water Evolution W(t)

$$\begin{aligned}\frac{dW}{dt} =& -\alpha k_{equi}\big(\mu([W])A_{ns} - A_s\big) + (\alpha-\beta)k_{vol}(t)[A_s^{dm}]V_{app} \\ &+ [W]\Big((\beta-\gamma)\tilde{k}_{surf}[B_{int}] + (\alpha-\gamma)k_{surf}[A_s]\Big) \\ &+ (\lambda_s-\beta)k_s e_{exo}\tilde{ph}(x)[F_{sol}^{dm}]V_{app} + \gamma k_{abs}[B_{abs}^{dm}]S_{sol} - k_w(W-0.1M).\end{aligned}$$

◇ Evolution of the bolus mass M(t)

$$\frac{dM}{dt} = \frac{M}{M-W}\big(-k_w(W-0.1M) - k_{abs}[B_{abs}^{dm}]S_{sol} + \text{Secretions}\big)$$

◇ Evolution of bolus volume V(t)

$$\frac{dV}{dt} = -k_w(W-0.1M) + \text{Secretions}$$

Conclusion et perspectives

Dans le premier chapitre, un modèle générique de la digestion a été présenté. Un système d'équations différentielles couplées décrit les phénomènes principaux de la digestion pour un bolus homogène : le transport du bolus par les ondes péristaltiques, la dégradation volumique et surfacique du bolus par les enzymes pancréatiques et bordure en brosse et ensuite l'absorption des nutriments. Le modèle étant mécaniste, il a contribué à une meilleure compréhension de ces phénomènes et des lois qui les régissent.

Dans le deuxième chapitre, nous avons justifié par des méthodes d'homogénéisation mathématique le choix du modèle basé sur d'équations différentielles ordinaires pour décrire la digestion en démontrant que ce modèle tient compte d'une façon moyennée de la présence des différentes échelles du temps et de l'espace dans la digestion intestinale : (i) l'influence des ondes péristaltiques sur l'avancement du bol alimentaire, (ii) l'influence des villosités intestinales sur l'augmentation de la surface de contact des aliments avec la paroi intestinale, (iii) l'absorption passive et active à travers la paroi intestinale.

Dans le troisième chapitre, l'influence du changement de la structure du bolus a été étudiée. Le bolus homogène du Chapitre 1 a été remplacé par un bolus non-homogène qui contient des fibres alimentaires. Des propriétés des fibres alimentaires comme la capacité de rétention d'eau ainsi que les nutriments ont été pris en compte. Les résultats numériques sont cohérents avec des données de la littérature : les fibres solubles et insolubles diminuent la digestibilité totale, les fibres solubles diminuent aussi la vitesse du transit du bolus alors que les fibres insolubles l'augmentent.

Les thèmes suivants peuvent contribuer à rendre le modèle plus pertinent pour ouvrir des pistes de recherche :

Nécessité d'identification des paramètres

Une étape importante afin de rendre ce modèle opérationnel est l'identification de ses paramètres. En effet, les expériences du chapitre 1 et le chapitre 3 ont montré l'influence des paramètres sur des résultats finaux de la digestion. Pour identifier les paramètres, des données issues des expérimentations seront nécessaires. Dans un premier temps, afin de rendre l'identification de ces paramètres possible, nous pourrons réduire les équations du modèle en choisissant un bolus suffisamment simplifié (homogène, solubilisé, enzymes endogènes, ...) pour ensuite complexifier le bolus au fur et à mesure. Cependant, l'identification de certains paramètres comme le coefficient d'équilibre $A_s \leftrightarrow A_{ns}$ ou la quantité d'eau associée à la matière sèche (W_{as} , W_{int}, ...) reste compliquée du point de vue expérimental et nécessitera des approches d'expert de ce domaine.

Détermination de la condition initiale

La condition initiale du modèle actuel est choisie en se basant sur le ratio de la matière sèche dans le bolus à l'entrée de l'intestin grêle et elle est indépendante du prétraitement des aliments dans l'estomac, car notre modèle ne s'intéresse qu'à la digestion intestinale. Cependant, la prise en compte de ce dernier permettra de traiter des bols avec une matrice alimentaire plus complexe. Par exemple, dans notre modèle présenté au Chapitre 3, nous avons introduit dans la condition initiale, la quantité d'eau bue (W_{drink}), de l'eau secrétée dans l'estomac (W_{sec}) et de l'eau associée aux aliments (W_{feed}), les vraies valeurs de ces quantités ne peuvent être définies qu'en prenant en compte le prétraitement de l'aliment dans l'estomac (la digestion partielle des aliments, l'absorption d'eau et les sécrétions, etc). Nous pourrons ensuite avoir une estimation raisonnable du volume et la composition du bolus à l'entrée de l'intestin grêle.

Ainsi, il est envisageable de coupler ce modèle avec un modèle de la digestion dans l'estomac pour lequel, la condition initiale sera la composition de l'aliment ingéré. Après la première étape de la digestion et de la solubilisation dans l'estomac, l'aliment entre dans l'intestin grêle par la vidange gastrique. La vidange gastrique peut être représentée par une fonction dont la période et l'efficacité dépendent de la composition de l'aliment dans l'estomac.

Bolus et sa composition

1. *Passage à un bolus hétérogène :* nous avons étudié la digestion pour un bolus homogène et ensuite pour un bolus hétérogène en intégrant les fibres alimentaires dans sa composition. Il est donc intéressant de prendre en compte les trois catégories de nutriments au sein du bolus : les glucides, les lipides et les protides. L'objectif est d'étudier leur cinétique de digestion en présence des éventuelles interactions. En effet, les interactions entre les aliments variées au sein d'un bolus sont connues pour être des étapes impactantes de la digestion. Ainsi, certains aliments peuvent limiter la digestion des autres ou au contraire la favoriser. L'intégration de ces données dans le modèle le rendrait évidemment plus compliqué (augmentation de nombre des équations et des paramètres), mais peut permettre d'obtenir un modèle plus opérationnel.
2. *Changement de la longueur du cylindre :* dans le modèle actuel, un cylindre de la longueur fixe ℓ et du rayon variable $R(t)$ représente le bol alimentaire. Le volume du bolus à l'entrée de l'intestin grêle définit son rayon $R(0)$. Cette quantité a un maximum que nous appelons r_{max}. Dans le modèle actuel, la condition d'entrée est toujours définie pour satisfaire cette contrainte. Cependant, il est clair que le volume du bolus à l'entrée de l'intestin grêle varie en fonction de la composition de l'aliment dans l'estomac, nous pouvons ainsi envisager d'étaler (augmenter ℓ) le bolus lorsque $R(0) > r_{max}$.
3. *Bolus consécutifs :* l'évolution d'un seul bolus dans la lumière intestinale a été étudiée dans cette thèse. De la même manière, l'évolution de plusieurs bolus indépendants (qui ne se rejoignent pas) peut être étudiée et modélisée. Il est toutefois possible d'envisager un regroupement éventuel de ces bolus dans l'iléon et modéliser l'influence de ce regroupement sur la digestibilité totale. Cependant, nous ne pensons pas que cet aspect soit un point majeur comparé aux autres voies pour développer le modèle.

Bibliographie

[1] B. Darcy, J.P. Laplace, and P.A. Villiers. Digestion dans l'intestin grêle chez le porc. *Ann. Zootech*, 30 :31–62, 1981.

[2] W.M.S. Russel and R.L. Burch. The principles of humane experimental technique. *Methuen & Co Ltd, London.*, 1959.

[3] J. Vanmilgen and P. Lescoat. Modelling digestion and metabolism in the pig : an alternative to animal esperimentation ? *Bull. Acad. Vét. France - N°5 http ://www.academie-veterinaire-defrance.org/*, Tome 161- N°5 :435–440, 2008.

[4] J. Clairambault. Modélisation dans le domaine biomédical. ECP 2009-10 Modeling in Biomedical, 2009-10.

[5] R. Lambert P. Meunier, Y. Minaire. *La digestion*. 1988.

[6] L. Montagne and J. Flament. *La digestion des aliments*. Agrocampus ouest.

[7] G. Allaire. The theory of periodic homogenization.

[8] M. Taghipoor, G. Barles, C. Georgelin, J. R. Licois, and P. Lescoat. Mathematical modeling of transport and degradation of feedstuffs in the small intestine. *Journal of Theoretical Biology*, 294 :114–121, October 2011.

[9] W. H. Karasov. Optimal digestive responses to changing diet and foraging costs. In *Adams, N. & Slotow, R. (Eds), Proc. 22 Int. Ornithol. Congr. Durban, University of Natal*, 1999.

[10] S. R. McWilliams and W. H. Karasov. Phenotypic flexibility in digestive system structure and function in migratory birds and its ecological significance. *Comp Biochem Physiol A Mol Integr Physiol*, 128(3) :579–593, Mar 2001.

[11] J.D. Logan, A. Joern, and W. Wolesensky. Chemical reactor models of optimal digestion efficiency with constant foraging costs. *Ecological Modelling*, 168(1–2) :25–38, 2003.

[12] V. P. Srivastava. Effects of an inserted endoscope on chyme movement in small intestine– a theoretical model. *Applications and Applied Mathematics*, 2 :79–91, 2007.

[13] A. Wilfart, L. Montagne, H. Simmins, J. Noblet, and J.van Milgen. Digesta transit in different segments of the gastrointestinal tract of pigs as affected by insoluble fibre supplied by wheat bran. *Br J Nutr*, 98(1) :54–62, Jul 2007.

[14] D. Bastianelli, D. Sauvant, and A. Rérat. Mathematical modeling of digestion and nutrient absorption in pigs. *J Anim Sci*, 74(8) :1873–1887, Aug 1996.

[15] J.D. Logan, A. Joern, and W. Wolesensky. Location, time, and temperature dependence of digestion in simple animal tracts. *Journal of Theoretical Biology*, 216 :5–18, January 2002.

[16] R. Miftahof and N. Akhmadeev. Dynamics of intestinal propulsion. *Journal of Theoretical Biology*, 246(2) :377 – 393, 2007.

[17] A. Shu-Han Lin, M. L. Buist, N. P. Smith, and A. J. Pullan. Modelling slow wave activity in the small intestine. *Journal of Theoretical Biology*, 242(2) :356 – 362, 2006.

[18] L. Bueno, J. Fioramonti, and Y. Ruckebusch. Mechanisms of propulsion in the small intestine. *Ann Rech Vet*, 8(3) :293–301, 1977.

[19] X. T. Zhao, M. A. McCamish, R. H. Miller, L. Wang, and H. C. Lin. Intestinal transit and absorption of soy protein in dogs depend on load and degree of protein hydrolysis. *J Nutr*, 127(12) :2350–2356, Dec 1997.

[20] B. Séve. Ileal standardised digestibility of amino acids in feedstuffs for pigs.

[21] J. P. Laplace. The transit of digesta in the different parts of the digestive tract of the pig. *Prog Clin Biol Res*, 77 :847–872, 1981.

[22] V. Rayner and G. Wenham. Small intestinal motility and transit by electromyography and radiology in the fasted and fed pig. *J Physiol*, 379 :245–256, Oct 1986.

[23] C. Gariepy D. S.A. Pommier, C. Pomar. Petitclerc, influence du genotype, de la castration, de la somatocrinine et déunerestriction energetique sur la qualité des viandes et les proprietés de transformation des carcasses de porcs. rapport final d l'entente auxiliaire canada-quebec sur le developpement agro-alimentaire. Quebec, Canada 1993.

[24] J. Rivest, J. F. Bernier, and C. Pomar. A dynamic model of protein digestion in the small intestine of pigs. *J Anim Sci*, 78(2) :328–340, February 2000.

[25] Livio C. Piccinini. Homogeneization problems for ordinary differential equations. *Rend. Circ. Mat. Palermo (2)*, 27(1) :95–112, 1978.

[26] M. Taghipoor, G. Barles, C. Georgelin, J. R. Licois, and P. Lescoat. Mathematical homogenization in the modelling of digestion in the small intestine. September 2011.

[27] L.C. Evans. The perturbed test function method for viscosity solutions of nonlinear PDE. *Proc. Roy. Soc. Edinburgh Sect. A*, 111(3-4) :359–375, 1989.

[28] L.C. Evans. Periodic homogenisation of certain fully nonlinear partial differential equations. *Proc. Roy. Soc. Edinburgh Sect. A*, 120(3-4) :245–265, 1992.

[29] G. Barles, F. Da Lio, P.-L. Lions, and P. E. Souganidis. Ergodic problems and periodic homogenization for fully nonlinear equations in half-space type domains with Neumann boundary conditions. *ArXiv e-prints*, October 2009.

[30] A. V. Mernone, J. N. Mazumdar, and S. K. Lucas. A mathematical study of peristaltic transport of a casson fluid. *Mathematical and Computer Modelling*, 35(7-8) :895–912, 2002.

[31] D. Randall, W. Burggren, K. French, and R. Eckert. *Eckert Animal Physiology : Mechanisms and Adaptations*. W.H. Freeman & Company, 4th edition, 1997.

[32] X. T. Zhao, M. A. McCamish, R. H. Miller, L. Wang, and H. C. Lin. Intestinal transit and absorption of soy protein in dogs depend on load and degree of protein hydrolysis. *J Nutr*, 127(12) :2350–2356, December 1997.

[33] J. Keener and J. Sneyd. *Mathematical Physiology (Interdisciplinary Applied Mathematics) 2 Vol Set*. Springer, 2nd edition, December 2008.

[34] K.e. Yamauchi. Review of a histological intestinal approach to assessing the intestinal function in chickens and pigs. *Animal Science Journal*, 78 :356–370, 2007.

[35] H. Ishii. *Perron's method for Hamilton-Jacobi Equations,. Duke Math. J*, 55 :369–384., 1987.

[36] M. G. Crandall, H. Ishii, and P. L. Lions. user's guide to viscosity solutions of second order partial differential equations. *Bull. Amer. Math. Soc. (N.S.)*, Bull. :Amer.Math.Soc.27 1–67, 1992.

[37] G. Barles. Nonlinear neumann boundary conditions for quasilinear degenerate elliptic equations and applications. *Journal of Diff. Eqns*, 154 :191–224, 1999.

[38] G. Barles. *Solutions de viscosité des équations de Hamilton-Jacobi (Mathématiques et Applications) (French Edition)*. Springer, 1 edition, March 1995.

[39] C. Wenk. The role of dietary fibre in the digestive physiology of the pig. *Animal Feed Science and Technology*, 90(1–2) :21 – 33, 2001. <ce :title>The Role of Dietary Fibre in Pig Production</ce :title>.

[40] B. McCleary and L. Prosky, editors. *Advanced Dietary Fibre Technology*. Wiley-Blackwell, 1 edition, 2 2001.

[41] J. W Anderson, P. Baird, R. H. Davis, S. Ferreri, M. Knudtson, A. Koraym, V. Waters, and C. L. Williams. Health benefits of dietary fiber. *Nutr Rev*, 67(4) :188–205, Apr 2009.

[42] A. Tharakan. *Modelling of physical and chemical processes in the small intestine*. PhD thesis, University of Birmingham, December 2009.

[43] K.E. and Bach Knudsen. The nutritional significance of "dietary fibre" analysis. *Animal Feed Science and Technology*, 90(1-2) :3 – 20, 2001. The Role of Dietary Fibre in Pig Production.

[44] M. Siljeström, E. Westerlund, I. Björck, J. Holm, N.-G. Asp, and O. Theander. The effects of various thermal processes on dietary fibre and starch content of whole grain wheat and white flour. *Journal of Cereal Science*, 4(4) :315 – 323, 1986.

[45] E. Jiménez-Moreno, J. M. Gonzàlez-Alvarado, R. Làzaro, and G. G. Mateos. Effects of type of cereal, heat processing of the cereal, and fiber inclusion in the diet on gizzard ph and nutrient utilization in broilers at different ages. *Poult Sci*, 88(9) :1925–1933, Sep 2009.

[46] T. M. Burkhalter, N. R. Merchen, L. L. Bauer, S. M. Murray, A. R. Patil, J. L. Brent, and G. C. Fahey. The ratio of insoluble to soluble fiber components in soybean hulls affects ileal and total-tract nutrient digestibilities and fecal characteristics of dogs. *J Nutr*, 131(7) :1978–1985, Jul 2001.

[47] M. Rezaei, M. A. Karimi Torshizi, and Y. Rouzbehan. The influence of different levels of micronized insoluble fiber on broiler performance and litter moisture. *Poult Sci*, 90(9) :2008–2012, Sep 2011.

[48] FAO, Rome : Food Report of the Joint FAO/WHO Expert Consultation. Paper 66, and Agriculture Organization, editors. *Carbohydrates in human nutrition*. FAO Food and Nutrition, 1998.

[49] Barbara O. and Schneeman. Dietary fiber and gastrointestinal function. *Nutrition Research*, 18(4) :625 – 632, 1998.

Résumé :

L'objectif de cette étude est de modéliser la digestion dans l'intestin grêle : le transport des aliments par les ondes péristaltiques, la dégradation par les enzymes endogènes et exogènes et l'absorption active et passive. Un modèle mécaniste basé sur les équations différentielles ordinaires a été utilisé pour représenter la digestion. Les équations décrivent l'évolution de la position et de la composition du bolus provenant de l'estomac. Nous montrons ensuite par les méthodes d'homogénéisation mathématiques que ce modèle peut être considéré comme une version macroscopique des modèles plus réalistes, qui contiennent des phénomènes biologiques à des échelles inférieures de l'intestin grêle. Enfin, nous étudions l'influence du changement de la structure de bolus sur la digestion en intégrant les fibres alimentaires dans sa composition. Les deux principales caractéristiques des fibres alimentaires qui interagissent avec la fonction de l'intestin grêle, à savoir, la viscosité et la capacité de rétention d'eau ont été modélisées.

Mots clés :

Modélisation, EDO, Digestion, Intestin grêle, Péristaltique, Homogénéisation, Solutions de viscosité, Fibres alimentaires.

Abstract :

The purpose of this study is to model the digestion in the small intestine : transport of the the bolus by the peristaltic waves, feedstuffs degradation according to the endogenous and exogenous enzymes and nutrients absorption. A mechanistic model based on ordinary differential equations is used to represent the digestion. The equations describe the evolution of the position and composition of the bolus of feedstuffs coming from the stomach. We prove by using the homogenization methods, that this model can be considered as a macroscopic version of more realistic models which contain the biological phenomena at lower scales of the small intestine. Finally, we investigate the digestion of a non-homogeneous feedstuffs matrix by integrating the dietary fibre in the bolus. The two main physiochemical characteristics of dietary fibre which interact with the function of the small intestine, i.e. viscosity and water holding capacity are modelled.

Keywords :

Modelling, ODE, Digestion, small intestine, peristaltic, Homogenization, Viscosity solutions, Dietary fibres.